Synthesis and Characterization of Unsymmetrical Perylene Derivatives and Perylene Oligomers

by

Runkun Sun

A dissertation submitted to the Graduate Faculty in Chemistry in partial fulfillment of the requirements for the degree of Doctor of Philosophy

The City University of New York.

2013

This manuscript has been read and accepted for the Graduate Faculty in Chemistry in satisfaction of the dissertation requirement for the degree of Doctor of Philosophy

Prof. Shi Jin

Date | Chair of Examining Committee

Prof. Maria C. Tamargo

Date | Executive Officer

Prof. Qiaosheng Hu

Prof. Yu Chen

Prof. Zhonghua Yu

Supervisory of Committee

The City University of New York

Abstract

Synthesis and Characterization of Unsymmetrical Perylene Derivatives and PDI Oligomers

By

Runkun Sun

Adviser: Professor Shi Jin

Since the discovery of highly fluorescent property of perylene tetracarboxylic diimide (PDI) derivatives in 1959, more and more researchers' attention has been attracted to related fields. Ever since, many kinds of PDI derives have been synthesized and characterized. And many special properties of PDI derivatives also have been found, such as strong absorbance, special redox property and self-assembly induced by π-π interaction etc. All these properties endow PDI derivatives wide applications in photovoltaic field and semi-conducting materials area. At the same time, those important applications also encourage researchers to do more exploration on the synthesis and characterization of PDI derivatives. As one of those researchers, my thesis mainly focuses on developing new synthetic methods and characterization of novel PDI derivatives.

In **Chapter 1**, the history of perylene, PDI derivatives and PDI oligomers was reviewed. Their corresponding properties and applications were briefed discussed. Furthermore, the synthetic methods for different kinds of PDI derivatives, both advantages and disadvantages, were also discussed.

In **Chapter 2**, with the investigation of known reactions which were used to

prepare the key intermediate, perylene monoimide monoanhydride, a new synthetic method was developed. The key intermediate could be prepared with high yield conveniently. With the key intermediate, several unsymmetric PDI derivatives were prepared with decent yield. The optical property of one unsymmetric PDI was studied.

In **Chapter 3**, the synthesis of peryelene diester monoanhydride (PEA) and perylene monoimide monoanhydride (PIA) was explored. We discovered a new way to prepare PEA and PEI. Several PEA and PEI with complex structure were prepared with decent yield. The first unsymmetric PEA was synthesized.

In **Chapter 4**, the synthesis of several perylene oligomers was discussed. Based on our experience gained in the Chapter 3 and our investigation of Langhals' strategy, a new approach to grow perylene oligomers was developed by us. With our strategy, the key intermediate, perylene dimer dianhydride, could be obtained with high yield. Starting from this intermediate, a few perylene oligomers were obtained. The extraordinary absorption ability of PDI oligomers was studied.

Acknowledgements

First of all, I would give my sincerely thanks to my adviser- Professor Shi Jin. He is a great professor with full passion on the science. During my exploration of research projects in my study, his guidance plays a vital role. Besides these, he also teaches me how to face failure, overcome frustration and be a professional researcher, which will benefit me for my whole life. I am really appreciated.

My special thanks also go to Professor Qiaosheng Hu from College of Staten Island, Professor Zhonghua Yu from The City College of CUNY, and Professor Yu Chen from Queens College of CUNY. As my committee members, they spend large amount efforts on my project and give many valuable suggestions. I am really appreciated.

My special thanks also go to my colleagues in Professor Jin' research Group, Chenming Xue, Bin Wang, Yijin Xu, Guolin Lu, Hao Zhang and Minzhi Chen. With their help and suggestions, my research journey becomes much easier.

My thanks also go to all the Professors and Staffs of Chemistry Department, College of Staten Island. Thank you for your helps and suggestions, and I really enjoy the time. Besides, I would like specially thank Professor Nan-Loh Yang for admitting me and giving continuous financial support for all these years.

My deepest thanks go to my families, my father Mr Jingbin Sun, my mother Mrs Wenmei Zhang, my sisters Mrs Fuyun Sun, Mrs Xiuzhi Sun, Mrs Yuling Sun, my wife Jianhua Bao and my son Willson Sun. Thank you for your unconditionally encouragement, support and love.

Dedication

This Dissertation is dedicated to my parents, my wife, and my son. Their unconditional love, their continuous support and their encouragements help me clear most burdens on my way to the destination.

谨以此文献给我的父母，妻子和孩子。在他们无微不至的关爱，不懈的支持和鼓励之下，我才能越过层层障碍完成学业.

Table of Contents

BIBLIOGRAPHY

LIST OF FIGURES

LIST OF SCHEMES

LIST OF TABLES

1. Introduction

1.1. History of Perylene

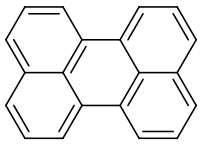

Scheme 1-1. Structure of Perylene

Perylene represents one kind of condensed aromatic rings. The extended conjugated system endows it some special properties, such as strong fluorescence, and the ability to transfer charge. Consequently, perylene and its derivatives attracted more and more attention. In 1953, the accurate structure of perylene with X-ray crystallography was reported by J. G, White etc.[1]

To date, a large amount of perylene derivatives have been synthesized and characterized. Their applications have been utilized in several fields.

1.2. Overview of Perylene Tetracarboxylic Acid Dianhydride (PDA)

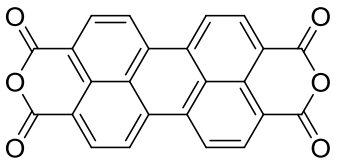

Scheme 1-2. Structure of PDA

PDA forms molecular crystals with a monoclinic structure. In the bulk, the molecules form stacks with an inter-planar distance of 3.2 Å between adjacent

molecules.[2] Inside a stack, molecules do not exactly overlap on top of each other. Instead, they shifts with respect to each other along the long molecular axis parallel to molecular planes by ~1.1 Å， and this leads to an ~11.3 °tilt of the molecular stacks.[3,4] This planar stacking of PDA molecules drew considerable attention from worldwide researchers who working on vapor-deposit organic films.[5-10] It has been reported that PDA can form ordered thin films on various substrates, such as Au, Ag, Si, KCl, NaCl, glass, polymers, graphite and etc.[2, 11-15]

PDA's deposition on KCl [15] and graphite [11](bottom) are shown in **Figure 1-1**.

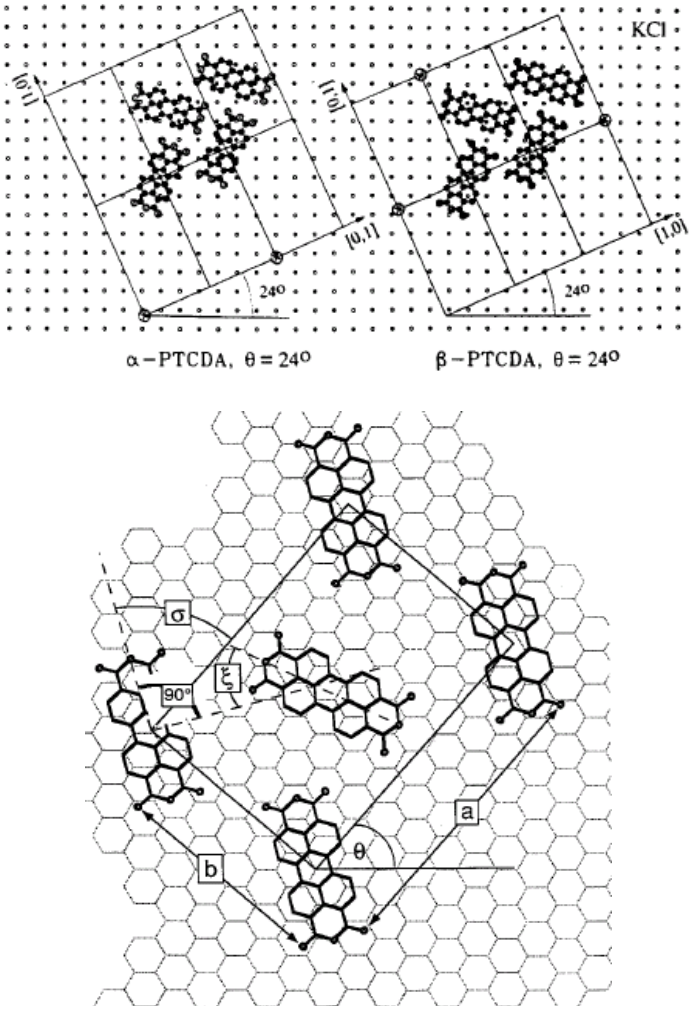

Figure 1-1[11, 15] PDA deposited on KCl and graphite

Besides those important applications as organic thin films, PDA also plays an

important role in the synthesis of perylene derivatives. Most of perylene tetracarboxylic diimide (PDI) were prepared from PDA.[16-20] Some perylene tetracarboxylic derivatives which can be prepared from PDA are shown in the **Scheme 1-3**.

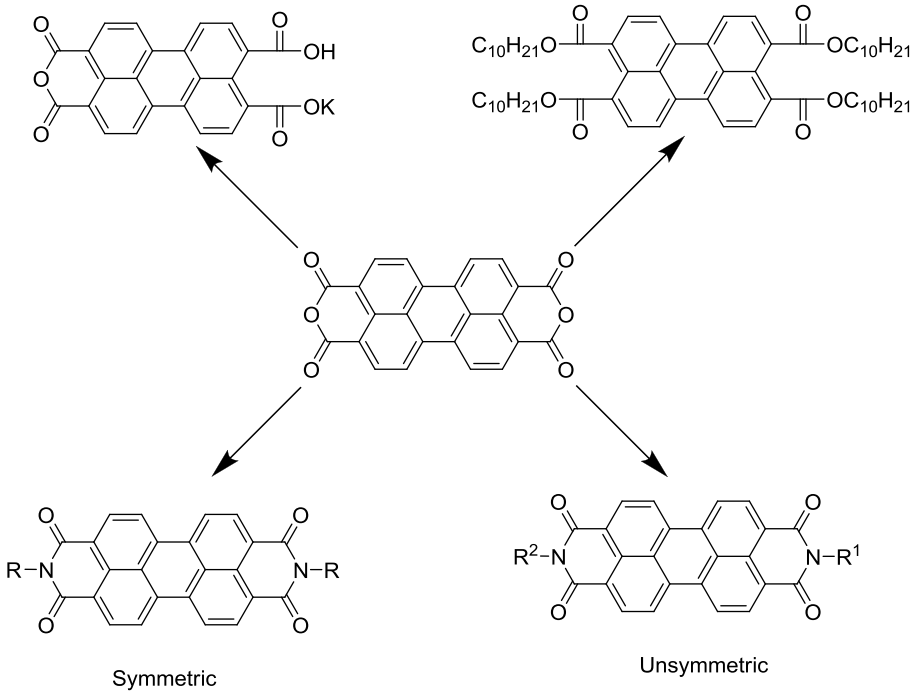

Scheme 1-3. Derivatives of PDA

1.3. Overview of Perylene Tetracarboxylic Diimide (PDI)

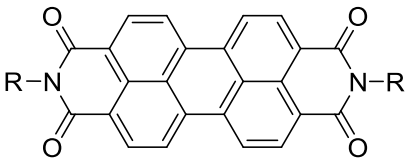

Scheme 1-4. Structure of PDI

1.3.1. History of PDIs

PDIs, discovered in 1913 by Kardos, are well known lightfast red dyes.[21-23] In 1950s, some PDIs were found very useful as high grade industry pigments due to their

unique properties: insolubility, light stability, weather stability, chemical inertness and wide coverage of visible color, from red to violet, even black.[24]

As most PDIs, especially PDIs with short alky groups, don't have good solubility in normal organic solvents, their high fluorescent property was not discovered for long time, until it was reported in 1959.[25] After that discovery, PDIs attract more and more attentions from researchers, and many other applications have also been discovered. To date, PDIs are among the best n-type organic semiconductors, which is related to their high electron affinity.[26-28] PDIs also have been investigated for long time as the active component in field effect transistors, photovoltaic materials, highly efficient fluorophores, and versatile blocks of self-assembly materials.[29-41]

The past years have witnessed the increasing interest of PDIs, which is due to the combination of their favorable properties. PDIs and perylene tetracarboxylic monoimide monoanhydride (PIA) have been proven as the best fluorophores for single molecule spectroscopy.[42] Recently, Müllen and coworkers reported that dendrimers with PDIs at well-defined position can enable unprecedented dye-dye interaction at single molecule level.[43-46]

1.3.2. Synthesis of PDIs

As shown in **Scheme 1-5**, if substituents at two sides of the perylene ring are same, they are considered as symmetric PDIs. Otherwise, they are unsymmetric PDIs. The synthesis routes of these two kinds of PDIs are quite different.

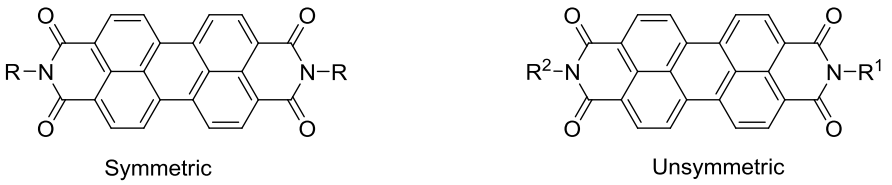

Scheme 1-5. Structure of symmetric and unsymmetric PDIs

1.3.2.1. Synthesis of Symmetric PDIs

Normally, PDA acts as the starting material in the synthesis of symmetric PDIs. The direct condensation of PDA and a primary amine will give corresponding symmetric PDIs. PDA itself was synthesized via the strategy shown in **Scheme 1-6**. Acenaphthene was oxidized to naphthene-1,8-dianhydride. Then it was converted to imide with ammonia, and subsequently dimerized in molten alkali. Finally, saponification in hot concentrated sulfuric acid gives the product PDA.[47]

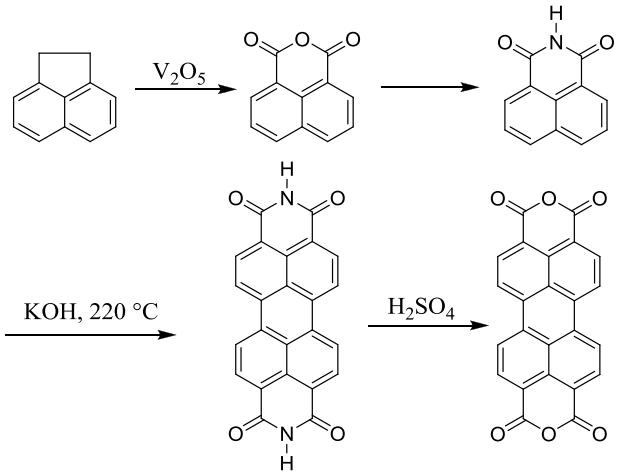

Scheme 1-6. Preparation of PDA

The condensation of PDA and primary amines can be carried out under various circumstances with good yield, such as in water, or benzene.[48-49] The reaction is shown in **Scheme 1-7**.

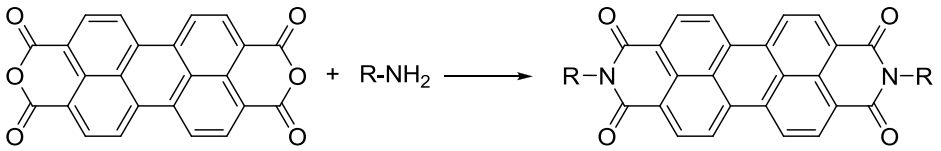

Scheme 1-7. Synthesis of symmetric PDIs

When aromatic amines or other less reactive amines are involved in the condensation, quinoline or molten imidazole as solvent is preferred. And zinc salt is often added as catalyst. One reaction is shown in **Scheme 1-8**.[53]

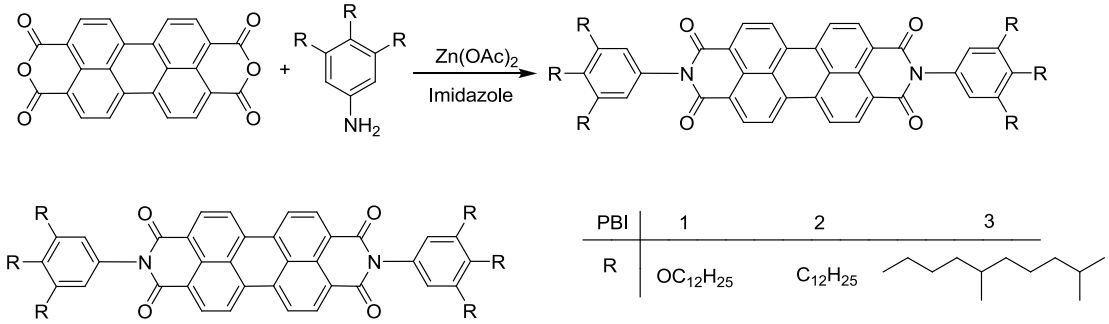

Scheme 1-8. Synthesis of symmetric PDIs

Besides zinc salts, such as zinc acetate and zinc chloride, lead and copper salts can be used too, but they are less effective and more difficult to remove from the reaction system. The mechanism of the catalysis effect of zinc salts is not clear. Some researchers claim them as dehydration reagents, and Langhals has other explanation.[54] In his point of view, a zinc salt will form a complex with PDA, which enhance the solubility of PDA dramatically. Thus, the reaction speed will be accelerated. PDA is insoluble in normal organic solvents, and the solution does not have fluorescence or color. After adding a zinc salt, the solubility of PDA is strongly enhanced. UV-Vis and fluorescence spectrum of PDA could be obtained, as shown in **Figure 1-2**.[54]

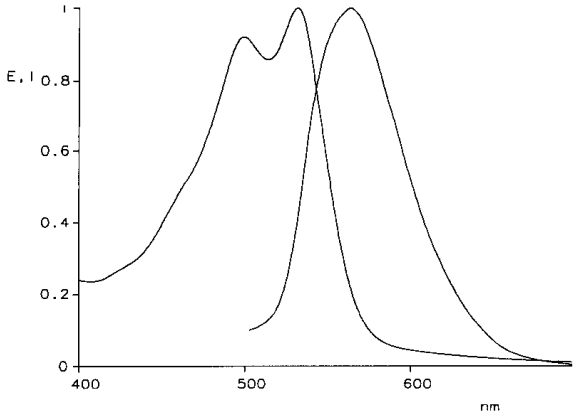

Figure 1-2[54] UV-Vis spectrum of PDA

Besides the direct condensation of primary amines with PDA, there is another method to synthesize PDIs, dimerization of substituted naphthalene imides. This method was applied in the preparation for short-chain aliphatic PDIs.[55-56] The reaction is shown in **Scheme 1-9**.

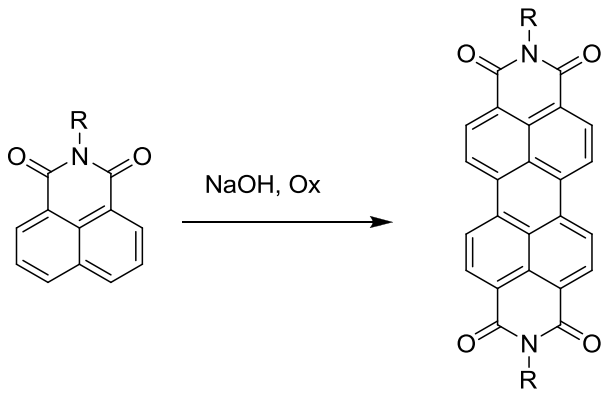

Scheme 1-9. Dimerization method to synthesize PDIs

Another stepwise dimerization was reported by Shein, but the reaction was limited to special cases because of complicated synthesis. [57-58]

1.3.2.2. Synthesis of Unsymmetric PDIs

Comparing to the synthesis of symmetric PDIs, the synthesis of unsymmetric

PDIs is more complicated. As Langhals reported, it is impossible to synthesize unsymmetric PDIs by stepwise condensation of different primary amines. In the reaction of an amine and PDA, even when far less than equivalent amount of the amine was added, the product turned out as the symmetric PDI, not the desired perylene monoimide monoanhydride (PIA) and excess PDA remains unreacted.[59] Without the formation of a PIA, the unsymmetric PDIs can't be prepared in this way. The reaction is shown in **Scheme 1-10**.

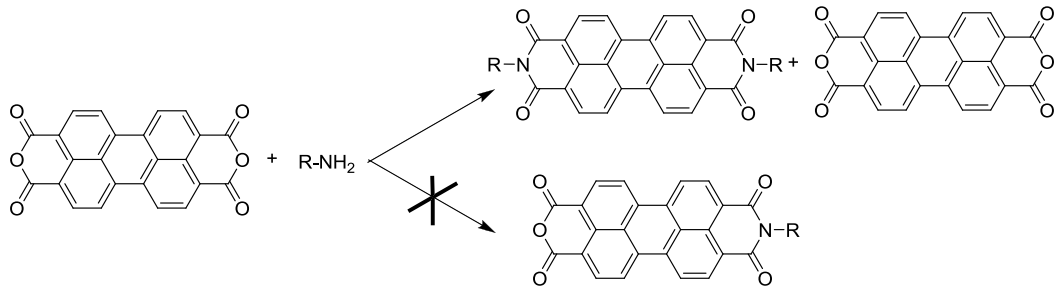

Scheme 1-10. Preparation of perylene monoimide by ratio control

Condensations involving a mixture of two amines and PDA have been carried out, and the unsymmetric PDI is one of the three major products.[54] Besides the usually challenging separation, the reactivity of that two amines must be similar to get a sensible yield. The reaction is shown in **Scheme 1-11**.

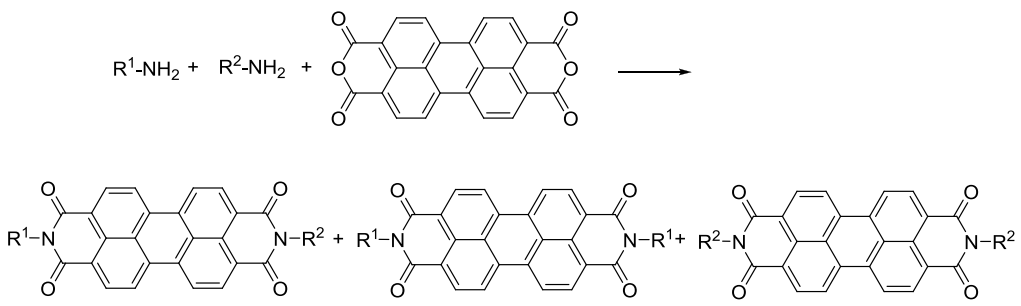

Scheme 1-11. Condensation of mixed amines

Another method was found by Nagao, Misono and coworkers. It involves a partial acidic hydrolysis of PDIs in concentrated sulfuric acid at 180-200 ℃.[60] With such a drastic condition, the applicability of this method is limited into a quite narrow area with simple aliphatic N-substituents, such as R= methyl, ethyl, propyl and butyl. Problems will occur when aromatic substituents are involved, because sulfonation may take place. The strategy is shown in **Scheme 1-12**.

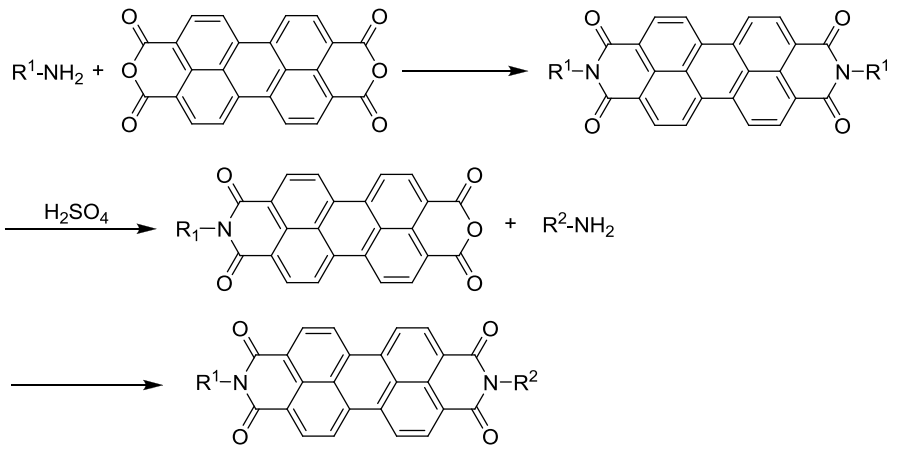

Scheme 1-12. Nago's method for unsymmetric PDIs

Another method was reported by Troster.[61] PDA is first converted into water soluble potassium perylene tetracarboxylate. Then a quantitative amount of orthophosphoric acid is added into the system to acidify the salt, and the perylene monoanhydride monocarboxylic monopotassium salt will precipitate out of the system due to its extreme low solubility in water. PIAs can be prepared by the condensation of the perylene monoanhydride monocarboxylic monopotassium salt and an appropriate primary amine in water. With this strategy, unsymmetric PDIs can be prepared in a large scale. However, the aqueous reaction environment limits the reactants to water soluble amines; otherwise the yield will be quite low. The

method is shown in **Scheme 1-13**.

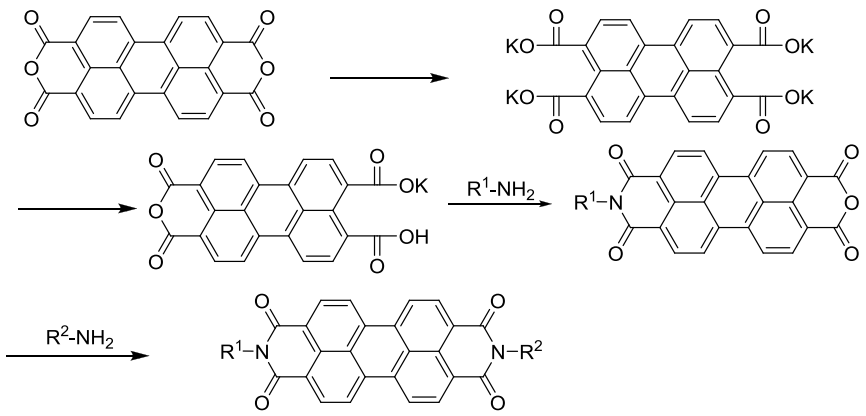

Scheme 1-13. Troster's method

Alternatively, alkaline saponification of symmetric PDIs was tried by Langhals.[62] With a partial hydrolysis of symmetric PDIs, PIAs can be obtained. Then via another condensation of a PIA with a primary amine, unsymmetric PDI can be prepared. The method is shown in **Scheme 1-14**.

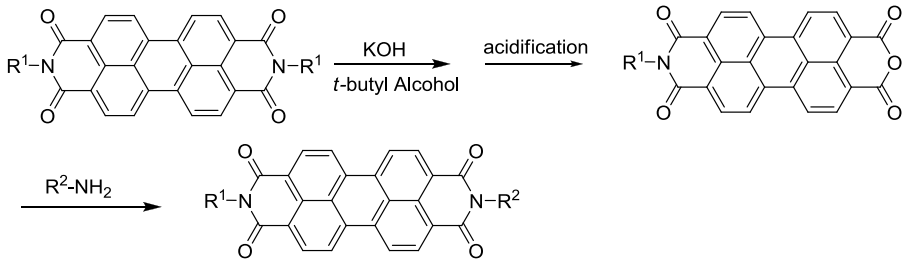

Scheme 1-14. Langhals' method

1.3.2.3. Synthesis of Bay-Substituted PDIs

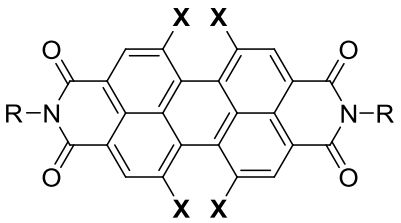

Scheme 1-15. Structure of bay-area modified PDIs

As shown in the **Scheme 1-15**, substituents can be introduced at a carbocyclic position (bay area), labeled as **X**. The first successful preparation was reported by Seabold and coworkers at BASF.[63] Four phenoxy groups were incorporated in bay-area with high yield by nucleophilic replacement of chlorine substituent. The reaction is shown in **Scheme 1-16**.

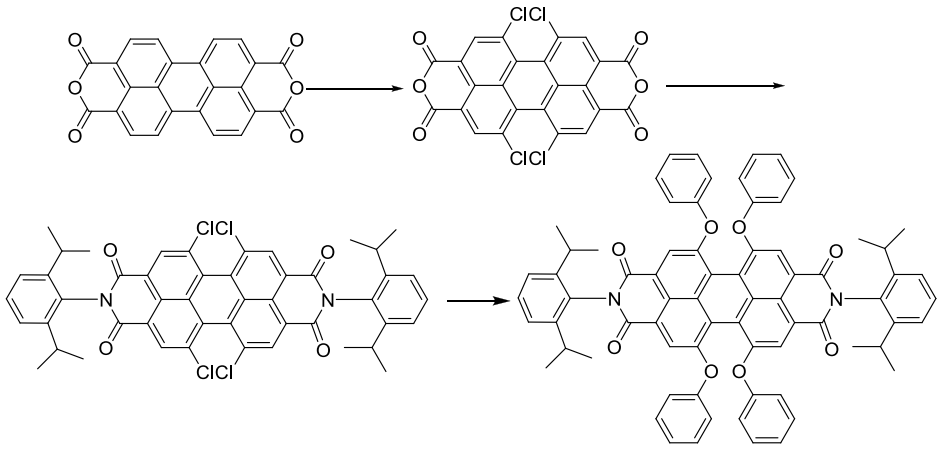

Scheme 1-16. Bay-area modified PDI

With this strategy, the introduction of other nucleophiles were proved to be difficult, and few successful reactions were reported.[64]

Although the discovery of tetrachlorinated perylene dianhydride was known for a while, only very recently, the synthesis of dibrominated perylene dianhydride was reported by H. Arms etc.[65] The synthesis of bay-modified PDIs was then greatly promoted, as the replacement of a bromine atom by a nucleophile is straightforward. Series of PDIs having bay-area substituents were prepared with this staring material.[66-71] The reactions are outlined in **Scheme 1-17**.

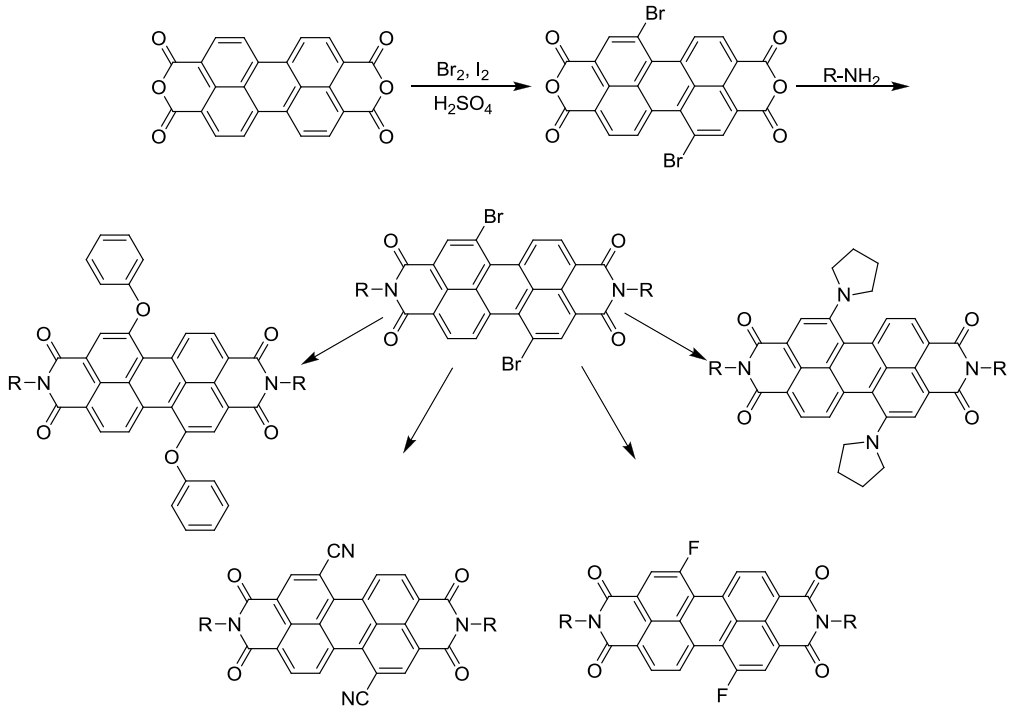

Scheme 1-17. Bay-area modified PDIs

1.3.3. Properties and Applications of PDIs

1.3.3.1. Optical Properties

PDIs are among the best lightfast colorants to date.[72] Their extraordinary absorbance and fluorescence capability originates from the extensive π-conjugated system. Their excellent photo stability and thermal stability benefit a lot from the heterocyclic ring structure.[54] Some derivatives can be sublimed at 550 ℃ without decomposition,[74] some are resistant to ionizing[75] radiation, and some other aggressive conditions[76]. For example, they can be dissolved in concentrated sulfuric acid and recycled back by dilution without decomposition.[77]

As far as the optical properties of PDIs are concerned, it's worth noting that both HOMO and LUMO of PDIs have nodes at imide nitrogen atom.[73] This naturally

brings the electronic decoupling between the perylene core and N-substituents. These orbital are shown in **Figure 1-3**.

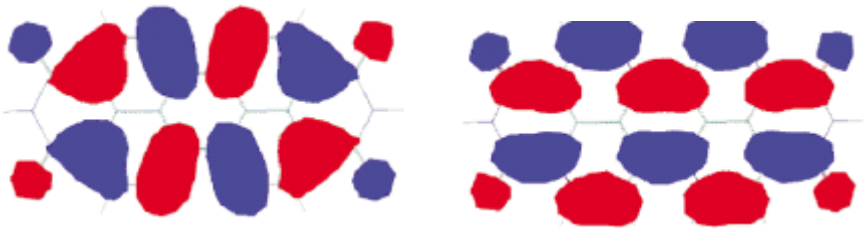

HOMO **LUMO**

Figure 1-3[73] HOMO and LUMO of PDIs

Based on this, N-substituents can be tuned freely without a pronounced effect on the electronic absorption spectrum. To improve the solubility, some PDIs with swallowtail substituents have been synthesized by Langhals.[78] For the PDI with 1-nonyldecyl as N-substituent, the solubility is up to 35 g/100 ml in *n*-Heptane. In contrast, *n*-decyl PDI is insoluble in *n*-Hexane.[105] Those PDIs are shown in **Scheme 1-18**.

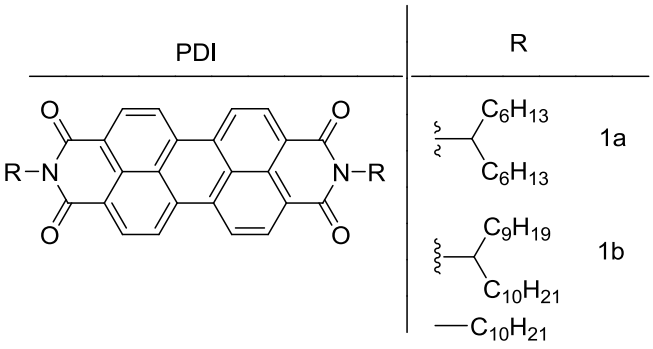

Scheme 1-18. PDIs with swallowtails

High soluble PDIs can form red purple solution with yellow fluorescence. The typical UV-Vis and fluorescence spectra of PDIs in chloroform are shown in **Figure**

1-4.[54] The UV-Vis absorption peaks are usually found at 526, 490, 459, 432 and 369 nm, and the fluorescence peaks appear at 628, 579, 537nm. The molar absorption coefficient constant is 95,000 L mol^{-1} cm^{-1}, which is pretty high among the chromophores. Many PDIs have a tendency to aggregate, which causes the broadening and hypsochromic shift of the UV-Vis spectrum, and quenching of fluorescence.

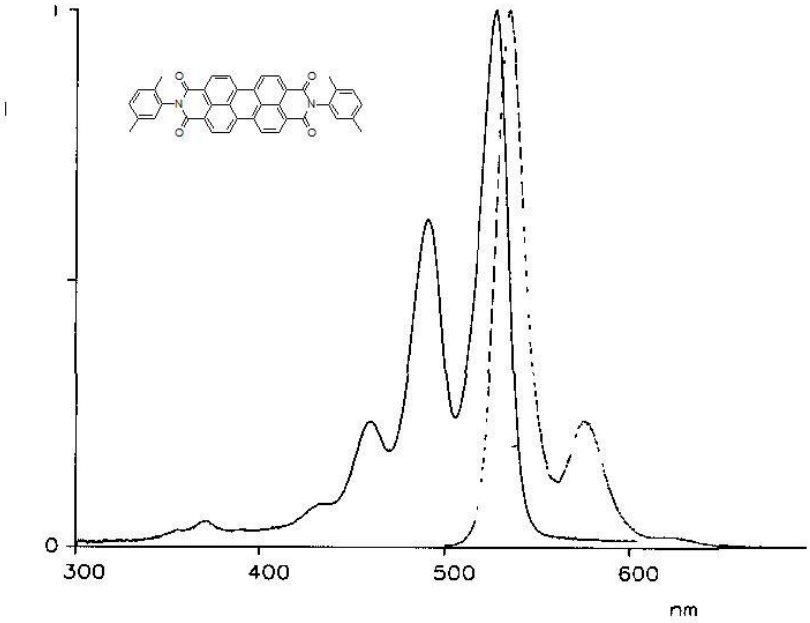

Figure 1-4[54] UV-Vis and fluorescence spectra of a PDI in chloroform

Normally, the UV-Vis spectra of PDIs are not affected significantly by the solvent. However in concentrated sulfuric acid, as presented in **Figure 1-5**, an 80 nm bathochromic shift of λ_{max} was observed, due to the protonation of carbonyl groups. The shape of the spectrum and molar absorption coefficient didn't change much, and this fact suggests that the UV-Vis spectrum in concentrated sulfuric acid could be a good tool for the quantitatively determination of PDIs that are insoluble in normal

organic solvents.

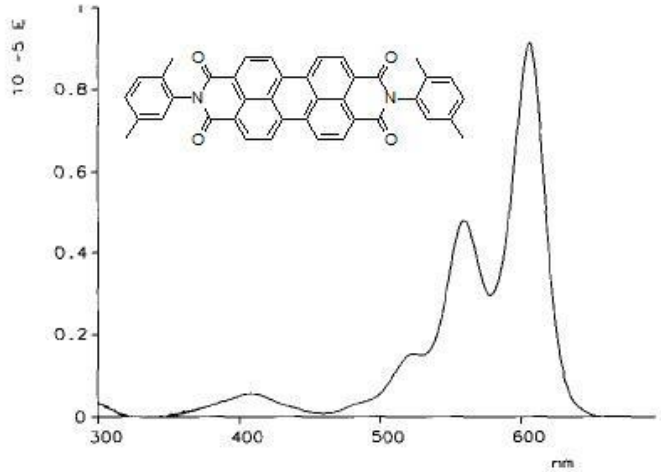

Figure 1-5[54] UV-Vis spectrum of a PDI in concentrated sulfuric acid

Because of the unit fluorescence quantum yield, high stability in air, and excellent solubility in common organic solvents, **1a** in **Scheme 1-18**, was suggested as a standard for the determination of fluorescence quantum yiled.[79] However, the quantum yield will decrease, if aryl substituents connected to an imide nitrogen are not at the orthogonal conformation. One sample with an aryl substituent was reported with a quantum yield of 70%, and the introduction of electron-rich alkoxyphenyl N substituents suppressed the quantum yield to <5%.[34, 80]

More pronounced changes in absorption and emission bands will happen, if substituents were introduced to the bay area of a PDI. When two phenoxy groups were introduced to a single PDI core, the λ_{max} exhibits a 20 nm red-shift. With four phenoxy groups, the shift can be as much as 50 nm.[35] When two electron-rich tetra hydro pyrrole groups were installed at the bay area, the absorption peak can have a red-shift of 160 nm and the emission is already in infrared region.[35] In contrast, the

introduction of electron-withdrawing groups has less effect on the spectrum.

1.3.3.2. Redox Properties and Photovoltaic Applications

PDIs are fairly electron-deficient colorants, which are prone to reduce and rather difficult to oxidize. For most PDIs, two reversible reductions and one reversible oxidation can be found in cylic voltammetry. The PDIs without bay-area modification exhibit a first reduction potential of -0.44V vs SCE (saturated calomel electrode) in CH_2Cl_2. This is comparable to that of C_{60}, a widely used powerful electron acceptor.[81] For bay-substituted PDIs, their redox potentials are greatly affected by those substituents. The introduction of electron-withdrawing groups such as chlorine and cyano groups leads to stronger oxidants, which have high reduction potential; the introduction of phenoxy or other electron donating groups does not favor reductions.

The electron-deficiency of PDIs contributes a lot to their excellent photo stability. Because of their high reduction potentials, in a photo-excited state, they are even better oxidants. This makes the photo-oxidation, the major destruction mechanism of dyes, unfavorable. This property has been widely applied in preparation the long-last photovoltaic materials.[30-31]

Besides the high photo-stability, the charge carrier mobility of PDIs also makes them among the best organic semi-conductors, which is important to photovoltaics too. Some of air stable n-type semi-conductors are shown in **Scheme 1-19**.[83-85]

	 C_{60}	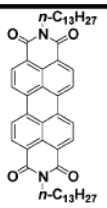 PDI-13	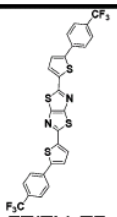 $FT(Th)_2TF$	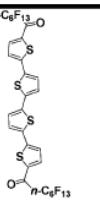 DFHCO-4T	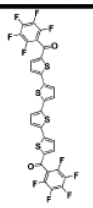 DFCO-4T	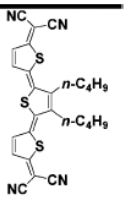 DCMT
E_{red1} (S.C.E.)	-0.5 V	-0.46 V	-1.54 V	-0.88 V	-1.05 V	-0.19
$\mu(cm^2V^{-1}s^{-1})$	0.5	2.1	1.2	1.7	0.5	0.2

Scheme 1-19[85] n-type organic semiconductors

Among these n-type organic semi-conductors, **PDI-13** has the best charge carrier mobility. One important type of organic photovoltaic devices is organic thin film-based solar cell. A typical device consists of a very thin organic film sandwiched between two different electrode materials. This kind of devices with good efficiency containing a PDI/phthalocyanine heterojunction was firstly reported by Tang in 1985, and the power conversion efficiency is ~1%.[87] New systems with higher power conversion efficiency was reported by Schmidt-Mende.[88]

The structure of heterojunction solar cell was shown in **Figure 1-6**.[89]

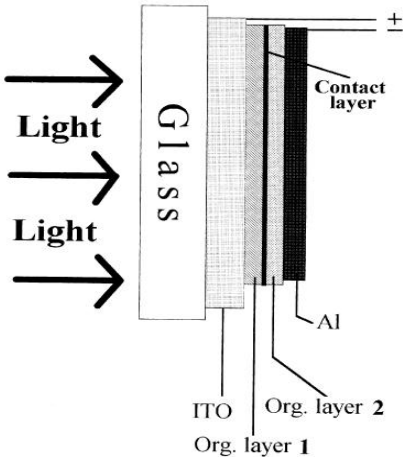

Figure 1-6[89] Heterojunction solar cell structure

The molecular structure of HBC-PhC_{12} (the electron donor) and its packing scheme are shown in **Figure 1-7.** The distance between adjacent molecules is 34 Å, and the distance between two disks is 3.5 Å. For the PDI in the figure, the distance between two π-packed disks is also 3.5 Å.[88]

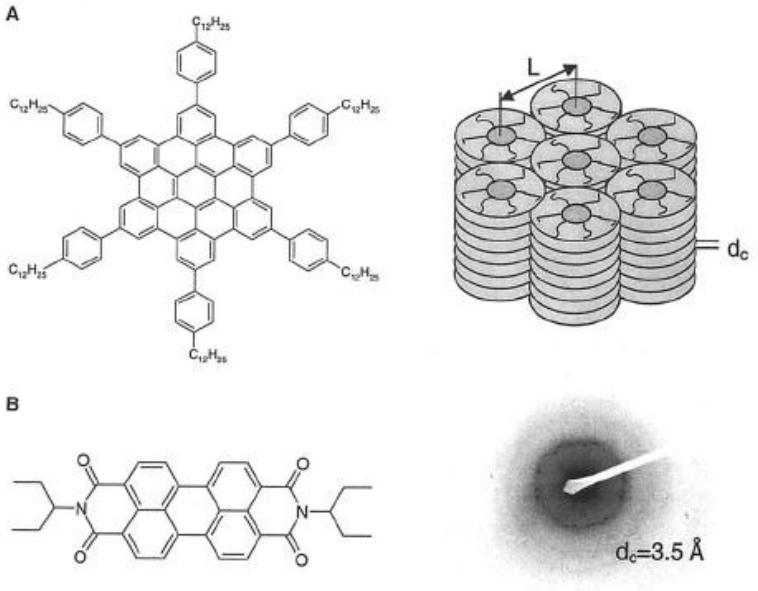

Figure 1-7[88] Molecule structure of HBC-PhC_{12}

The HOMO, LUMO data of two components are shown in **Figure 1-8**.

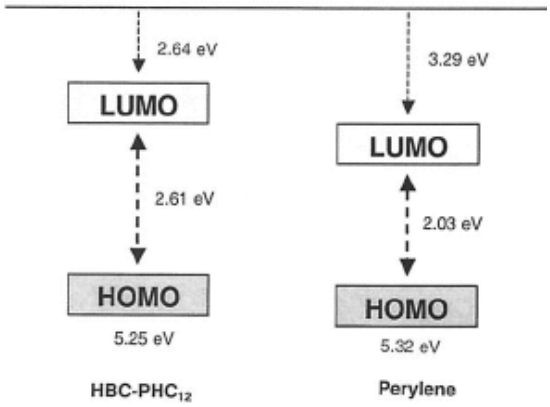

Figure 1-8[88] HOMO, LUMO data of HBC and perylene

The mechanism of energy transport and charge separation is shown in **Figure 1-9**.[89]

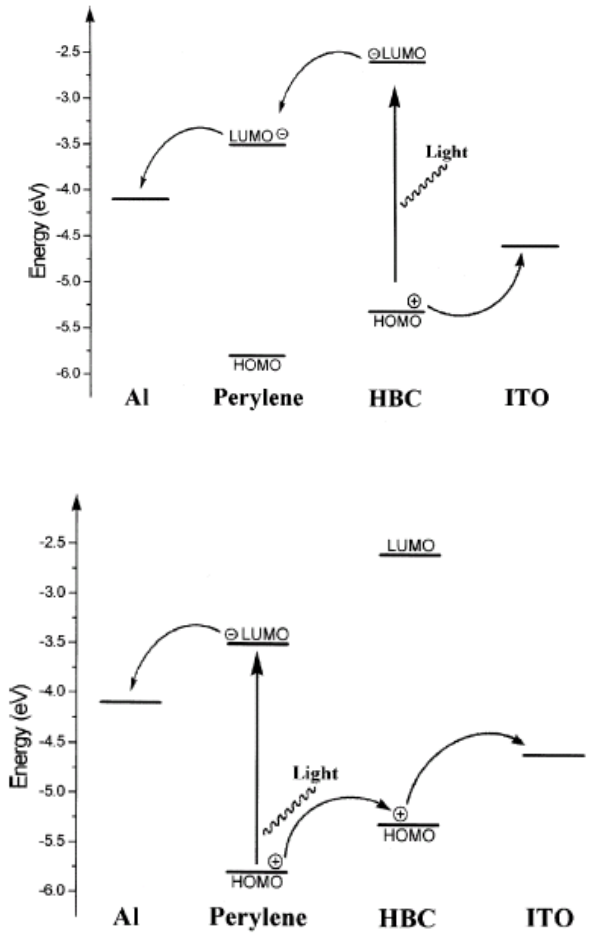

Figure 1-9[89] Charge separation mechanism

Good photo-stability, large absorption coefficient, appropriate and tunable HOMO, LUMO levels together with high charge carrier mobility suggest that PDIs could be promising photovoltaic materials in the future.

1.3.3.3. Structure, π-π Stacking and Self-assembly

The structure of PDIs has been studied for long time, and the planar structure was proved by X-ray diffraction of a number of PDI single crystals [90-91] The specific data is shown in **Figure 1-10**.[16]

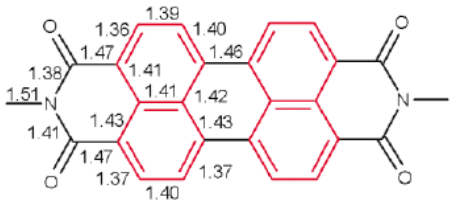

Figure 1-10. X-ray data of PDI

This planar structure is affected little by the substituents on terminal nitrogen, but affected significantly by the bay-area substituents. When bulky groups were introduced into the bay area, the steric hindrance makes the twisted structure more favorable rather than the planar structure. One example is shown in the **Figure 1-11**.[16]

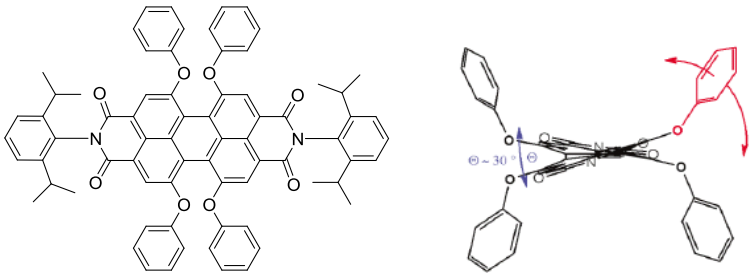

Figure 1-11. Structure of a bay-area modified PDI

This twisted structure has a strong influence on the packing behavior of PDIs, and the strong **π-π** interaction between PDIs molecules is considerably weakened. The decrease **π-π** interaction substantially enhances their solubility.[90]

π-π interaction is a kind of widely existed force in aromatic systems. In a small aromatic ring system, ab initial calculations suggest that **π-π** interaction doesn't have much influence on the stacking of molecules. However, the importance of **π-π** interaction increases rapidly with the increase of the size of the planar

π-conjugated system. In large planar π-conjugated molecules such as PDIs, the **π-π** interaction has a strong influence on the packing of PDIs, both in solid phases and in liquid phases.

In a solid phase, the crystallography studies of PDIs suggest that there is a parallel orientation between PDIs molecules. The distance between two adjacent molecules is around 3.2- 3.5 Å. The packing mode is affected by substituents, and the color is affected greatly by the packing mode. Therefore, PDIs with different colors, from red, orange, to black, can be achieved with this strategy.[92] There are two major packing modes for PDIs, J-aggregation and H-aggregation. J-aggregation usually leads to a bathochromic shift in a UV-Vis spectrum, while a hypsochomic shift is typically observed with the formation of H-aggregates. These shifts greatly broaden the accessible color range of PDIs, which is important to pigments. These aggregates are shown in **Figure 1-12**.[93]

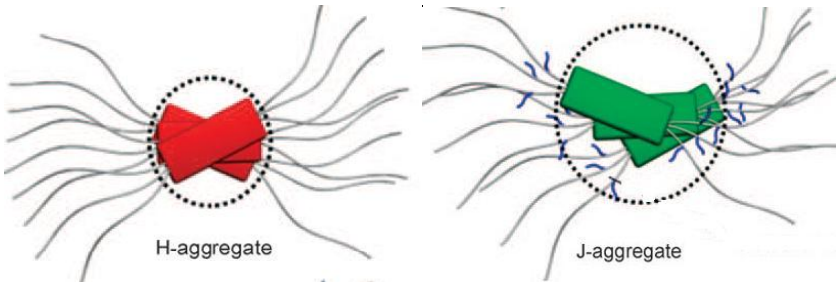

Figure 1-12[93] J-aggregate and H-aggregate

In a liquid phase, **π-π** interaction-dominated aggregation also exists. Though this kind of behavior has been found for long time, only recently, the Gibbs energy change of the aggregation process was determined by Würthner etc.[94] Via the concentration dependent UV-Vis spectroscopy study, the aggregation constants of

series of PDIs were determined. The structures of these PDIs are shown in **Scheme 1-20**.[94]

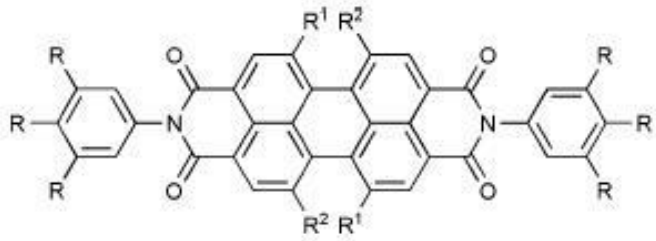

a: R = $OC_{12}H_{25}$, $R^1 = R^2 = H$
b: R = $OC_{12}H_{25}$, $R^1 = H$, $R^2 = p$-*t*BuPhO
c: R = $OC_{12}H_{25}$, $R^1 = R^2 = p$-*t*BuPhO
d: R = $OC_{12}H_{25}$, $R^1 = R^2 = Cl$
e: R = $C_{12}H_{25}$, $R^1 = R^2 = H$

Scheme 1-20[94] PDIs with self-assembly behavior

The aggregation constants of PDIs in methylcyclohexane at 20 ℃ are shown in **Table 1-1**. [94]

	K/M^{-1}	$-\Delta G^0_{298}$/kJ mol^{-1}
a	1.5×10^7	40.9
b	6×10^5	33.1
c	1×10^5	29.0
d	700	16.2

Table 1-1[94] Aggregation constant of PDIs

These aggregations could appear at pretty low concentration due to the large constant. Different type of aggregation mode, H-aggrgate or J- aggregate, will lead to different colors. The concentration-dependent fluorescence of sample **e** in **Scheme 1-20**, at 10^{-6}, 10^{-5}, 10^{-4}, 10^{-3} and 10^{-2} M^{-1} are shown in **Figure 1-13**.[94]

Figure 1-13. Concentration-dependent fluorescence of samples

In a liquid crystalline phase, **π-π** interaction also plays an important role in the packing process. The principle is similar to that in a solid phase. Liquid crystalline PDIs were found by Cormier and Gregg for the first time in 1997.[95] Subsequently, lots of attention was attracted into this area and more liquid crystalline PDIs were obtained.

Many liquid crystalline PDIs exhibit a hexagonal columnar mesophase. The temperature range over which a liquid crystalline phase is observed varies with different PDIs, and some PDIs have a temperature range as wide as 62-244 ℃.[89]

Besides the **π-π** interaction, some other driving forces have also been exploited in self-assembly behaviors of PDIs. They include hydrogen bonding, metal-ligand-coordination and ionic interaction.

The hydrogen bonding mostly works cooperatively with **π-π** interaction, and some time can lead to a unique structure, such as helical structure. One example is shown in **Figure 1-14**.[96]

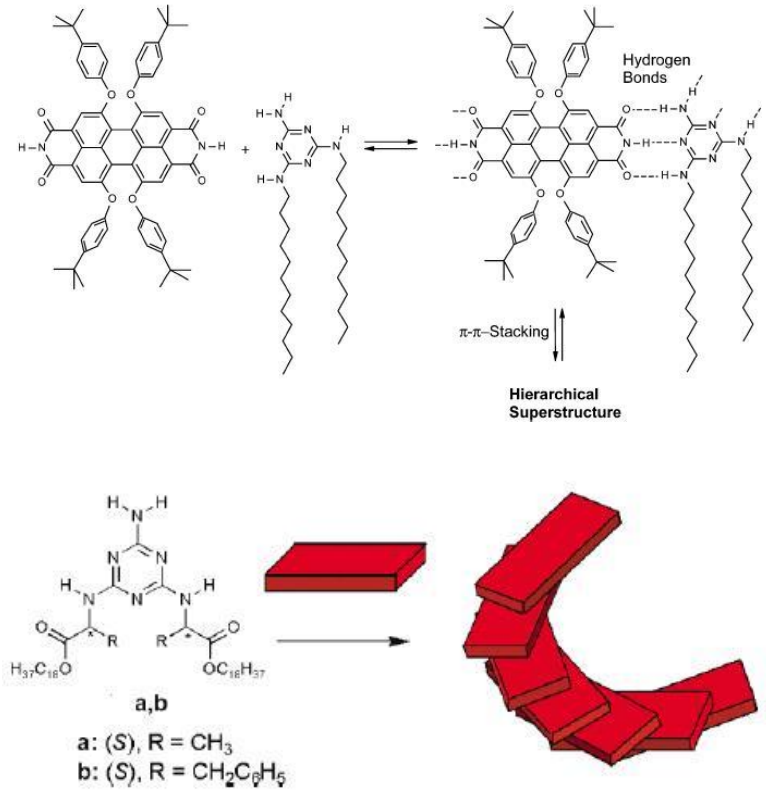

Figure 1-14[96] Self-assembly behavior of PDIs

Metal-ligand-coordination could also be a strong driving force under certain conditions. The coordination bond could be powerful enough to overcome the **π-π** interaction, and drastically enhance the solubility of PDIs. This property has been applied in the preparation of well-defined nano-oligo chromophor, as exemplified in **Scheme 1-21**.[97]

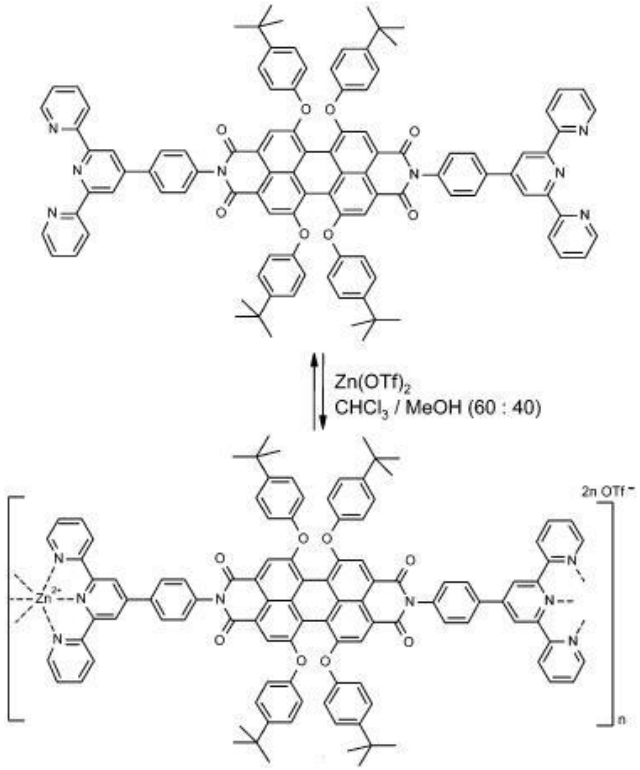

Scheme 1-21. Metal ligand PDIs

1.4. Overview of PDI Oligomers

The structure of PDI oligomers is shown in **Scheme 1-22.** They are constructed by directly connecting individual PDI units with N-N bonds. Comparing to the well-known PDIs, PDI oligomers are much less studied. To date, the synthesis and characterization of them were only reported by two research groups.[98-99]

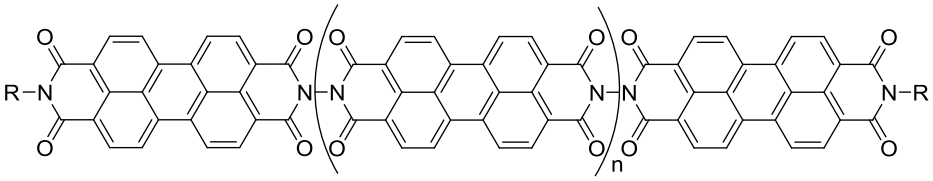

Scheme 1-22. PDI oligomers

1.4.1. Synthesis of PDI Oligomers

The only synthesis strategy was reported by Langhals in 1998,[98] and the other group applied this strategy in the preparation of novel substituted PDI trimers.[99] The strategy is shown in **Scheme 1-23**.[98]

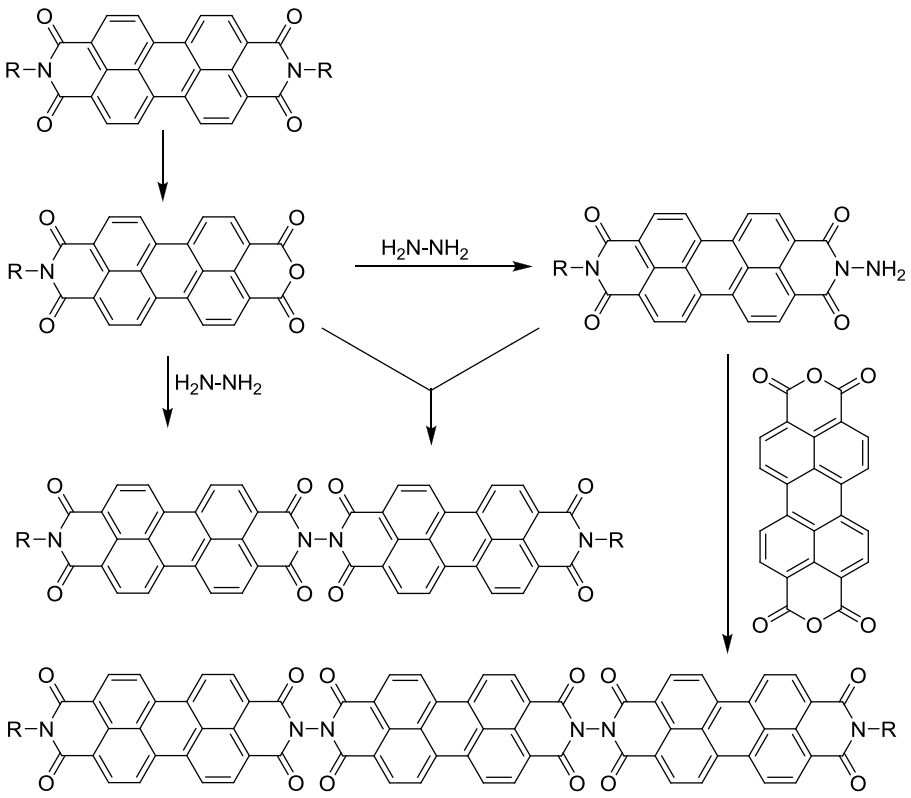

Scheme 1-23. Synthesis route of PDI oligomers

The rare report of synthesis of PDI oligomers is partially due to the difficulties involved in the preparation process. First problem is the low solubility of PDIs and PDI oligomers in organic solvents. To overcome this issue, two strategies were applied. One method is to introduce a bulky solubilization group to the nitrogen terminal, which was used by Langhals.[98] The other is to introduce functional groups at the bay-area, which can substantially decrease the **π-π** interaction and enhance

solubility. The second method was used by Wasielewski.[99]

The second problem is the synthesis of the key intermediate PIA. With Langhals' strategy, PDI dimer and trimer are synthesized with good yield. However, due to the intrinsic problem of the saponification reaction, the limit of this strategy is PDI trimer. To prepare longer PDI oligomers, new method need to be explored.

1.4.2. Properties and Applications of PDI Oligomers

Besides general properties of PDIs, PDI oligomers also exhibit other unique properties. PDI oligomers have a rigid rod structure, and all the PDI units arranged in one-dimension, which makes the one-dimensional transport of electrons and energy possible. A few PDI dimers and trimers have been prepared and characterized by Wasielewski's group. And they found that electron hopping $>10^7$ S^{-1} between two PDI units of PDI dimer.[99] For the trimer, similar phenomenon was observed too. These results demonstrated that linear perylene oligomers could be potential n-type semi-conducting materials for fast long distance electron transport.

This rigid rod structure also offers PDI oligomers a great chance to build intense dyes with a very high absorption coefficient. When chromophores, like PDI units, are arranged in a highly ordered fashion with a very short distance separating adjacent units, strong exciton interaction will be expected.[100]

For PDI oligomers, their transition moments are linear and the distance between two adjacent molecules is the shortest. Therefore, their exciton interaction is among the strongest, and this interaction causes dramatically increase of their absorption

coefficient. For the PDI oligomers in **Scheme 1-23**, the normal absorption coefficient of PDIs is around 85,000 L mol^{-1} cm^{-1} but for the PDI dimer is 240,000 L mol^{-1} cm^{-1}, far beyond the two times of monomer. The coefficient of trimer is 420,000 L mol^{-1} cm^{-1}, which is almost 5 times of that of monomer. At the same time, the quantum yield of fluorescence still is around 100%.

In this thesis, the synthesis and characterization of PDI oligomers also will be discussed.

2. Synthesis and Characterization of Unsymmetric Perylene Tetracarboxylic Diimides

2.1. Introduction and Design

Perylene tetracarboxylic diimides (PDIs) have been attracting considerable attention as lightfast colorants,[1-3] highly efficient fluorophores,[4-6] the best n-type organic semiconductors[7-9] and versatile building blocks in selfassembly.[10-12]

PDI **2-1** shown in **Scheme 2-1** does not dissolve in any organic solvents. To solve this problem, solubilizing groups were introduced in the PDI core, often in form of N-substituents.

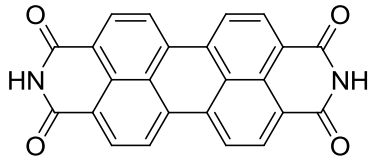

2-1

Scheme 2-1. Structure of PDI

The synthesis of symmetrically N-substituted PDIs can be achieved with a direct condensation of perylene tetracarboxylic dianhydride (PDA) with an appropriate primary amine.

However, in many instances, it is preferred to install two N-substitution groups in an unsymmetrical fashion. These include the situations when the PDI moieties are incorporated into complex molecular and supra-molecular architectures, or into polymers as the side groups. The synthesis of unsymmetric PDIs is important, and there are not many available methods reported in literatures.

Preparation of unsymmetric PDIs by step-wise condensation of PDA with two

different primary amines by controlling the stoichiometric ratio was proved not working.[13]

Unsymmetric PDIs could be obtained by simultaneous condensation of PDA and a mixture of two primary amines.[1] To apply this strategy, two different amines should have similar reactivity. Moreover, the isolation of target unsymmetric PDIs from the mixture is usually quite challenging.

If one has the access to an appropriate perylene tetracarboxylic monoimide monoanhydride (PIA) with a structure shown in **Figure 2-2**, a convenient condensation with a primary amine with another different R group would produce an unsymmetrically substituted PDI. Various PIAs, particularly those with symmetric secondary alkyl groups (swallowtails), have been widely integrated into donor-acceptor dyads and triads,[16-17] donor–bridge acceptor molecules,[18] fluorescent sensors and light switches,[19-21] supramolecular assemblies,[22-23] and PDI multichromophores[24-27]and PDI side chain polymers,[28-30] owing to the strong solubilizing power of swallowtails.

There are two commonly used approaches toward PIAs in literatures.

One was reported by Troster,[14] which was shown in **Scheme 1-13**. However, only water soluble amines offer a decent yield.

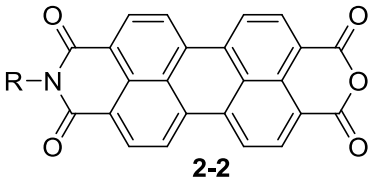

2-2

Scheme 2-2. Structure of PIA

The second approach, a partial saponification, was reported by Langhals.[15]

Moderate yields and the strong basic environment limit the application of this strategy.

Here we would like to present our new approach to a versatile class of PIAs shown in **Scheme 2-3**. They have a few unique features. The first feature is the good extensibility. The carboxylic group and anhydride group are good positions for the introduction of new groups. By tuning the R group, the **π-π** interaction between perylene cores can be tailored by steric means. This tuneability is necessary to achieve a delicate balance between good solubility and the ability to form π stacks with extensive inter molecular **π**-orbital overlap, which is crucial for various optoelectronic applications.[31] Another advantage is that the configuration of the N-bound unsymmetric center is controllable by using an optically pure α-amino acid as the starting material.

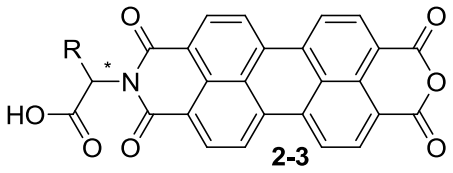

2-3

Scheme 2-3. Synthesis of PIA with an alpha amino acid

2.2. Results and Discussions

2.2.1. Synthesis and Characterization of PIAs

To synthesize PIA **2-3** with a high yield, a few methods were tried, as shown in **Figure 2-1**. Synthesis of PIA **2-3** with R = methyl was initially attempted according to two general procedures established byTroster[14] and Langhals[15] (method **T** and **L**), with optically pure L-alanine as the amine source. Compound **2-4** was synthesized according to a literature procedure.[14] It is known that both procedures produce a

mixture of PDA, PDI **2-5** and the aimed PIA **2-3**. PIA **2-3**, PDI **2-5** and PDA are similarly soluble in aqueous alkaline solution and poorly soluble in common organic solvents, which make it impractical to isolate PIA **2-3** from the reaction mixture efficiently. So it is necessary to find a method that can produce PIA **2-3** at the highest possible yield. Moreover, it is also important to evaluate the result of these reactions.

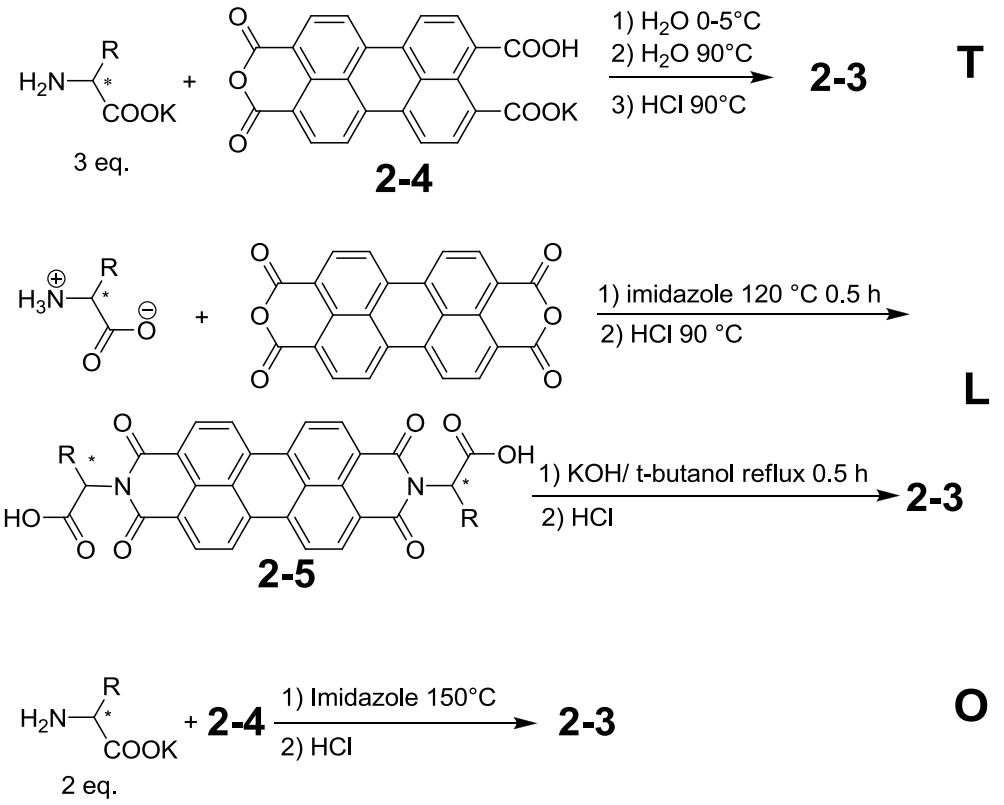

T-----Troster's method; **L**-----Langhal's method; **O**-----Our method

All chirality centers are in S configuration.**2-3a**, **2-5a**: R = methyl

2-3b: R = 2-methylpropyl **2-3c**: R=1-methylethyl

Figure 2-1. Preparation of PIA **2-3**

The IR and UV-Vis data of PDA, PDI and PIA are shown in the **Table 2-1**. C=O stretching vibration bands of anhydride and imide groups appear at different

positions in an IR spectrum. Thus FT-IR spectroscopy can provide important information in terms of the ratio of anhydride and imide functional groups in a reaction product mixture. A pure PIA would feature both anhydride (1733 and 1772 cm^{-1}) and imide (1660 and 1701 cm^{-1}) C=O stretching vibration bands at nearly the same intensity. The problem is that, an equimolar mixture of PDI and PDA would produce a very similar IR spectrum as that of pure PIA. This can be distinguished by UV-Vis spectroscopy. All perylene tetracarboxylic derivatives are soluble in concentrated sulfuric acid, mainly driven by the protonation of carbonyl groups. As the result, their UV-Vis spectra in concentrated sulfuric acid can be conveniently collected and analyzed. The two strongest UV-Vis absorption peaks of PIA are at 610 and 570 nm, respectively. In contrast, an equimolar mixture of PDA and PDI would exhibit four UV-Vis bands at 618, 573, 546 and 510 nm. Evidently, the combination of IR and UV-Vis spectroscopy can be applied to the evaluation of the products from **Figure 2-1** semi-quantitatively.

	IR (cm^{-1})		**UV-Vis (nm)**
	Imide	**Anhydride**	
PDA		**1733, 1772**	**510, 546**
PDI	**1660, 1701**		**573, 618**
Monoanhydride monoimide	**1660, 1701**	**1733, 1772**	**570, 610**

Table 2-1. IR and UV-Vis spectra of PDA, PDI and PIA

The corresponding spectra of crude products in **Figure 2-1** are shown in **Figure**

2-2. It is obvious that method **T** (**3a-T**) produces a large amount of PDA, as indicated by the significantly stronger anhydride bands in the IR spectrum and the intense UV–Vis absorption peak at 548 nm. Although method **L** is more efficient than method **T**, it has been reported that the yield of the monoimide monoanhydride by partial saponification is at most about 50% due to the random nature of the reaction. The formation of PDA in method **L** (**3a-L**) is unambiguously identified by a shoulder at 548 nm. As isolation of PIA **2-3a** is difficult, it would be ideal if a more efficient procedure is available.

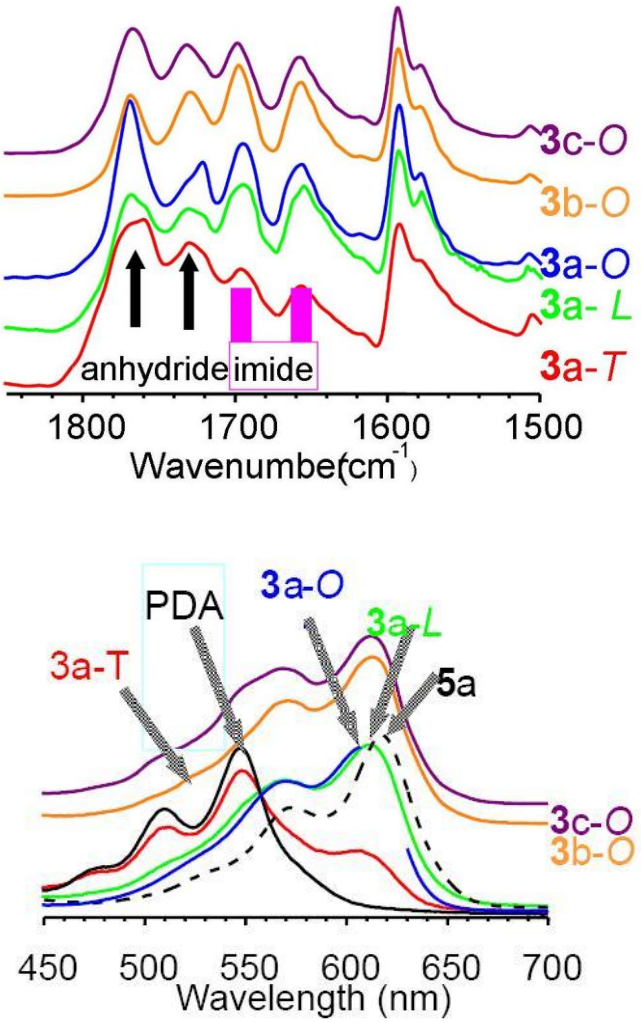

Figure 2-2. UV-Vis and IR spectra of PIA **2-3**

Procedure **T** has been successfully applied to synthesize PIAs in yields greater than 85% from water-soluble primary amines with a primary alkyl group or its steric equivalent. In our case, it is speculated that the steric hindrance caused by the methyl group in L-alanine slows down the nucleophilic attack of amino group to the anhydride group, so that competing basic hydrolysis of the anhydride group dominates the reaction, which produces the precursor of PDA. The yield of PIA **2-3a** could be considerably improved if the hydrolysis reaction is suppressed. Base on this analysis, we improved the reaction condition. In procedure **O**, reactions were carried out in imidazole melt instead of water to minimize the hydrolysis. The crude product is obtained in essentially quantitative yield. Gratifyingly, IR and UV spectra suggest that the crude product is mostly PIA **2-3a** and contains no PDA, as indicated by the absence of a peak or shoulder at 548 nm. Moreover, the formation of PDI **2-5a** is also reduced when compared with procedure **L**, as indicated by the slightly blue-shifted UV-Vis absorption maximum peak.

Procedure **O** also works with α-amino acids with different R groups. For instance, PIA **2-3b** and PIA **2-3c** have also been synthesized by using L-leucine and L-valine as the amine sources, respectively. PIA **2-3c** is always contaminated by PDA and its preparation is significantly more sensitive to moisture than that of PIA **2-3b**, which is more sensitive than PIA **2-3a**. Both can be rationalized by the increase of the steric hindrance toward nucleophilic attacks of the amino group to the anhydride group, which increases the relative rate of the competing hydrolysis due to

trace amount of water. From L-alanine to L-leucine, then to L-valine, though the reaction condition becomes more and more rigorously anhydrous, the contamination of PDA in the product becomes more and more obvious. The reaction conditions when preparing PIA **2-3a**, **b** and **c** were outlined in **Scheme 2-4**, **Scheme 2-5** and **Scheme 2-6,** respectively.

L-alanine as amine source:

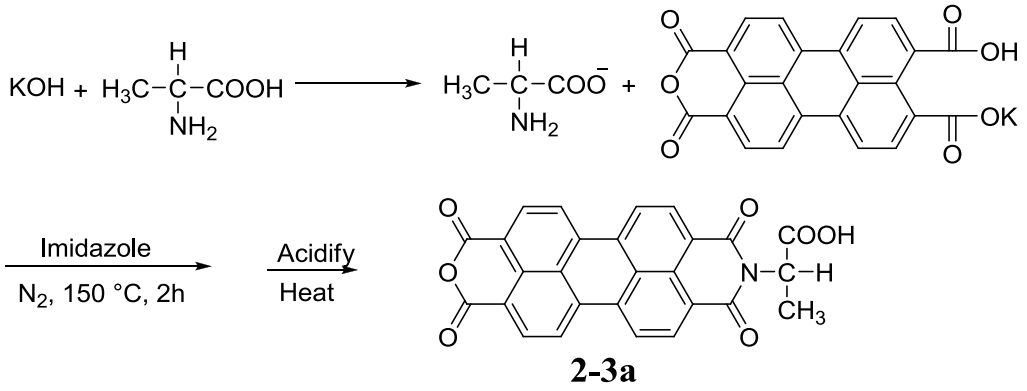

Scheme 2-4. Synthesis of PIA with alanine as amine source

L-leucine as amine source:

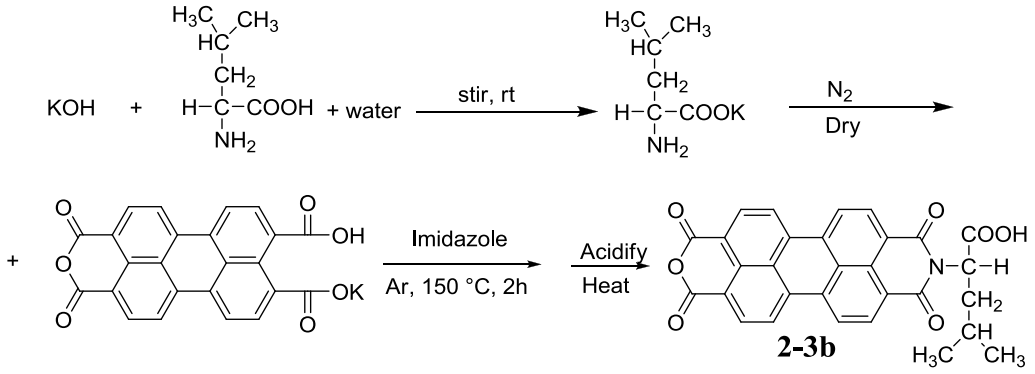

Scheme 2-5. Synthesis of PIA with leucine as amine source

L-valine as amine source:

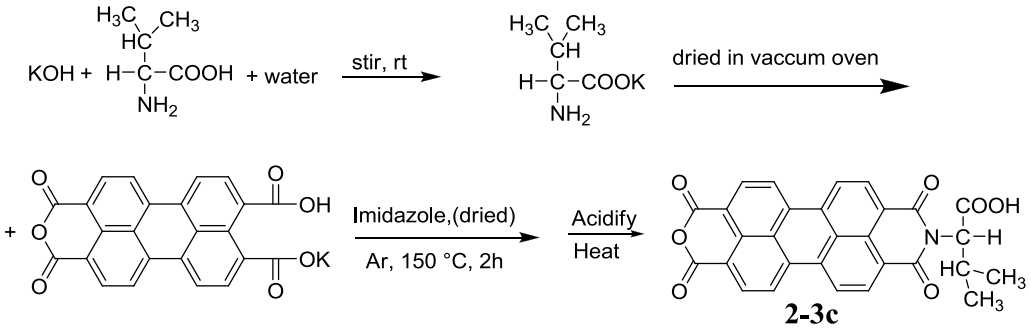

Scheme 2-6. Synthesis of PIA with valine as amine source

2.2.2. Extension of PIA 2-3a by Imidization

With PIA **2-3a** as the starting material, unsymmetric PDIs can be prepared conveniently by reacting with an primary amine source.[1] Some unsymmetric PDIs can be obtained with relatively high yield, and the common reaction condition is shown in the **Scheme 2-7**.

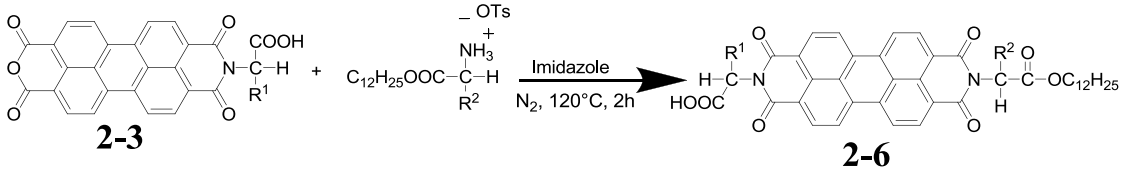

Scheme 2-7. Synthesis of unsymmetric PDI **2-6**

With this method, several intermediates were obtained. Their structures and yields are shown in **Scheme 2-8**. All products were purified through column and confirmed by NMR, FT-IR and MS.

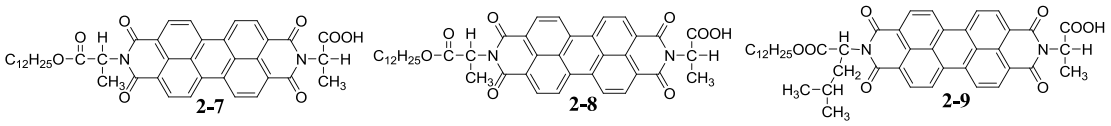

L-Ala-PDI-L-Ala-C12H25

Yield= 67%

D-Ala-PDI-L-Ala-C12H25

Yield= 75%

L-Ala-PDI-L-Leu-C12H25

Yield= 73%

Scheme 2-8. Unsymmetric PDI intermediates

During our exploration for the synthesis method of those unsymmetric PDI

intermediate compounds, we also tried the direct condensation with a mixture of two primary amines. The reaction is showed in **Scheme 2-9**.

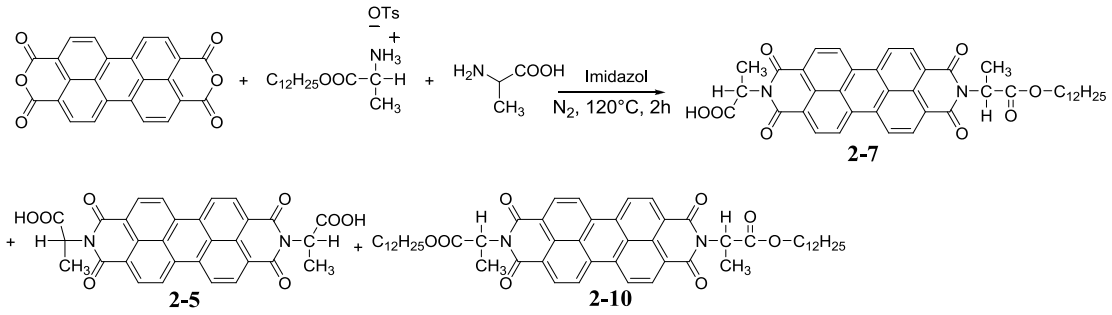

Scheme 2-9. Mix condensation of different amines

The isolated yield of unsymmetric PDI **2-7** is about 25%. Although the yield is not high, this approach involves less preparation steps. In addition, the separation of three expected products (two symmetrically di-substituted PDIs and the desired unsymmetrically di-substituted PDI) is not difficult due to the large polarity differences among them. It could be a back-up plan**.**

All these intermediates are soluble in common organic solvents such as chloroform and THF, which makes the column purification feasible. This friendly accessibility will substantially widen their potential applications in perylene derivatives' preparation and research.

2.2.3. Synthesis and Characterization of Unsymmetric PDIs

The unsymmetric PDI intermediates described in the previous section can be further extended to preparation of PDI derivatives with more complicated structures.

To study the self-assembly behavior and optical property of unsymmetric PDI derivatives, we designed PDI **2-12,** which is shown in **Scheme 2-10.** A long hydrophobic group, C-12 ester, and a long hydrophilic tetraethylene glycol chain,

were introduced unsymmetrically into a PDI. The interaction between these groups may endue this compound some interesting assembly properties. The optically pure amine source, L-alanine, also provides two chirality centers at both sides of PDI. It should be an optically active chiral compound. Its optical properties will be discussed in the section **2.3.** The isolate yield of this reaction turns out to be around 50%.

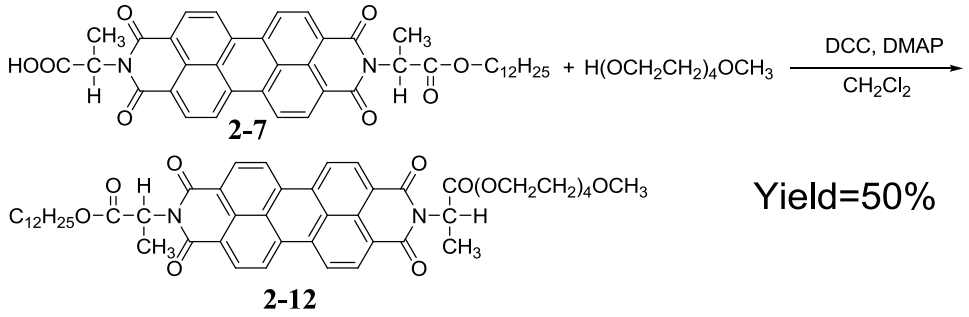

Scheme 2-10. Synthesis of unsymmetric PDI **2-12**

For the two previous samples, only one amino acid (L-alanine) was introduced into the terminal of a PDI. But for some cases, the installation of different amino acids could be necessary. So we designed and synthesized PDI **2-13** with the method shown in **Scheme 2-11**. The unsymmetric PDI intermediate was prepared with the method outlined in **Scheme 2-7.** The introduction of another -$C_{12}H_{25}$ group is straight forward, and the isolate yield is 80%.

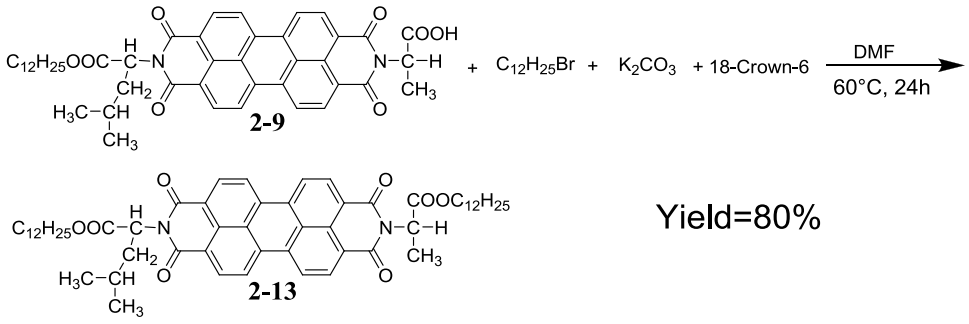

Scheme 2-11. Synthesis of unsymmetric PDI **2-13**

2.3. Characterization

FT-IR, NMR, UV-Vis, MS and circular dichroism (CD) measurements have been carried out to characterize those unsymmetric PDIs.

PDI **2-12** has chirality centers at nitrogen terminals, which is from corresponding optically pure amino acids.[32] The spectra of PDI **2-12,** in **Figure 2-3**, was obtained under condition 1.2 × 10^{-4} M in 1/3 THF/H_2O (v/v). This spectrum gives solid evidences to us that this unsymmetric PDI is optically active.

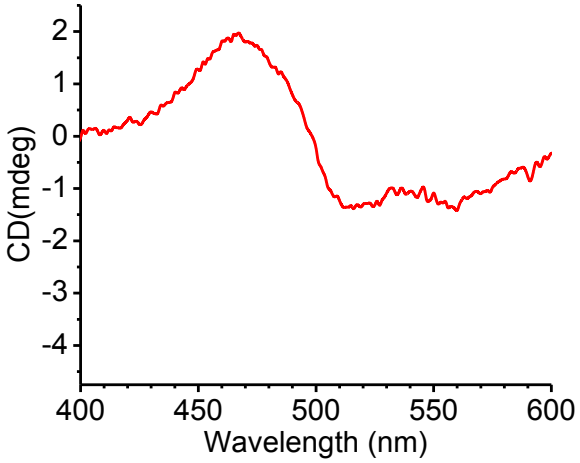

Figure 2-3. CD spectrum of PDI **2-12**

2.4. Conclusion

We did some study on the synthesis of unsymmetric PDIs. A new and convenient method has been developed by us to prepare key intermediate PIA **2-3**. The evaluation of PIA **2-3** can be done with combination of FT-IR and UV-Vis spectra. With this key intermediate, several unsymmetric PDIs were obtained with decent

yields. At the same time, a few unsymmetric PDIs with more complex structure have been prepared. The circular dichroism result provides solid evidence for the chirality of PDI **2-12**.

2.5. Experiments

2.5.1. Instruments and Characterizations

^{1}H and ^{13}C NMR spectra were recorded on a Varian 300 or 600 MHz NMR spectrometer with deuterated chloroform ($CDCl_3$), DMSO or THF as the solvent at room temperature. The chemical shifts were reported using TMS as the internal standard. Mass measurement was carried out in CUNY-Hunter MS center. The IR spectra were acquired on a Bruker Vertex 70V FT-IR spectrometer at a resolution of 4 cm^{-1}. Circular dichroism (CD) spectra were measured on an Aviv 62ADS spectrometer with a bandwith of 2 nm. UV-Vis spectra were recorded on LAMBDA 650 UV-Vis Spectrophotometer.

2.5.2. Materials and Synthesis

All reagents and chemicals were purchased from Fisher scientific or VWR international and used as received.

Perylene-3,4,9,10-tetracarboxylic acid monoanhydride monopotassium carboxylate (compound **2-4**) was prepared according to a literature procedure.[1]

Perylene-3,4,9,10-tetracarboxylic acid monoanhydride monopotassium carboxylate (compound **2-4**) was prepared according to a literature procedure.[1]

***N*, *N*'-di((*S*)-1-carboxyethyl)-3,4,9,10-perylenetetracarboxyldiimide (**PDI

2-5a) was synthesized according to our previously published procedure.[31]

***N-(S)*-1-carboxyethyl-3,4,9,10-perylenetetracarboxylic-3,4-anhydride-9,10-imide (**PIA **2-3a)**

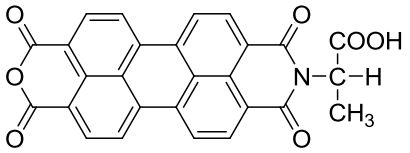

2-3a

Procedure T (**Troster's** Method) is a literature protocol

Procedure L (Langhals' Method**)** is a literature protocol with 5a as the diimide

Procedure O (Our Method**)**

Into a 25 mL Schlenk flask were charged L-alanine (3.80 mmol), KOH (3.80 mmol) and imidazole (5 g). The mixture was purged with argon and stirred at 120 ℃ for 30 minutes and a clear solution was obtained. Then the temperature was increased to 150 ℃ before compound **2-4** (1.90 mmol) and imidazole (10 g) were added. The reaction was allowed to continue at 150 ℃ until the mixture was completely soluble in water. It typically takes about 90 minutes. Then the mixture was cooled to 90 ℃ and deionized water (10 mL) was added under argon. The red solution was filtered to remove trace amount of compound **2-4**. The filtrate was acidified with 12 M HCl solution to pH 3~4. Subsequently, the mixture was heated to 90 ℃ and stirred for 30 minutes. The red precipitate was collect by suction filtration and washed thoroughly with deionized water the filtrate was neutral. Product was dried in vacuum oven at 75 ℃ until constant weight. Yield: 870 mg (99%)

FT-IR (cm^{-1}): 3300-2800 (Carboxylic OH), 2956 (CH3), 1766 (symmetric

anhydride C=O), 1733 (antisymmetric anhydride C=O), 1699 (symmetric imide C=O symmetric), 1660 (antisymmetric imide C=O), 1594 (aromatic ring stretch).

UV-Vis spectra: 570 nm, 609 nm.

***N-(S)*-1-carboxy-3-methylbutyl-3,4,9,10-perylenetetracarboxylic-3,4-anhydride-9, 10-imide (**PIA **2-3b)**

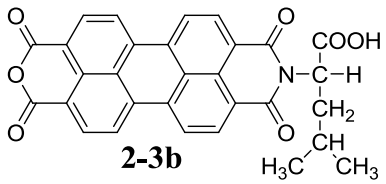

2-3b

Into a 25 ml Schlenk flask were charged L-leucine (3.51 mmol), KOH (3.51 mmol) and water (5 ml). The mixture was stirred at room temperature for 30 minutes and a clear solution was obtained. Then the mixture was heated at 100 ℃ and purged with argon until it was dry. Then the temperature was increased to 150 ℃ before compound **2-4** (1.75 mmol) and imidazole (15 g) were added. The reaction was allowed to continue at 150 ℃ until the mixture was completely soluble in water. It typically takes about 90 minutes. Then the mixture was cooled to 90 ℃ and deionized water (10 mL) was added under argon. The red solution was filtered to remove trace amount of compound **2-4**. The filtrate was acidified with 12 M HCl solution to pH 3~4. Subsequently, the mixture was heated to 90 ℃ and stirred for 30 minutes. The red precipitate was collected by suction filtration and washed thoroughly with deionized water the filtrate was neutral. Product was dried in vacuum oven at 75 ℃ until constant weight. Yield: 859 mg (97%)

FT-IR (cm^{-1}): 3300-2800 (Carboxylic OH), 2956 (CH_3), 1767 (symmetric

anhydride C=O), 1730 (antisymmetric anhydride C=O), 1699 (symmetric imide C=O), 1659 (antisymmetric imide C=O), 1594 (aromatic ring stretch).

UV-Vis spectra: 571 nm, 611 nm.

***N-(S)*-1-carboxy-2-methylpropyl-3,4,9,10-perylenetetracarboxylic-3,4-anhydride-9,10-imide** (compound **2-3c**)

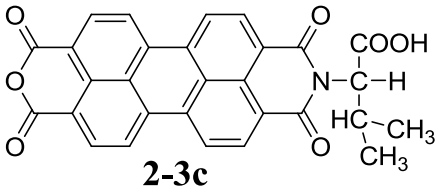

2-3c

Before the reaction, imidazole was dried in a desiccator with activated 4A molecular sieves for 2 days and compound **2-4** was dried in vacuum oven under 90 ℃ over night. Then into a 25 mL Schlenk flask were charged L-valanine (3.44 mmol), KOH (3.44 mmol) and water (5 g). The mixture was stirred at room temperature for 30 minutes and a clear solution was obtained. Then the mixture was heated at 100 ℃ and purged with argon to evaporate away the water until it was dry. The mixture was dried in vacuum oven at 120 ℃ for another 2 hours. Then it was taken out and protected with argon. Then the temperature was increased to 150 ℃ before compound **2-4** (1.15 mmol) and imidazole (15 g) were added. The reaction was allowed to continue at 150 ℃ until the mixture was completely soluble in water. It typically takes about 90 minutes. Then the mixture was cooled to 90 ℃ and deionized water (10 mL) was added under argon. The red solution was filtered to remove trace amount of compound **2-4**. The filtrate was acidified with 12 M HCl solution to pH 3~4. Subsequently, the mixture was heated to 90 ℃ and stirred for 30 minutes. The red precipitate was collected by suction filtration and washed

thoroughly with deionized water the filtrate was neutral. Product was dried in vacuum oven at 75 ℃ until constant weight. Yield: 564 mg (99%).

FT-IR (cm^{-1}): 3300-2800 (Carboxylic OH), 2956 (CH3), 1764 (anhydride C=O), 1730 (anhydride C=O), 1699 (symmetric imide C=O symmetric), 1660 (antisymmetric imide C=O), 1593 (aromatic ring stretch).

UV-Vis spectra: 548 nm (shoulder), 569 nm, 611 nm.

***(S)*-2-(dodecyloxy)-1-methyl-2-oxoethyl ammonium 4-toluenefulfonate** was synthesized according to a literature procedure.[1]

***N*-*(S)*-1-carboxyethyl-*N'*-*(S)*-2-dodecyloxy-1-methyl-2-oxoethyl-3,4,9,10-perylenetetracarboxyldiimide (**PDI **2-7)**

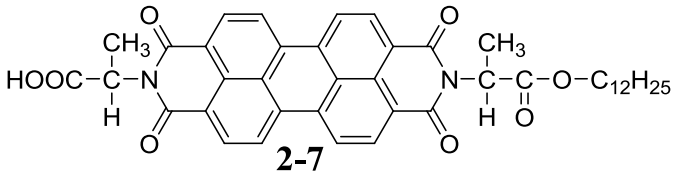

2-7

(S)-2-(dodecyloxy)-1-methyl-2-oxoethyl ammonium 4-toluenefulfonate and PIA **2-3a** were dried in vacuum oven at 60 ℃ over night. Then into a 25 mL Schlenk flask were charged PIA **2-3a** (4.32 mmol), *(S)*-2-(dodecyloxy)-1-methyl-2-oxoethyl ammonium 4-toluenefulfonate (4.75 mmol), and imidazole (15 g). The mixture was purged with argon and stirred at 120 ℃. The reaction progress was monitored with TLC. It typically takes about 90 minutes. Then the mixture was cooled down to 90 ℃, deionized water was added under argon. The solution was allowed to cool down to room temperature then acidified with 12 M HCl solution to pH 3~4. The red product was collected by suction filtration and washed with deionized water.

Product was dried in vacuum oven at 60 ℃ over night. Then the product was purified with column chromatography on silica gel using 20/1 (v/v) $CHCl_3$/acetic acid as the eluent. Yield: 2 g (66%).

^{1}H NMR (300 MHz, DMSO-d_6): δ 8.26–8.179 (m, 8H, Ar**H** in perylene ring); 5.75 (q, 1H, J = 6.9 Hz, -N-C**H**); 5.65 (q, 1H, J = 6.9 Hz, N-C**H**); 4.13-3.96 (m, 2H, -COC**H**$_2$-); 1.71–1.67 (m, 6H, -CH-C**H**$_3$); 1.48–1.39 (m, 2H, -COCH$_2$C**H**$_2$-); 0.93–0.59 (m, 21H,-C**H**$_2$-).

HRMS (ESI): (M+*e*): Calcd for $C_{42}H_{42}N_2O_8$ 702.2941; found, 702.2961.

The ^{1}**H-NMR** spectrum of one key intermediate PDI **2-7** is shown in the following.

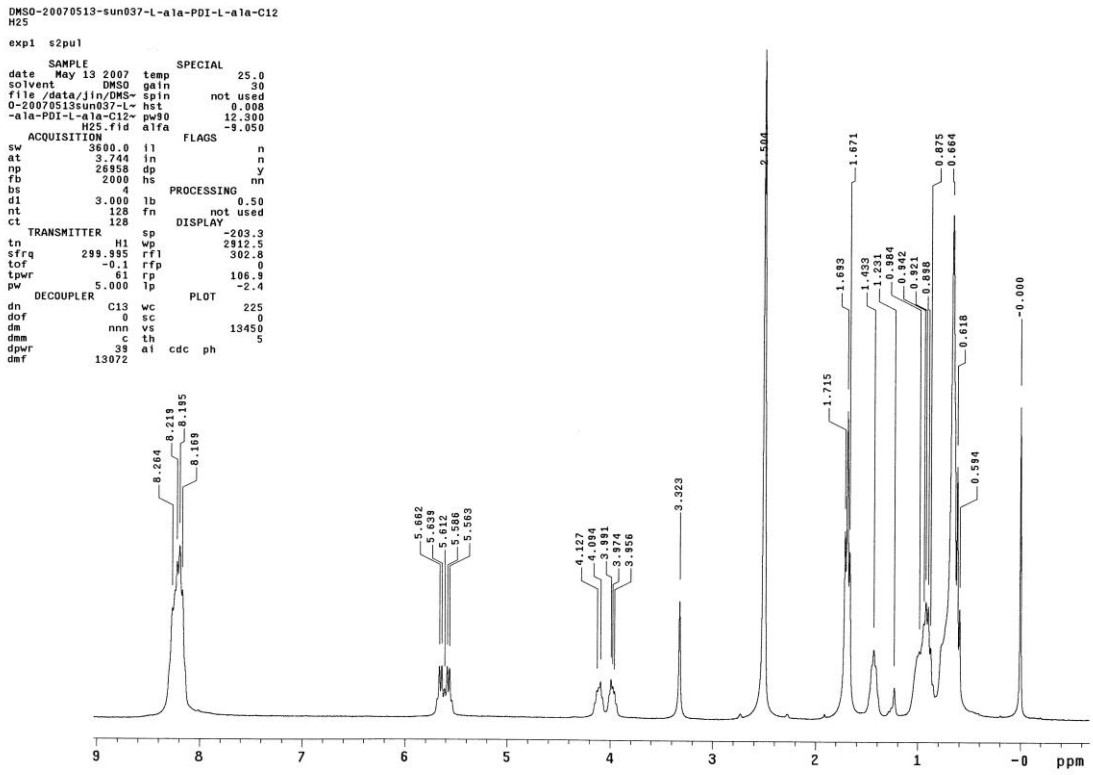

N-(S)-2-dodecyloxy-1-methyl-2-oxoethyl-N'-(S)-2-(2-(2-(2-(2-methoxyethoxy)ethoxy)ethoxy)-1-methyl-2-oxoethyl-3,4,9,10-perylenetetracarboxyldiimide

(compound **2-12)**

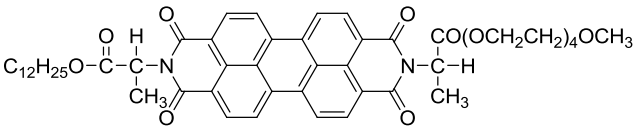

2-12

Into a 25 ml round bottom flask were charged PDI **2-7** (0.285 mmol), tetraethyleneglycol monomethyl ether (0.341 mmol), DCC (0.341 mmol), DMAP (0.17 mmol) and 20 ml CH_2Cl_2. Then the mixture was sealed and stirred at room temperature. The progress was monitored with TLC. After three days, 2 ml water was added into the mixture. Then it was filtered to obtain a red organic filtrate. The solvent was removed on a rotary evaporator giving the crude product. The crude product was dried in vacuum oven at 60 ℃ over night before it was purified with column chromatography on silica gel using 10/1 (v/v) $CHCl_3$/acetone as the eluent. Yield: 126 mg (50%).

^{1}H-NMR (300 MHz, $CDCl_3$, 298 K, TMS) δ = 8.70-8.61 (dd, 8H, J= 7.8Hz Ar**H** in perylene ring) , 5.817-5.77 (dd, 2H, J= 6.3 -C**H**-N) , 4.396-4.15 (m, 4H,–COOC**H$_2$**-), 3.72-3.68 (q, 2H, J= 4.2 Hz, -CH_2**CH_2**O-)**,** 3.61-3.51 (m, 12H, --OC**H$_2$**C**H$_2$**O-), 3.36 (s, 3H, -OC**H$_3$**), 1.76-1.74 (d, 6H, J= 6.9Hz, -C**H$_3$**) ,1.63-1.60 (m, 2H, -C**H$_2$**), 1.24-1.14 (m, 18H, –(C**H$_2$**)$_9$-), 0.87-0.83 (t, 3H, J= 6.6, -C**H$_3$**) **.**

^{13}C NMR (CDCl3, 600 MHz, 298K, TMS): δ (ppm) = 170.481 (ester **C**=O) ,

170.432 (ester **C**=O) **,** 162.772 (imide **C**=O) , 162.716 (imide **C**=O) , 134.757(Ar) **,** 134.715(Ar) **,** 131.795 (Ar) **,** 129.478(Ar) **,** 128.488(Ar), 123.334 (Ar) **,** 123.306 **(**Ar) **,** 1(Ar) **,** 123.215(Ar) **,** 123.166(Ar)**,** 72.093 (-O-**C**H_2) **,** 70.745 (-O-**C**H_2)**,** 70.731 (-O-**C**H_2)**,** 69.166 (-O-**C**H_2)**,** 65.908 (-COO-**C**H_2)**,** 64.798 (-COO-**C**H_2)**,** 59.217(-O-**C**H_3)**,** 49.773 (N-**C**H(COO)), 49.675(N-**C**H(COO)), 32.073(dodecyl **C**H_2)**,** 29.854(dodecyl **C**H_2)**,** 29.798(dodecyl **C**H_2)**,** 29.728(dodecyl **C**H_2)**,** 29.700(dodecyl **C**H_2)**,** 29.531(dodecyl **C**H_2) 29.384(dodecyl **C**H_2)**,** 28.660(dodecyl **C**H_2)**,** 26.112(dodecyl **C**H_2)**,** 22.861(dodecyl **C**H_2)**,** 14.997(-**C**H_3)**,** 14.309(-**C**H_3)**.**

FT-IR (cm^{-1}): 2923 (antisymmetric CH_2), 2852 (symmetric CH_2), 1743 (ester C=O), 1700 (symmetric imide C=O symmetric), 1659 (antisymmetric imide C=O), 1592 (aromatic ring stretch).

MS (APPI): m/z 893.3 [M + *e*].

^{1}H NMR spectrum of PDI **2-12**

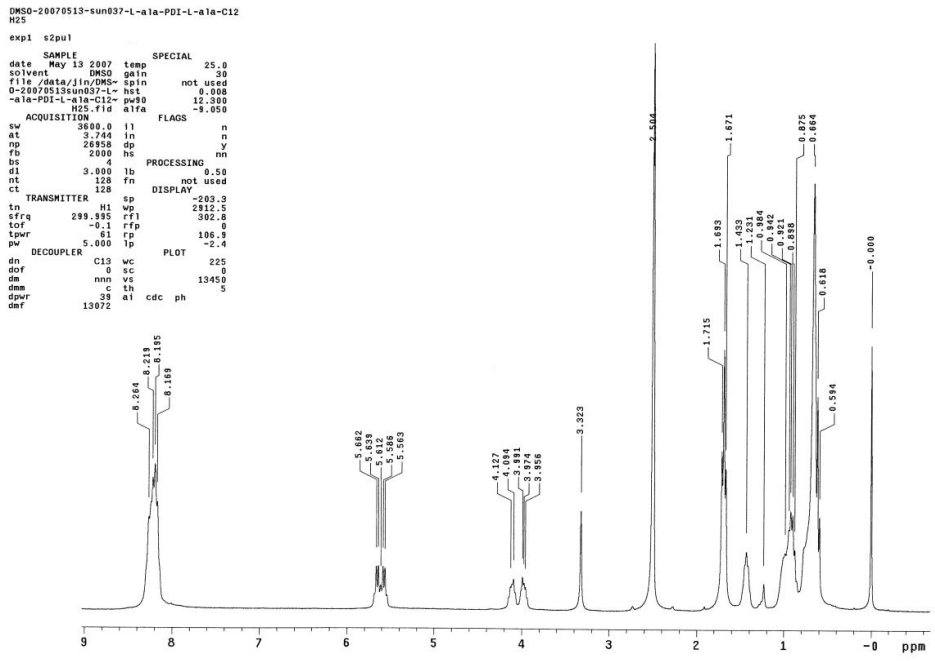

^{13}C NMR spectrum of PDI **2-12**

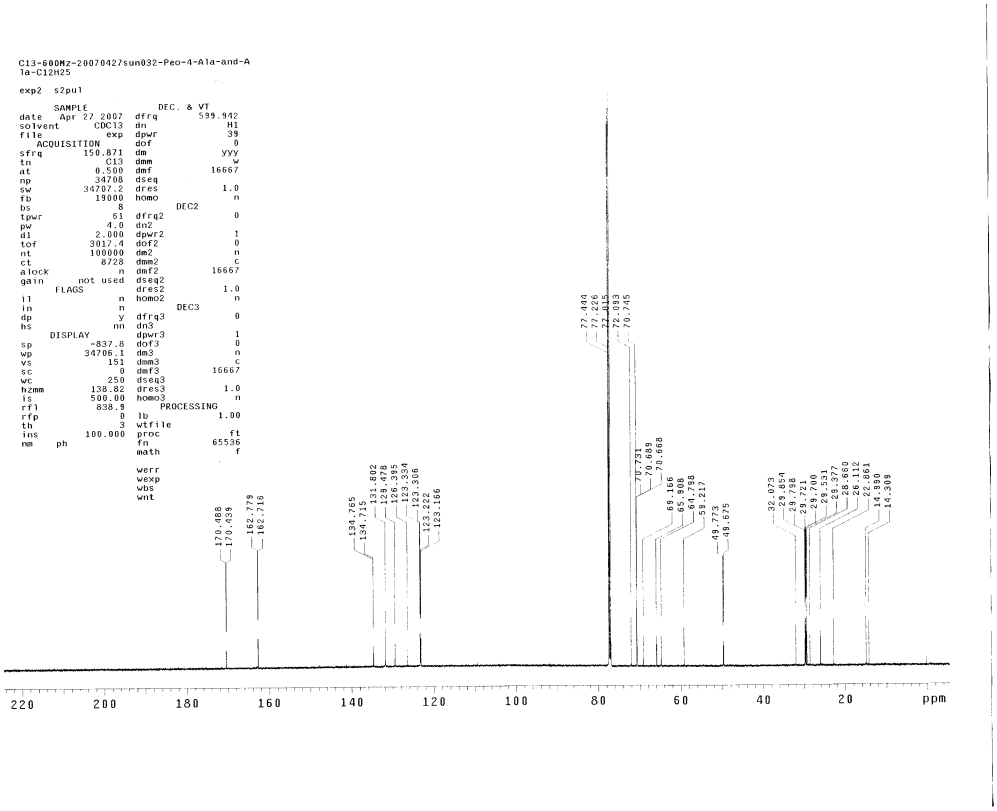

3. Synthesis of Perylene Monoimide Monoanhydride and Perylene Diester Monoanhydride

3.1. Introduction

Perylene monoimide monoanhydride (PIA) is an important intermediate for the synthesis of unsymmetric perylene tetracarboxylic diimides (PDI). The synthesis of PIA has been reported quite a few times.[1-3] Our group also developed an new method to synthesize PIAs, which is discussed in **Chapter 2**.[4] Starting from PIA 2-**3a**, a number of unsymmetric PDIs have been prepared conveniently, which also has been discussed in **Chapter 2.** However, our method also has its own limitations. First, only PIA 2-3a can be prepared with a very high yield. Second, this approach requires that at least one of the N-substitutent must be an α-substituted carboxylic acid derivatives. To overcome these limitations, our group has developed perylene di**e**ster mono**a**nhydride (PEA), a new type of versatile intermediate for the synthesis of unsymmetrically substituted perylene tetracarboxylic derivatives. The general structures of PIAs, PEAs, as well as the structure-related perylene tetracarboxylic tetraesters (PTEs) are shown in **Scheme 3-1**.

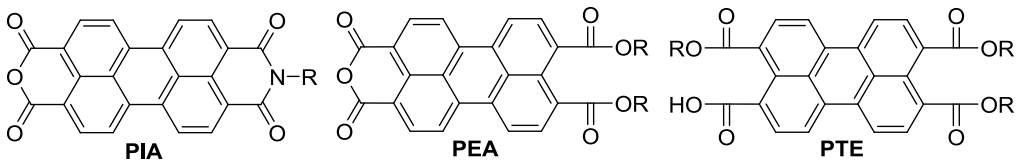

Scheme 3-1. Structure of PIA, PEA and PTE

The first PEA was prepared by an acid-catalyzed partial tandem hydrolysis -cyclization of a PTE, as shown in **Scheme 3-2**.

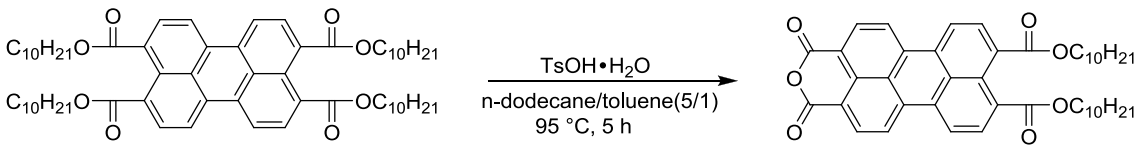

Scheme 3-2. Synthesis of PEA

From the synthesis point of view, PEA has a few distinct advantages over the corresponding PIA. First, as the two ester carbonyl groups in a PEA are not coplanar with the perylene ring, the π-stacking interaction in a PEA is considerably weaker than that of the corresponding PIA. Therefore, with the same R group, the solubility of a PEA in a common organic solvent is much higher than that of its PIA counterpart. Second, the ester carbonyl in PEA is much less reactive than an anhydride carbonyl. Therefore a highly selective condensation of the anhydride group can be performed when ester groups remain untouched. Afterwards, the two ester groups can be converted to an anhydride group which can be readily available to condense with another primary amine yielding an unsymmetrically substituted PDI. This provides a more versatile approach to unsymmetric PDIs and a potentially powerful method to prepare linear rigid rod PDI oligomers. Third, PEAs can serve as the starting materials of unsymmetrically substituted PTEs that have not been synthesized by any other methods.

As discussed in **Chapter 1.4.1**, the only currently available method by Langhals cannot be applied to prepare rigid rod PDI oligomer longer than the trimer. To this end, the application of a PEA has the potential to break this limit. A possible synthetical route would be:

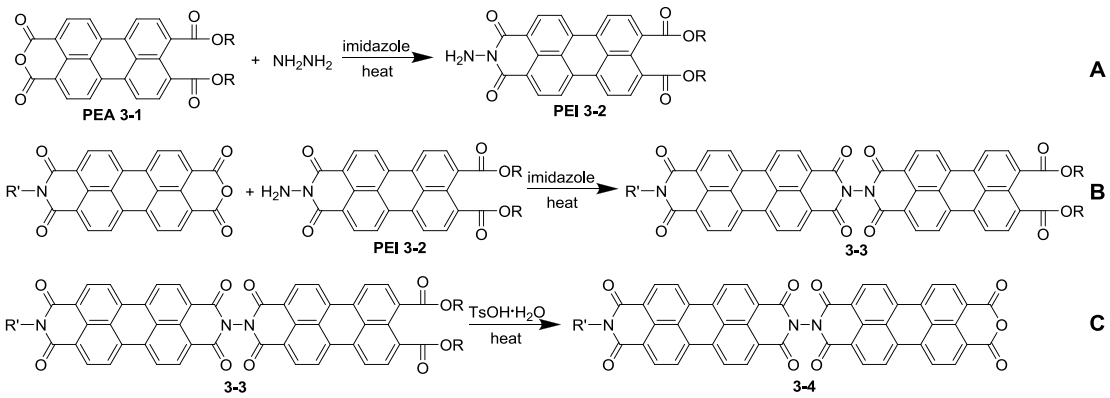

Scheme 3-3. Preparation of linear rigid-rod oligomers

A PEA will be first converted to a perylene tetracarboxylic di**e**ster mono**i**mide (PEI) **3-2**. PEI **3-2** features a primary amine group which potentially can condense with an anhydride group forming an imide linkage. At the other end of the molecule, there are two ester groups, which could be converted to an anhydride group, just like the reaction shown in **Scheme 3-3**. The diester-anhydride conversion is probably driven by the formation of the six-membered ring in the anhydride. Thus, PEI **3-2** can be a used as the key reagent in an iterative growth of a linear rigid-rod PDI oligomer.

As presented in **Scheme 3-3**, PEI **3-2** will react with a PIA and lead to the formation of perylene dimer diester **3-3** which can undergo a tandem hydrolysis -cyclization reaction forming perylene dimer monoanhydride **3-4**. Evidently, dimer C can react with PEI **3-2** again according to the procedure B shown in **Scheme 3-3**. The product of this reaction, a perylene trimer diester, can be converted to the corresponding perylene trimer monoanhydride. Every iteration of procedures B and C will increase the length of a perylene oligomer monoanhydride by one PDI unit.

Note that besides that tandem hydrolysis-cyclization shown in procedure C in **Scheme 3-3**, such a functional group conversion (diester → anhydride) can also be achieved in two steps, in the form of a basic hydrolysis followed by an acidification. Once the desired length of a perylene oligomer monoanhydride is reached, a dimerization reaction with hydrazine as the coupling agent will produce the final linear rigid-rod PDI oligomer, as shown below in **Scheme 3-4**.

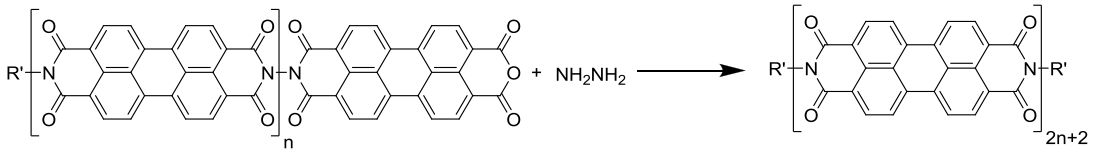

Scheme 3-4. Dimerization of a perylene oligomer monoanhydride

In order for such a preparation strategy to work well, a few conditions must be satisfied. In the procedure B in **Scheme 3-3**, PEI **3-2** is allowed to react with a PIA. For the reaction to be highly selective amine-anhydride reaction, the PIA must have a sufficiently high solubility. This is due to the fact that an ester group can also be nucleophilicly attacked by an amino group. Although it is known that typically an anhydride group is much more reactive than an ester group when it comes to a nucleophilic attack, one has to make sure that the concentration of available anhydride groups is comparable to that of ester groups. In case of procedure B, the PEI **3-2** is expected to be quite soluble in molten imidazole, therefore the concentration of available ester groups will be high and twice that of amino groups. If the PIA does not have a reasonable solubility in the reaction medium, ester groups may have a sizeable probability to react with amino groups. Thus, a PIA soluble in molten imidazole is needed for the sake of high procedure B selectivity. Of course, to make

the expected column chromatography purification feasible, perylene dimer monoanhydride **3-4** must have a sufficient solubility in a common solvent. All these require that R must have a high solubilization power, which will be explored in this chapter. In addition, the synthesis of PEAs and their applications in the preparation of perylene tetracarboxylic derivatives, especially unsymmetrically substituted ones, will also be investigated. The second requirement is that the hydrolysis-cyclization of the terminal diester groups must be fully accomplished without the cleavage of imide groups to any sizeable extent, which will be discussed in **Chapter 4**.

We have chosen PIA **3-5** as the highly soluble PIA as shown below.

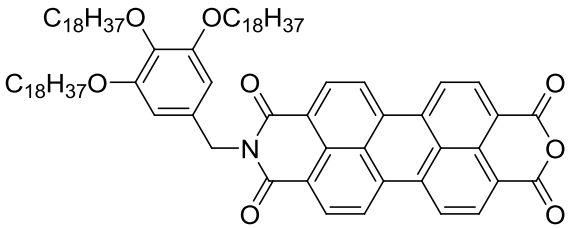

Scheme 3-5. Target PIA **3-5**

The trioctadecoxybenzyl group is expected to provide a highly solubilization power. Furthermore, a PIA with a dendritic N-substituents (shown below) may be readily derived from this N-substituent, which is likely to be even more soluble in a common organic solvent.

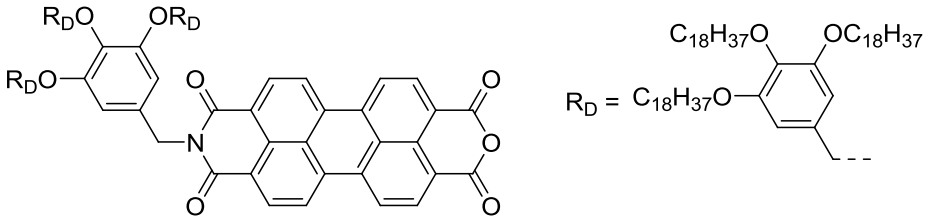

Scheme 3-6. PDI with dendrimer structure

The exploration started from the synthesis of PIA **3-5**.

3.2. Result and Discussion

3.2.1. The synthesis of PIA 3-5

The alcohol form (**3-6**) of PIA **3-5**'s N-substituent was first prepared according the procedure shown in **Scheme 3-7**.

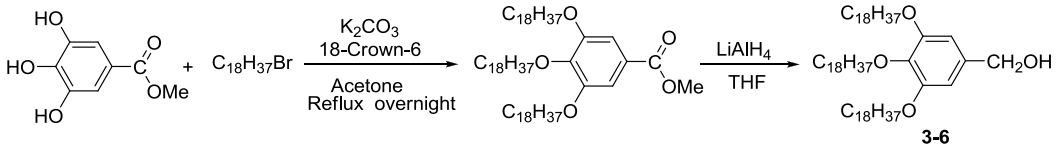

Scheme 3-7. The synthesis route of **3-6**

The first attempt to obtain PIA **3-5** was tried using direct functionalization of the acidic N-H of PIA **3-7** using Mitsunobu reaction, as depicted in **Scheme 3-8**. PIA **3-7** was prepared according to a literature procedure.[16]

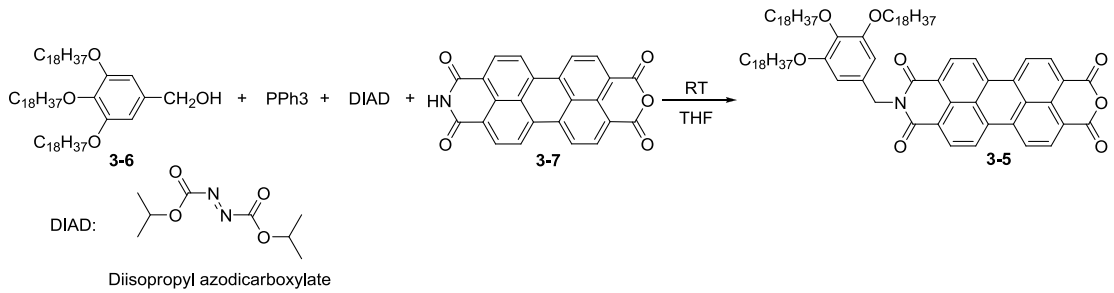

Scheme 3-8. Synthesis route of PIA **3-5**

Unfortunately, this reaction did not produce any detectable amount of desired PIA **3-5**, even after being stirred for more than three weeks. It is speculated that solubility of the PIA **3-7** in THF is too low to allow the reaction to proceed.

To solve this problem, PEI **3-8** was used to connect the solubilizing group to the perylene ring as shown in **Scheme 3-9** where the preparation of PEI **3-8** is also presented. PEI **3-8** is well-soluble in THF.

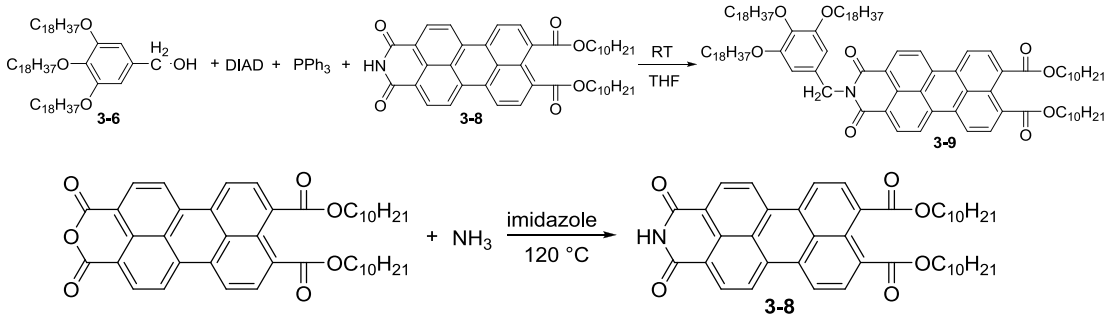

Scheme 3-9. Synthesis of PIA 3-9

Due to the much enhanced solubility of PEI **3-8** in THF, the reaction proceeds to completion after stirring at RT for 7 days. The PEI bearing the desired solubilizing group (PEI **3-9**) was obtained with an isolated yield of 85%.

The diester-anhydride conversion, which is supposedly to transform the PEI **3-9** to PIA **3-5**, were attempted a number of times, as shown in **Scheme 3-10**.

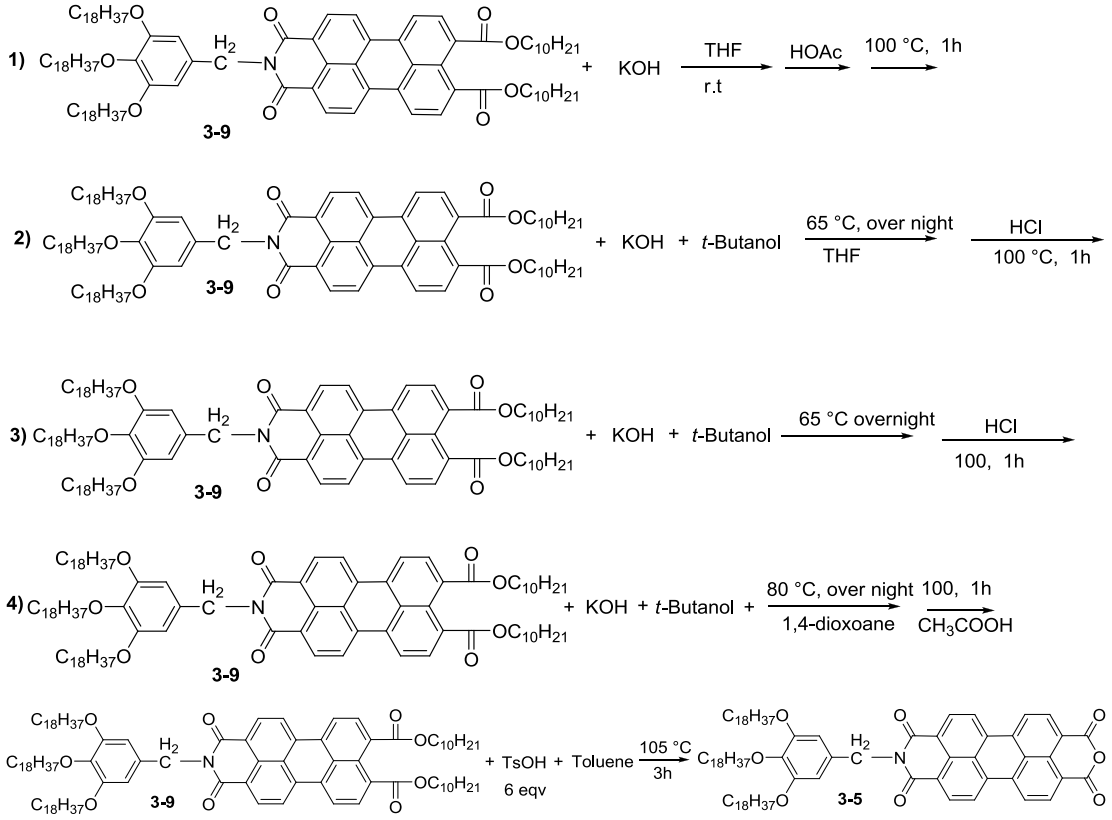

Scheme 3-10. Cyclization of PIA **3-9**

None of the reactions produced reasonable amount of PIA **3-5**. Most of them

yielded a complicated mixture that cannot be separated into collectable points/bands even on TLC. The failure of the acidic-catalyzed tandem hydrolysis-cyclization reaction can probably be attributed to the cleavage of ether linkages on the solubilizing group. Why those saponification-acidification procedures did not work is currently unknown.

3.2.2. Synthesis of PEI 3-10 and PIA 3-11

As our synthesis of PIA **3-5** was not successful, PIA **3-10** with a simple branched alky chain was proposed and synthesized with the same strategy, with the consideration that the ether linkages in PEI **3-9** are the most probably weak points. The synthesis PEI **3-10** is shown in **Scheme 3-11**. The yield was 76.2%.

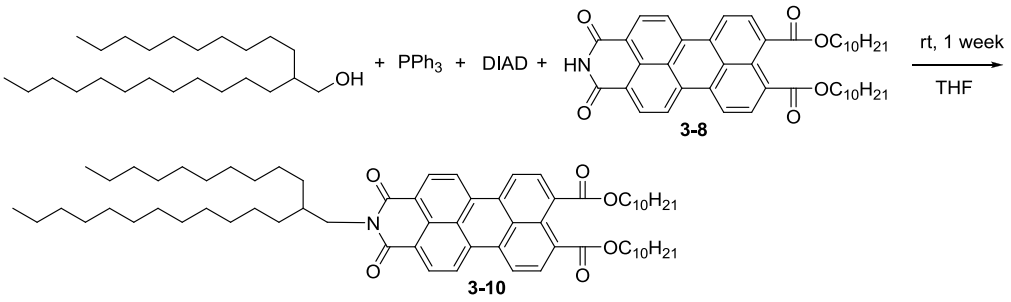

Scheme 3-11. Synthesis of PIA **3-10**

Without any ether linkages, the acid-catalyzed hydrolysis-cyclization of PEI **3-10** went smoothly. To optimize the condition of this reaction, a few different conditions were tested, which are shown in **Scheme 3-12**. With the best condition, the isolated yield was 93.6%

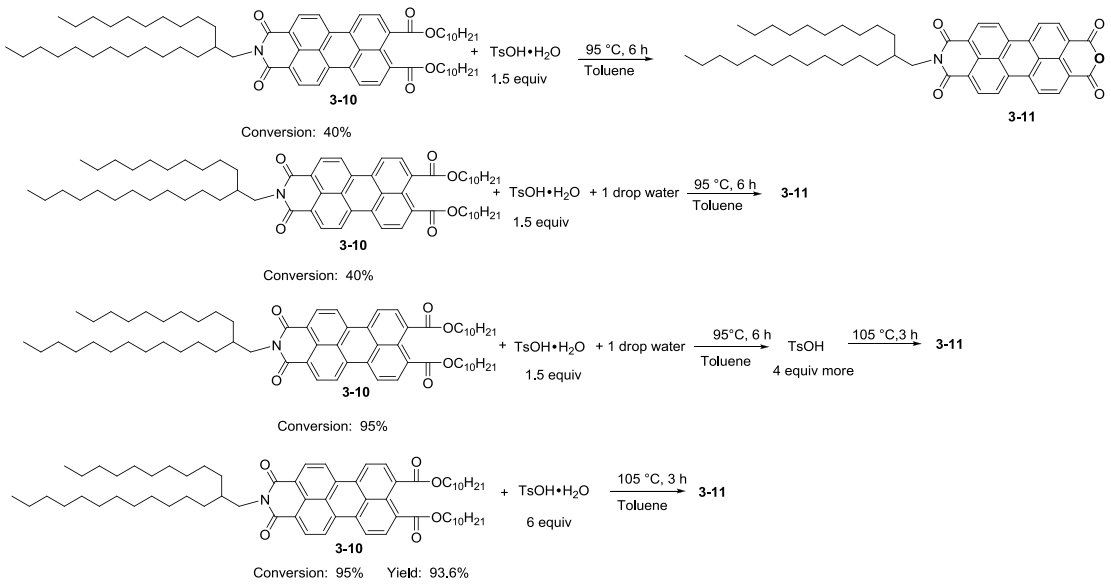

Scheme 3-12. Cyclization of PIA **3-10**

However, the solubility of PIA **3-11** in organic solvent is not good. Even in chloroform, which is among the best solvents for PDIs, the color of the saturated solution is lightly red, indicating a low solubility. This means if we would like to prepare PDI oligomers, we need to choose another solubilizing group.

3.2.3. Synthesis of PEA 3-12

The solubility of PIA **3-11** is actually much higher than that of *n*-alkyl counterparts, which demonstrates the effectiveness of using a branched alkyl chain to increase the solubility of PIAs. The problem is that the enhancement is not great enough to support the growth of PDI oligomers.

In our effort to develop PEAs, we have found that *n*-alkyl PTEs are highly soluble in most common organic solvents, except polar protic solvents such as methanol. It also came to our attention that all PEIs prepared by us exhibit good solubility. The observed strong solubilizing effect of the di-ester functionality can find its stem in the fact that the ester carbonyl groups are NOT coplanar to the

perylene ring. This makes it difficult for a PEI or PEA to form π-stacks efficiently, which increases the solubility.

If the solubilizing power of a branched alkyl chain (such as the one used in PIA **3-11**) is cooperatively combined with the strong solubilizing effect diester functionality, a highly soluble perylene tetracarboxylic monoanhydride may result and it may then be employed in the synthesis of linear rigid-rod perylene oligomers.

The structure of target PEA **3-12** is shown below.

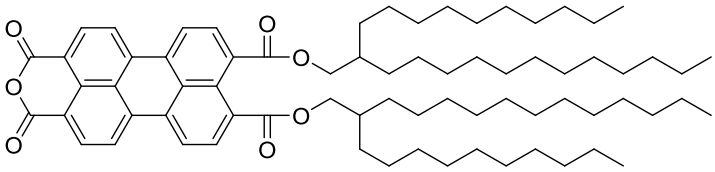

PEA 3-12

Scheme 3-13. Target molecule PIA **3-12**

3.2.3.1 Synthesis of PTE 3-13

As our group has discovered, acid-catalyzed partial tandem hydrolysis-cyclization is an efficient method to prepare PEAs. Therefore the corresponding PTE **3-13** is needed to prepare PEA **3-12**.

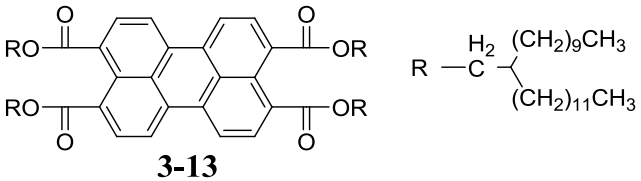

3-13

Scheme 3-14. PTE with branched chain

PTEs with simple *n*-alkyl substituents have been synthesized with nearly quantitative yield by using a phase-transfer approach. The same approach was first adopted to prepare PTE **3-13** as shown in Scheme **3-15**.

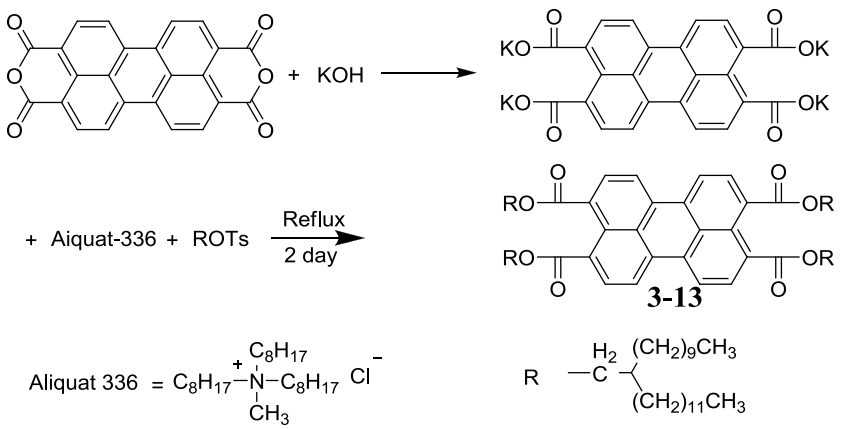

Scheme 3-15. Synthesis of PTE **3-13**

The yield was only ~30%. Likely the bulky alky chain had a substantial influence on the reactivity of the ROTs. The hydrolysis of ester/tosylate could also contribute to the low yield. Moreover, the small polarity difference between PTE **3-13** and the ROTs makes the separation really challenging.

A possible solution is to avoid the use of ROTs. This requires a different method to prepare PTE **3-13**. To this end, an ester-exchange was applied, as shown in Scheme **3-11**. It is known that under most circumstances, ester-exchange reactions are equilibrium reactions. The continuous removal of one alcohol is necessary to drive the reaction to completion. The most convenient method to continuously remove R^1OH is evaporation because the commercially available R_2OH features a very high boiling point. This calls for a R^1 group with a low-boiling-point R^1OH. By balancing the volatility and the accessibility, we chose R^1 = ethyl.

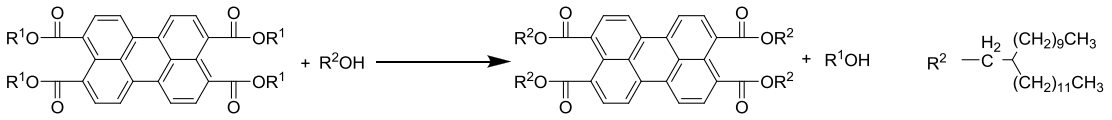

Scheme 3-16. Ester exchange reaction

Ethyl PTE was prepared via a phase transfer route with a yield of 75%. As shown below.

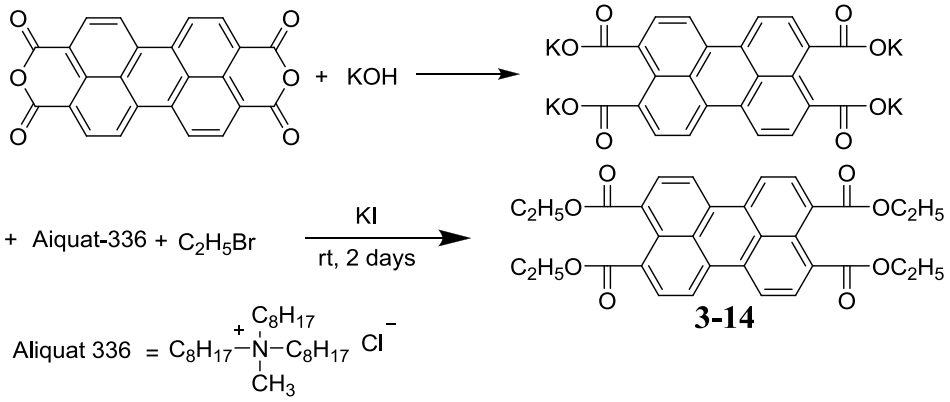

Scheme 3-17. Synthesis of PTE **3-14**

After choosing and preparing PTE **3-14**, the reaction condition of the ester-exchange should also be decided. Ester-exchange reactions are usually slow in the absence of catalysts. The presence of either an acid or a base will accelerate a reaction considerably. Here we choose a base as the catalyst. The actual catalyst is R^2OK that formed after removal of water via azeotropic distillation. Thus, the procedure is as presented in **Scheme 3-18**. Note that it is very important to keep the system as dry as possible, as the involvement of water is expected to transform an ester group to a carboxylate group which cannot react further under the given condition.

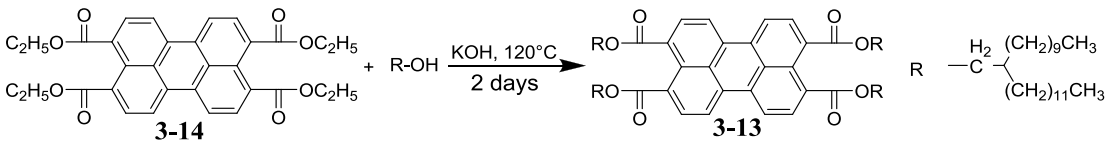

Scheme 3-18. Ester exchange reaction

The yield was 20%. Moreover, without the involvement of tosylate, the purification of PTE **3-13** here is easier than that in the first methods. With this

method, the preparation of ROTs also could be skipped.

3.2.3.2 Acid-catalyzed Hydrolysis-cyclization of PTE 3-13

The application of acid-catalyzed hydrolysis-cyclization to convert PTE **3-13** to PEA **3-12** was much more problematic than that in those *n*-alkyl counterparts. The PEA with two *n*-decyl chains was prepared at a yield of 74%. One important reason of the relative high yield is because in this case the PTE and corresponding PEA have vastly different solubility under the given reaction condition. In this way, the desired PEA will precipitate upon its formation and further hydrolysis-cyclization can be avoided (otherwise PDA will form). In case of PEA **3-12**, its solubility could be so high that it is always highly soluble in the reaction system. In this case, the further hydrolysis-cyclization of the two remaining ester groups on a PEA **3-12** molecule cannot be avoided. This was confirmed by the solubility test of PEA **3-12**. Even at room temperature, it can dissolve as much as 5 mg in 1 ml octane. At the reaction temperature that is required to promote the cyclization process, the solubility will be even higher.

Several different hydrolysis-cyclization conditions were tried, as shown below:

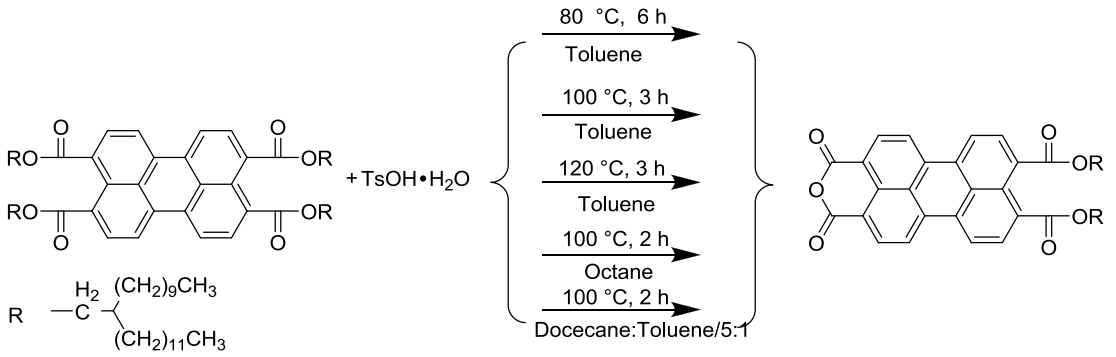

Scheme 3-19. Selective cyclization of PTE

This reaction is a stepwise reaction, and it was difficult to determine the

appropriate time to stop the reaction. If the reaction is stopped earlier than the right time, yield will be lower, as the conversion is not high enough yet. On the other hand, if the reaction was allowed to react too long, target PEA **3-12** will be converted back to PDA. As the reactant PTE **3-13** can be recycled during the purification process, to save our efforts, the reaction was stopped when PDA starts to form. Under the best condition (100 ℃, 2 h, Octane), the yield of PEA **3-12** was 30%.

If the best yield of PTE **3-13** is also taken into consideration, under the best scenarios, the yield from PDA to PEA was about 12%. It required recycling PTE **3-13**, and at least two column chromatography purifications were needed. Apparently, we need a better approach toward PEA **3-12**. It would be best if the hydrolysis-cyclization of PTE **3-13** could be avoided.

3.2.3.3 Ester-Exchange Approach toward PEA 3-12

Encouraged by the relatively good yield of the ester-exchange reaction shown in **Scheme 3-18**, we designed a related ester-exchange approach which can lead to the formation of PEA **3-12** without the problematic hydrolysis-cyclization step.

One thing makes this approach feasible the high yield preparation of PEA **3-14**, which is shown below.

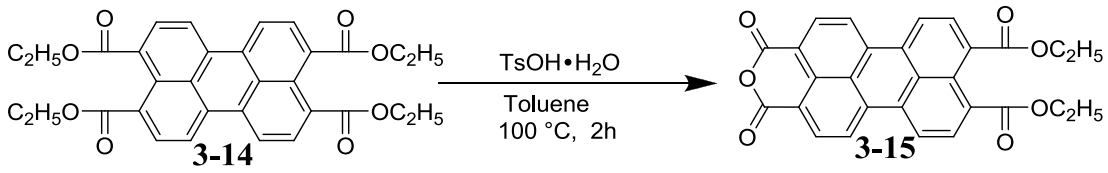

Scheme 3-20. Cyclization of PTE **3-20**

At the beginning of the reaction, the toluene solution is red and clear. During

the reaction, PEA **3-15** gradually formed and precipitated immediately. The isolated yield was 90%.

Then PEA **3-15** was subjected to a base-catalyzed ester-exchange reaction with ROH. Note that the base used here cannot be of a catalytic amount. It must be at least more than 1 molar equivalent of PEA **3-15**. The proposed mechanism is shown in **Scheme 3-21**.

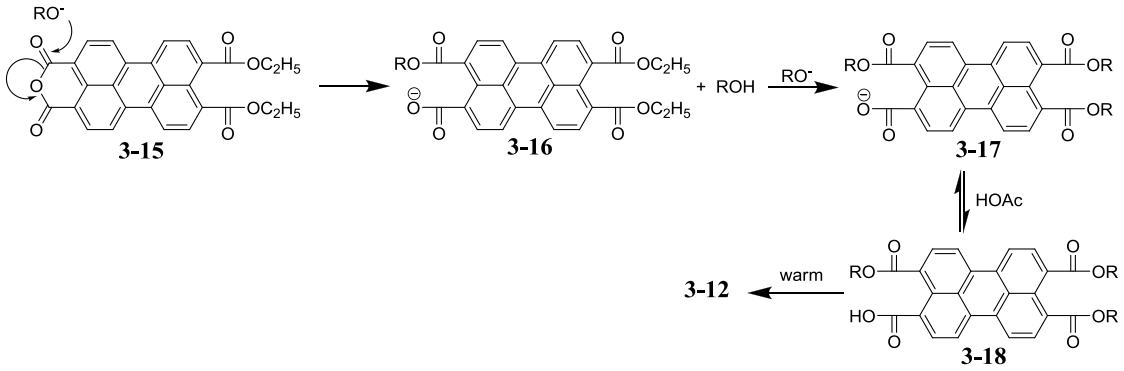

Scheme 3-21. Mechanism of ester exchange reaction

Due to the much higher reactivity, the anhydride group is first nucleophilicly attached by the RO^-, forming an ester and a carboxylate group. Due to the low reactivity of carboxylate groups, they will not participate any reactions before adding a weak acid (in our case, acetic acid). This step consumes one molar equivalent RO^-. Subsequently, the conventional ester-exchange reaction takes over and replaces the remaining two ethyl groups with the branched alkyl chains. Upon the completion of the reaction, ideally, all PEA **3-15** should be converted to PTE **3-17**. The next step is the addition of acetic acid. Since acetic acid is a weak acid, PTE **3-17** will be in equilibrium with PTE **3-18**, its acid form. However, PTE **3-18** is not stable, especially when being warmed. It undergoes an intramolecular cyclization reaction and produces PEA **3-12**. It is expected such an intramolecular reaction has a high

rate constant and high equilibrium constant, therefore all PTE **3-17** eventually will become PEA **3-12**. Note here no hydrolysis is involved, thus there is not clear need to control the reaction time to avoid the formation of PDA.

In our test, the yield of PEA **3-12** was about 20%. Just like the previous ester-exchange reaction, this reaction is also sensitive to water. The low yield may be attributed to the involvement of trace amount of water. Nevertheless, the yield of this reaction is better than the approach involving cyclization of PTE **3-13**, which was below 12%. On top of this, this procedure is less time-consuming than the cyclization approach.

It is worth noting that an unsymmetric PEA having two different ester groups was isolated (with a yield of 30%) during the process of purifying PEA **3-12**. The structure is shown below. Unsymmetric PEAs have never been reported before.

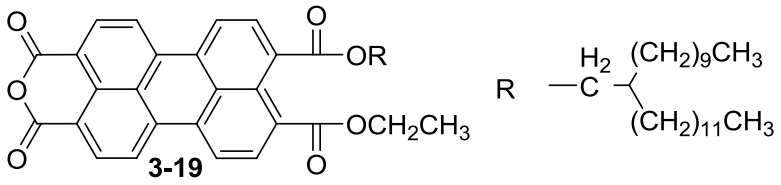

Scheme 3-22. Unsymmetric PEA **3-19**

3.3. Conclusions

To date, the synthesis of PEA and PEI has not been well developed. We did some studies on the synthesis, and developed a few new synthetic methods. At the same time, a few PEA and PEI has been obtained by us. Besides as building blocks for PDI oligomers, these compounds may have other potential applications in the

synthesis of PDI derivatives.

3.4. Experiments

3.4.1. Instruments and Characterizations

^{1}H and ^{13}C NMR spectra were recorded on a Varian 300 or 600 MHz NMR spectrometer with deuterated chloroform ($CDCl_3$), DMSO or THF as the solvent at room temperature. The chemical shifts were reported using TMS as the internal standard. Mass measurement was carried out in CUNY-Hunter MS center and Rutgers University at Newark. The IR spectra were acquired on a Bruker Vertex 70V FT-IR spectrometer at a resolution of 4 cm^{-1}. UV-Vis spectra were recorded on LAMBDA 650 UV-Vis Spectrophotometer.

3.4.2. Materials and Synthesis

All reagents and chemicals were purchased from Fisher scientific or VWR international and used as received. ALIQUAT 336 was kindly provided by Cognis Corporation.

3,4,9,10-tetra(decyloxycarbonyl)perylene (PTE**)**

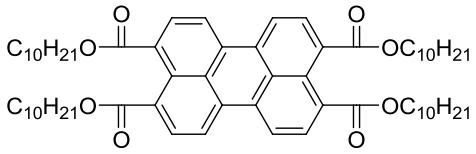

7.84 g (20 mmol) 3,4,9,10-perylenetetracarboxyldianhydride (PDA), 6.0 g (106 mmol) KOH and 100 ml deionized H_2O were added into a 200 ml beaker and stirred at 70 ℃ for 0.5 hour. The solution was filtered to a 250 ml round-bottomed flask. After pH value was adjusted to 8-9 with 1M HCl solution, 2.7 g (6 mmol) ALIQUAT 336 and 0.5 g (4 mmol) KI were added to the solution. The mixture was

stirred vigorously for 10 minutes followed by adding 35.4 g (160 mmol) decyl bromide. Then the solution was refluxed with vigorous stirring for 2 hours. Subsequently, the yellow product was extracted by $CHCl_3$. The $CHCl_3$ phase was washed with 15% NaCl aqueous solution three times. Then methanol was added to the $CHCl_3$ solution drop-wise to precipitate the yellow solid . The solid was collected by suction filtration and was dried in vacuum at 80 °C overnight. Yield (PTE) 19.3 g (97%) as a yellow solid.

Perylene-3,4-anhydride-9,10-di-(decyloxycarbonyl) (PEA **3-1)**

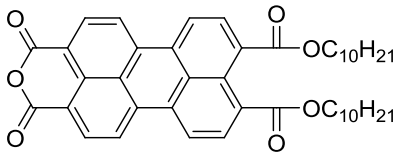

A 10 mL round-bottomed flask was charged with 1.647 g (1.67 mmol) **2**, 0.45 ml toluene and 2.25 ml *n*-dodecane before being heated to 95 ℃. After the yellow powder PTE was all dissolved, 0.316 g (1.67 mmol) *p*-toluenesulfonic acid monohydrate ($TsOH•H_2O$) was added to the solution and the solution was stirred at 95 ℃ for 5 hours. Then the dark red mixture was dissolved in 30 ml hot $CHCl_3$. This solution was purified by column chromatography with 20/1 (v/v) $CHCl_3$/acetone as the eluent. Yield PEA **3-10** 0.852 g (74%) as a dark red solid.

^{1}**H NMR (**$CDCl_3$, 600 MHz): δ (ppm) = 8.66 (d, J = 8.07 Hz, 2H, Ar), 8.55 (d, J = 8.16 Hz, 2H, Ar), 8.53 (d, J = 7.97 Hz, 2H, Ar), 8.15 (d, J = 7.92 Hz, 2H, Ar), 4.34 (t, J = 6.99 Hz, 4H, (COO)C**H$_2$**), 1.83 – 1.78 (m, 4H, (COO)CH_2C**H$_2$**), 1.47 – 1.27 (m, 28H, (COO)CH_2CH_2(C**H$_2$**)$_7$), 0.88 (t, J = 7.02 Hz, 6H, CH_2C**H$_3$**).

FT-IR (cm^{-1}): 2920 (antisymmetric CH_2), 2854 (symmetric CH_2), 1770

(anhydride C=O), 1723 (ester C=O), 1595 (aromatic ring stretch).

HRMS (M+*e*)$^-$: calcd for $C_{44}H_{50}O_7$ 690.35565; found 690.35515.

UV-Vis (in $CHCl_3$): 480, 507 nm (λ_{max}).

^{1}H NMR of PEA **3-1**

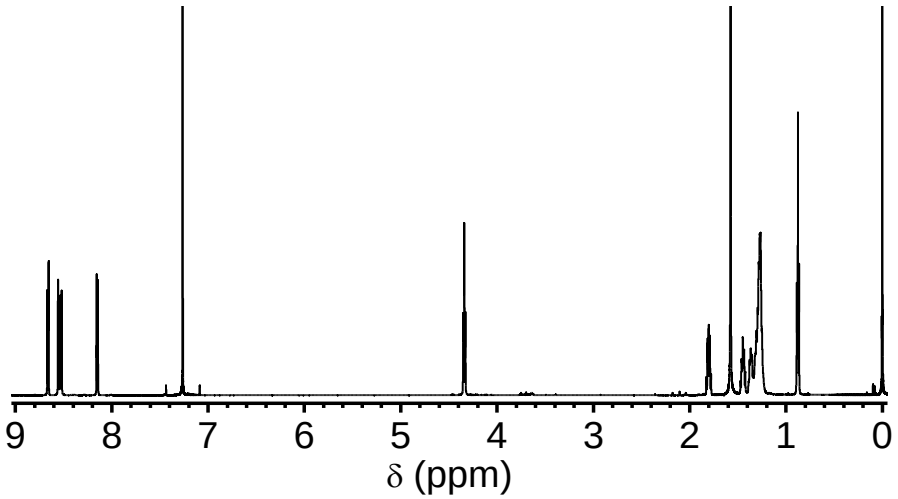

Perylene-3,4-dicarboximide-9,10-di-(decyloxycarbonyl) (PEI **3-8)**

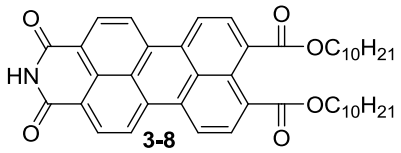

1.72 g decanoic acid and 1.46 g 28% ammonium hydroxide aqueous solution were mixed in a 20 ml vial. The vial was sealed and gently heated until a homogeneous solution formed. The solution was then cooled in refrigerator for crystallization to take place. After 12 hours, the crystals were collected by suction filtration and dried in vacuum at room temperature overnight. 0.607 g (3.24 mmol) collected crystalline solid, 0.972 g (1.41 mmol) PEA **3-1** and 8 g imidazole were charged to a 20 ml vial. The vial was purged with Argon for 5 minutes and sealed.

After that, it was heated to 120 ℃ for 1 hour. The reaction mixture was cooled to 90 ℃ and deionized water was added. The bright red solid was collected by centrifugation and dried in vacuum at 75 ℃ over night. The crude product was purified by column chromatography on silica gel using 50/3 (v/v) $CHCl_3$/acetone as the eluent to afford PEI **3-8** 0.859 g (88%) as a bright red solid.

^{1}H NMR ($CDCl_3$, 300 MHz): δ (ppm) = 8.59 (d, J = 8.13 Hz, 2H, Ar), 8.49 (s, 1H, N**H**), 8.46 (d, J = 8.13 Hz, 2H, Ar), 8.44 (d, J = 8.02 Hz, 2H, Ar), 4.34 (t, J = 6.93 Hz, 4H, $CO_2C\mathbf{H_2}$), 1.86 – 1.76 (m, 4H, $CO_2CH_2C\mathbf{H_2}$), 1.50 – 1.27 (m, 28H, $CO_2CH_2CH_2(C\mathbf{H_2})_7$), 0.87 (t, J = 6.6 Hz, 6H, $C\mathbf{H_3}$).

^{13}C NMR ($CDCl_3$, 75 MHz): δ (ppm) = 168.32 (ester **C**=O), 163.35 (imide **C**=O), 136.18 (Ar), 132.30 (Ar), 131.93 (Ar), 131.27 (Ar), 130.59 (Ar), 130.45 (Ar), 129.26 (Ar), 129.02 (Ar), 126.40 (Ar), 122.99 (Ar), 121.92 (Ar), 121.87 (Ar), 66.11 (OCH_2CH_2), 32.06 (CH_2), 29.74 (CH_2), 29.48 (CH_2), 28.75 (CH_2), 26.18 (CH_2), 22.84 (CH_2), 14.27 (CH_3).

FT-IR (cm^{-1}): 2924 (antisymmetric CH_2), 2854 (symmetric CH_2), 1720 (ester C=O), 1701 (symmetric imide C=O), 1648 (antisymmetric imide C=O), 1593 (aromatic ring stretch).

HRMS $(M+Na)^+$: calcd for $C_{44}H_{51}NNaO_6$ 712.36141; found 712.36110.

UV-Vis (in $CHCl_3$): 478, 508 nm (λ_{max}).

^{1}H NMR of PEI **3-8**

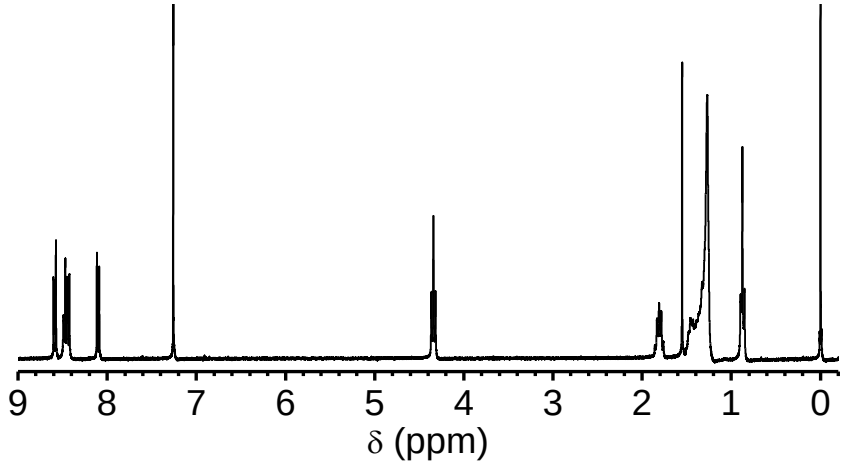

^{13}C NMR of PEI **3-8**

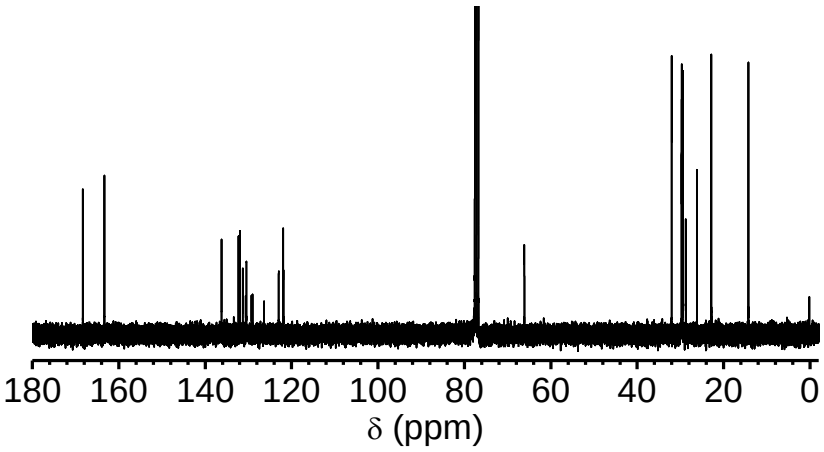

***N*-(3,4,5-trioctadecyloxylbenzyl)-perylene-3,4-dicarboximide-9,10-di-(decylo xycarbonyl) (**PEI **3-9)**

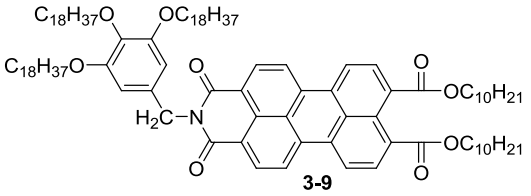

3-9

1.23 g (1.35 mmol) 3,4,5-trioctadecyloxylbenzyl alcohol (synthesized according to a literature protocol)[17] and 0.464 g PEI **3-8** (0.673 mmol) were dried in vacuum at

50 ℃ overnight before being added into a 25 ml round bottom flask together with 0.408 g (2.02 mmol) DIAD, 0.529 g (2.02 mmol) triphenylphosphine and 15 ml dry THF. The flask was sealed and the mixture was stirred at room temperature for 7 days. Then volatiles were removed on a rotary evaporator. The solid residue was purified by column chromatography on silica gel using 8/1 (v/v) petroleum ether/ethyl acetate as the eluent to afford PEI **3-9** 0.850 g (79.3%) as a red solid.

^{1}H NMR ($CDCl_3$, 600 MHz): δ (ppm) = 8.33 (d, J = 8.04 Hz, 2H, Ar), 8.17 (d, J = 8.07 Hz, 2H, Ar), 8.08 (d, J = 8.22 Hz, 2H, Ar), 8.01 (d, J = 7.92 Hz, 2H, Ar), 6.87 (s, 2H, Ar), 5.26 (s, 2H, NC**H**$_2$), 4.37 (t, J = 7.2 Hz, 4H, CO_2C**H$_2$**), 4.03 (t, J = 6.6 Hz, 4H, CH_2C**H$_2$**OAr (3,5)), 3.91 (t, J = 6.6 Hz, 2H, CH_2C**H$_2$**OAr (4)), 1.85 – 1.60 (m, 10H, OCH_2C**H$_2$**), 1.49 – 1.24 (m, 118H, C**H$_2$**), 0.87 (m, 15H, C**H$_3$**).

^{13}C NMR ($CDCl_3$, 150 MHz): δ (ppm) = 168.16 (ester **C**=O), 163.04 (imide **C**=O), 153.22 (OAr), 153.02 (OAr), 137.76 (Ar), 134.82 (Ar), 132.47 (Ar), 131.84 (Ar), 131.60 (Ar), 131.04 (Ar), 130.11 (Ar), 128.91 (Ar), 128.52 (Ar), 125.24 (Ar), 122.37 (Ar), 121.59 (Ar), 121.19 (Ar), 108.27 (Ar), 73.40 (ArO**C**H_2), 69.14 (ArO**C**H_2), 65.90 (ester O**C**H_2), 43.67 (N**C**H_2), 31.93 (**C**H_2), 30.35 (**C**H_2), 29.73 (**C**H_2), 29.68 (**C**H_2), 29.62 (**C**H_2), 29.53 (**C**H_2), 29.42 (**C**H_2), 29.38 (**C**H_2), 28.65 (**C**H_2), 26.20 (**C**H_2), 26.15 (**C**H_2), 26.12 (**C**H_2), 26.06 (**C**H_2), 22.70 (**C**H_2), 22.57 (**C**H_2), 22.08(**C**H_2), 21.95 (**C**H_2), 14.27 (**C**H_3).

FT-IR (cm^{-1}): 2955 (antisymmetric CH_3), 2918 (antisymmetric CH_2), 2870 (symmetric CH_3), 2854 (symmetric CH_2), 1724 (ester C=O), 1701 (symmetric imide C=O), 1659 (antisymmetric imide C=O), 1593 (aromatic ring stretch).

HRMS $(M+H)^+$: calcd for $C_{105}H_{166}NO_9$ 1586.25962; found 1586.25944.

UV-Vis (in $CHCl_3$): 478, 509 nm (λ_{max}).

^{1}H NMR of PEI **3-9**

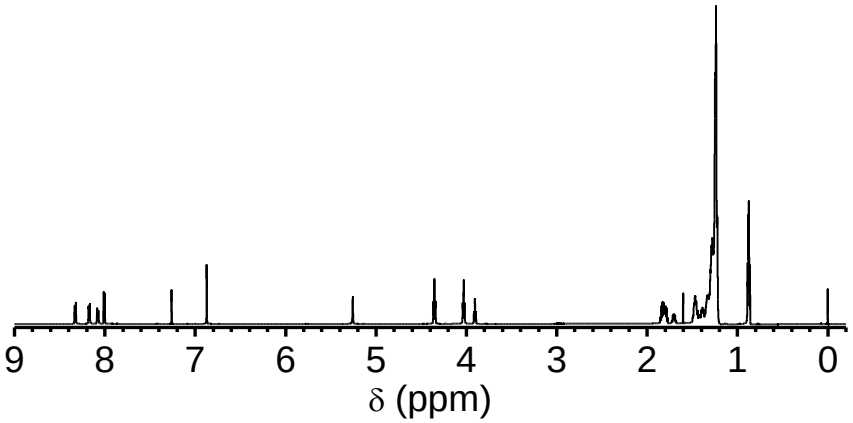

^{13}C NMR of PEI **3-9**

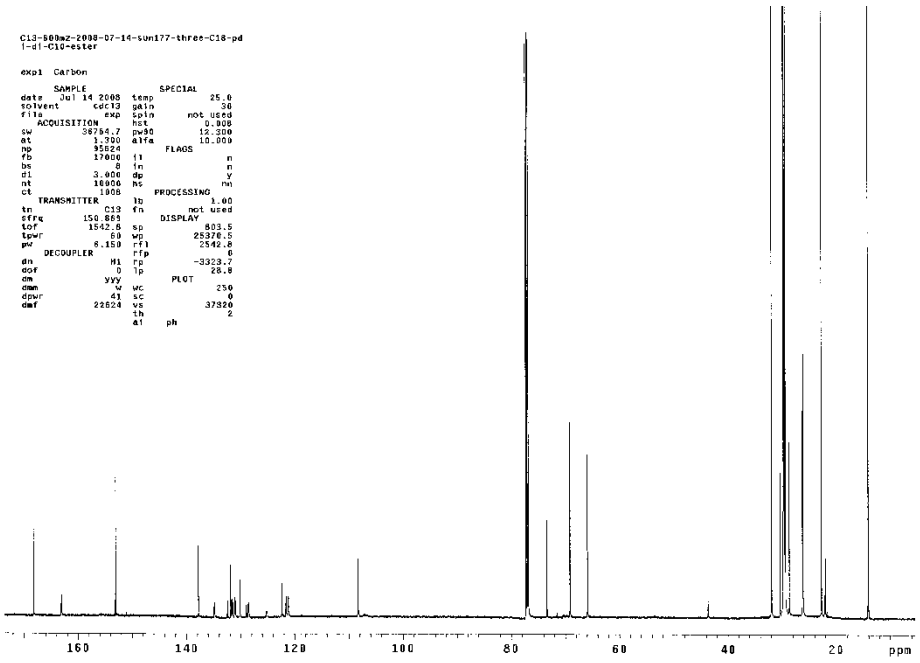

***N*-(2-decyltetradecyl)-perylene-3,4-dicarboximide-9,10-di-(decyloxycarbonyl) (**PEI **3-10)**

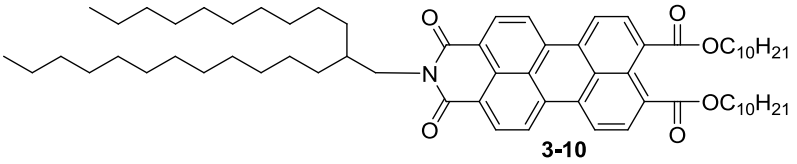

3-10

0.525 g (1.48 mmol) 2-decyltetradecan-1-ol and 0.34 g (0.49 mmol) PEI **3-8** were dried in vacuum at 50 ℃ overnight before being added into a 25 ml round bottom flask together with 0.398 g (1.97 mmol) diisopropyl azodicarboxylate (DIAD), 0.516 g (1.97 mmol) triphenylphosphine and 15 ml dry THF. The flask was sealed and the mixture was stirred at room temperature for 7 days. Then volatiles were removed on a rotary evaporator. The solid residue was purified by column chromatography on silica gel using 8/1 (v/v) petroleum ether/ethyl acetate as the eluent to afford PEI **3-10** 0.380 g (76.2 %) as an orange red solid.

^{1}**H NMR** ($CDCl_3$, 600 MHz): δ (ppm) = 8.54 (d, J = 8.04 Hz, 2H, Ar), 8.36 (d, J = 8.22 Hz, 2H, Ar), 8.35 (d, J = 8.08 Hz, 2H, Ar), 8.06 (d, J = 7.86 Hz, 2H, Ar), 4.34 (t, J = 6.0 Hz, 4H, COOC**H$_2$**), 4.13 (d, J = 7.8 Hz, 2H, NC**H$_2$**), 2.01 (m, 1H, C**H**), 1.82 – 1.78 (m, 4H, CO_2CH_2C**H$_2$**), 1.57 – 1.21 (m, 68H, C**H$_2$**), 0.87 (m, 12H, C**H$_3$**).

^{13}**C NMR** ($CDCl_3$, 150 MHz): δ (ppm) = 168.26 (ester **C**=O), 163.97 (imide **C**=O), 135.48 (Ar), 135.43 (Ar), 132.17 (Ar), 131.88 (Ar), 131.47 (Ar), 130.35 (Ar), 129.25 (Ar), 129.09 (Ar), 126.03 (Ar), 122.56 (Ar), 122.18 (Ar), 121.85 (Ar), 65.87 (O**C**H_2), 44.63 (N**C**H_2), 36.61 (**C**H), 31.90 (**C**H_2), 31.75 (**C**H_2), 30.04 (**C**H_2), 29.68 (**C**H_2), 29.64 (**C**H_2), 29.62 (**C**H_2), 29.56 (**C**H_2), 29.55 (**C**H_2), 29.34 (**C**H_2), 29.32 (**C**H_2), 29.25 (**C**H_2), 28.57 (**C**H_2), 26.55 (**C**H_2), 26.01 (**C**H_2), 22.67 (**C**H_2), 14.27

(**C**H_3).

FT-IR (cm^{-1}): 2955 (antisymmetric CH_3), 2922 (antisymmetric CH_2), 2871 (symmetric CH_3), 2853 (symmetric CH_2), 1722 (ester C=O), 1703 (symmetric imide C=O symmetric), 1657 (antisymmetric imide C=O), 1594 (aromatic ring stretch).

HRMS $(M+H)^+$: calcd for $C_{68}H_{100}NO_6$ 1026.75506; found 1026.75299.

UV-Vis (in $CHCl_3$): 476, 507 nm (λ_{max}).

^{1}H NMR of PEI **3-10**

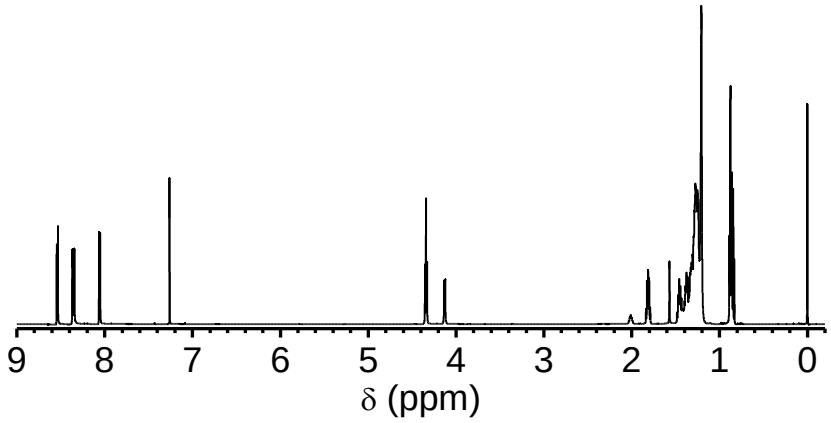

^{13}C NMR of PEI **3-10**

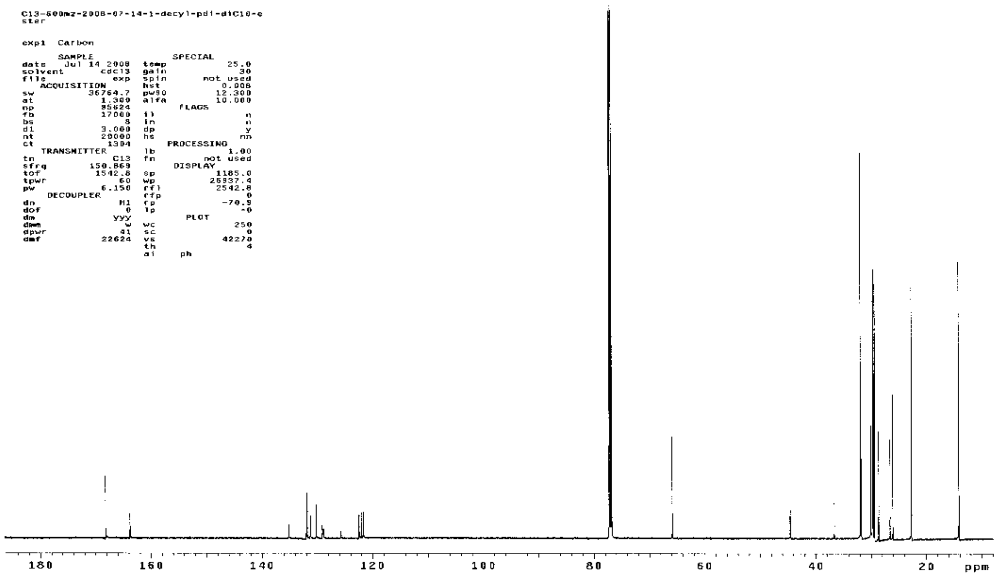

***N*-(2-decyltetradecyl)-perylene-3,4-dicarboximide-9,10-anhydride (**PEA **3-11)**

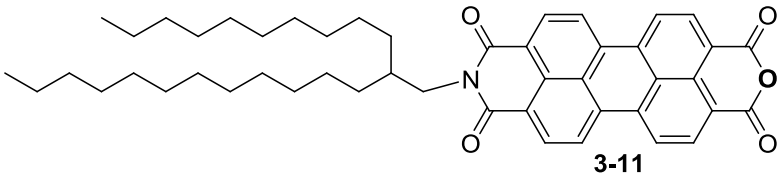

3-11

A 25 mL round bottom flask was charged with 0.185 g (0.18 mmol) PEI **3-10**, 0.205 g (1.08 mmol) TsOH•H_2O and 15 mL toluene. Then the flask was sealed and heated to 100 ℃ for 2 hours. Volatiles were removed on a rotary evaporator and the solid residue was washed twice by methanol. Afterwards, the solid residue was purified by column chromatography on silica gel using 10/1 (v/v) petroleum ether/ethyl acetate as the eluent to afford PEA **3-11** 0.120 g (93.2%) as a red solid.

^{1}H NMR ($CDCl_3$, 300 MHz): δ (ppm) = 8.68 (m, 8H, Ar), 4.13 (d, J = 7.2 Hz, 2H, NC**H_2**), 2.01 (m, 1H, C**H**), 1.52 – 1.19 (m, 40H, C**H_2**), 0.85 (m, 6H, C**H_3**).

FT-IR (cm^{-1}): 2954 (antisymmetric CH_3), 2918 (antisymmetric CH_2), 2871 (symmetric CH_3), 2850 (symmetric CH_2), 1763 (symmetric anhydride C=O), 1722 (antisymmetric anhydride C=O), 1693 (symmetric imide C=O), 1654 (antisymmetric imide C=O), 1594 (aromatic ring stretch).

HRMS $(M+e)^-$: calcd for $C_{48}H_{57}NO_5$ 727.42367; found 727.42390.

UV-Vis (in $CHCl_3$): 486, 523 nm (λ_{max}).

^{1}H NMR of PEA **3-11**

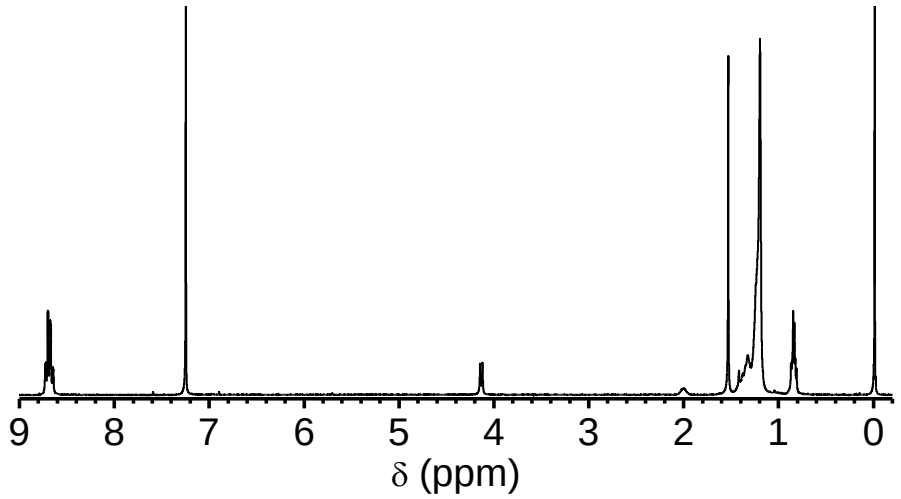

3,4,9,10-tetra(2-decyltetradecyloxycarbonyl)perylene (PTE **3-13)**

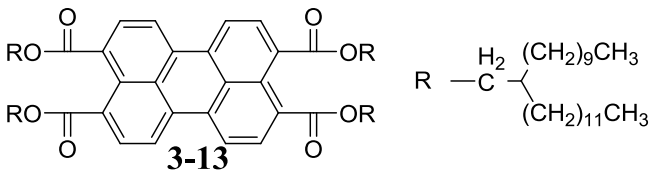

3-13

To prepare PTE **3-13**, two different methods were applied.

Firstly, a synthesis method is shown in **Scheme 3-15**. 0.784 g (2 mmol) 3,4,9,10-perylene tetracarboxyl dianhydride (PDA), 0.56 g (10 mmol) KOH and 30 ml deionized H_2O were added into a 100 ml round-bottomed flask and stirred at 70 °C for 2 hour. The solution was filtered to a 100 ml round-bottomed flask. After pH value was adjusted to 8-9 with 1M HCl solution, 0.808 g (2 mmol) ALIQUAT 336 and 0.03 g (0.2 mmol) KI were added to the solution. The mixture was stirred vigorously for 10 minutes followed by adding 8 g (16 mmol) ROTs. Then the solution was refluxed with vigorous stirring for 2 days. Subsequently, the green product was extracted by $CHCl_3$. The $CHCl_3$ phase was washed with 15% NaCl

aqueous solution three times. $CHCl_3$ was removed by rotary evaporator. The left liquid was dried in vacuum at 50 °C overnight. Yield (PTE **3-13**) 1.62 g (40%) as a green liquid.

Secondly, another synthesis method is shown as **Scheme 3-18**. 3.54 g (10 mmol) 2-decyltetradecan-1-ol, 0.112 g (2 mmol) KOH, 50 ml toluene were charged into a 100 ml flask and refluxed for 2 hours. The produced water was removed by water separator. Then 0.54 g (1 mmol) PTE **3-14** was added into the system. The mixture was refluxed with vigorous stirring for 2 days. Subsequently, toluene was removed by rotary evaporator. The green product was extracted by $CHCl_3$. The $CHCl_3$ phase was washed with 15% NaCl aqueous solution three times. $CHCl_3$ was removed by rotary evaporator. The left liquid was dried in vacuum at 50 °C overnight. Yield (PTE **3-13**) 0.41 g (20%) as a green liquid.

FT-IR (cm^{-1}): 2956 (antisymmetric CH_3), 2924 (antisymmetric CH_2), 2871 (symmetric CH_3), 2854 (symmetric CH_2), 1718 (ester C=O), 1592 (aromatic ring stretch).

HRMS (M+ benzopyrene)$^-$: calcd for $C_{140}H_{216}NO_8$ 2026.6051; found 2026.6524.

HRMS (MALDI) with benzopyrene as matrix.

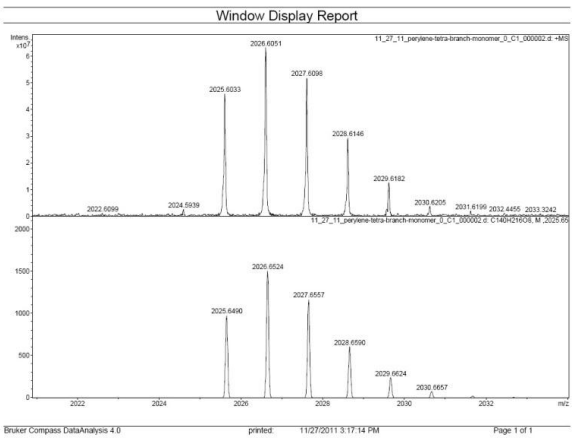

3,4,9,10-tetra(ethyloxycarbonyl)perylene (PTE **3-14)**

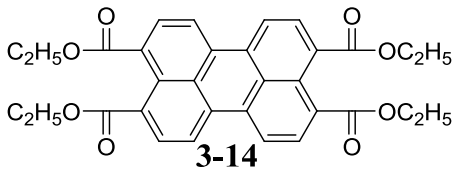

3-14

0.784 g (2 mmol) 3,4,9,10-perylenetetracarboxyldianhydride (PDA), 0.527 g (2 mmol) KOH and 50 ml deionized H_2O were added into a 100 ml beaker and stirred at 70 °C for 3 hour. The solution was filtered to a 100 ml round-bottomed flask. 0.808 g (2 mmol) ALIQUAT 336 and 0.032 g (0.2 mmol) KI were added to the solution. The mixture was stirred vigorously for 10 minutes followed by adding 4.36 g (40 mmol) ethyl bromide. After all reagents were added, the bottle was sealed to prevent the losing of ethyl bromide (b.p. 38.4 °C). Then the solution was vigorously stirred for 3 days at room temperature. Subsequently, the yellow product was collected with vacuum filtration, and washed 3 times with deionized H_2O. The crude product was dried in vacuum at 50 °C over night. Dried crude product was dissolved in 15 ml $CHCl_3$. Then methanol was added to the $CHCl_3$ solution drop-wise to precipitate the yellow solid. The solid was collected by suction filtration and was dried in vacuum at 80 °C overnight. Yield (PTE **3-14**) 0.756 g (70%) as a yellow solid.

FT-IR (cm^{-1}): 2981 (antisymmetric CH_3), 2932 (antisymmetric CH_2), 2906 (symmetric CH_3), 2868 (symmetric CH_2), 1710 (ester C=O), 1590 (aromatic ring stretch).

Perylene-3,4-anhydride-9,10-di-(ethyloxycarbonyl) (PEA **3-15)**

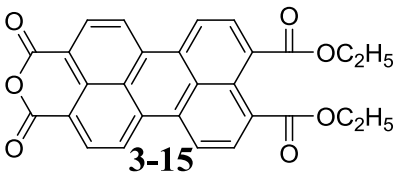

3-15

A 25 mL round-bottomed flask was charged with 0.54 g (1 mmol) PTE **3-14** and 15 ml toluene before being heated to 100 ℃. After the yellow powder PTE **3-14** was all dissolved, 0.19 g (1 mmol) *p*-toluenesulfonic acid monohydrate ($TsOH•H_2O$) was added to the solution and the solution was stirred at 100 ℃ for 2 hours. Then the mixture was cooled down to room temperature. The solid was collected by suction filtration, washed with 40 ml H_2O. This crude product was put in a vial with 20 ml toluene and heated to 100 ℃ for 0.5 hour. Then the mixture was cooled down to room temperature. With a vacuum filtration, purified product was obtained. This purification procedure was repeated 2 more time before the toluene solution's color became very light. Then, the purified product was dried in vacuum at 80 ℃ overnight. Yield PEA **3-15** 0.44 g (90%) as an orange red solid.

FT-IR (cm^{-1}): 2977 (antisymmetric CH_3), 2930 (antisymmetric CH_2), 2900 (symmetric CH_3), 2853 (symmetric CH_2), 1766 (symmetric anhydride C=O), 1728 (antisymmetric anhydride C=O), 1710 (ester C=O), 1590 (aromatic ring stretch).

Perylene-3,4-anhydride-9,10-di-(2-decyltetradecyloxycarbonyl) (PEA **3-12)**

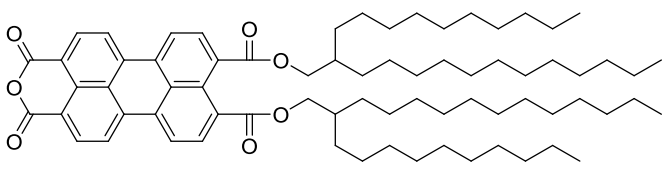

PEA 3-12

Two methods were applied in the synthesis of PEA **3-12**.

Firstly, a synthesis method is shown in **Scheme 3-19**. 50 mL round-bottomed flask was charged with 1.774 g (1 mmol) PTE **3-13**, 0.19 g (1 mmol) *p*-toluenesulfonic acid monohydrate ($TsOH•H_2O$) and 10 ml *n*-octane. Then the mixture was heated to 100 ℃ for 2 hours. Then *n*-octane was removed by rotary evaporator. The left red residue was dissolved in 5 ml $CHCl_3$. This solution was purified by column chromatography with 50/1 (v/v) $CHCl_3$/acetone as the eluent. Yield PEA **3-12** 0.324 g (30%) as a red solid.

Secondly, another synthesis method is shown in **Scheme 3-21**. 3.54 g (10 mmol) 2-decyltetradecan-1-ol, 0.112 g (2 mmol) KOH, 50 ml toluene were charged into a 100 ml flask and refluxed for 2 hours. The produced water was removed by water separator. Then 0.47 g (1 mmol) PEA **3-15** was added into the system. The mixture was refluxed with vigorous stirring for 2 days. Subsequently, toluene was removed by rotary evaporator. The reaction mixture was acidified with acetic acid and heated. The red product was extracted by $CHCl_3$. The $CHCl_3$ phase was washed with 15% NaCl aqueous solution three times. $CHCl_3$ was removed by rotary evaporator. This left residue was purified by column chromatography with 50/1 (v/v) $CHCl_3$/acetone as the eluent. Yield PEA **3-12** 0.216 g (20%) as a red solid.

^{1}H NMR ($CDCl_3$, 600 MHz): δ (ppm) = 8.62 (d, J= 7.98 Hz, 2H, Ar), 8.48 (t, 4H, Ar), 8.10 (d, J= 7.98 Hz, 2H, Ar), 4.26 (d, J= 6 Hz, 4H, -OC**H_2**CH), 1.83 (m, 2H, C**H**), 1.46 – 1.19 (m, 80 H, C**H_2**), 0.85 (m, 12 H, C**H_3**).

FT-IR (cm^{-1}): 2925 (antisymmetric CH_2), 2854 (symmetric CH_2), 1766

(symmetric anhydride C=O), 1728 (antisymmetric anhydride C=O), 1710 (ester C=O), 1590 (aromatic ring stretch).

HRMS $(M+e)^-$: calcd for $C_{72}H_{106}NO_7$ 1083.7967; found 1083.7886. (MALDI) with benzopyrene as matrix.

^{1}H NMR of PEA **3-12**

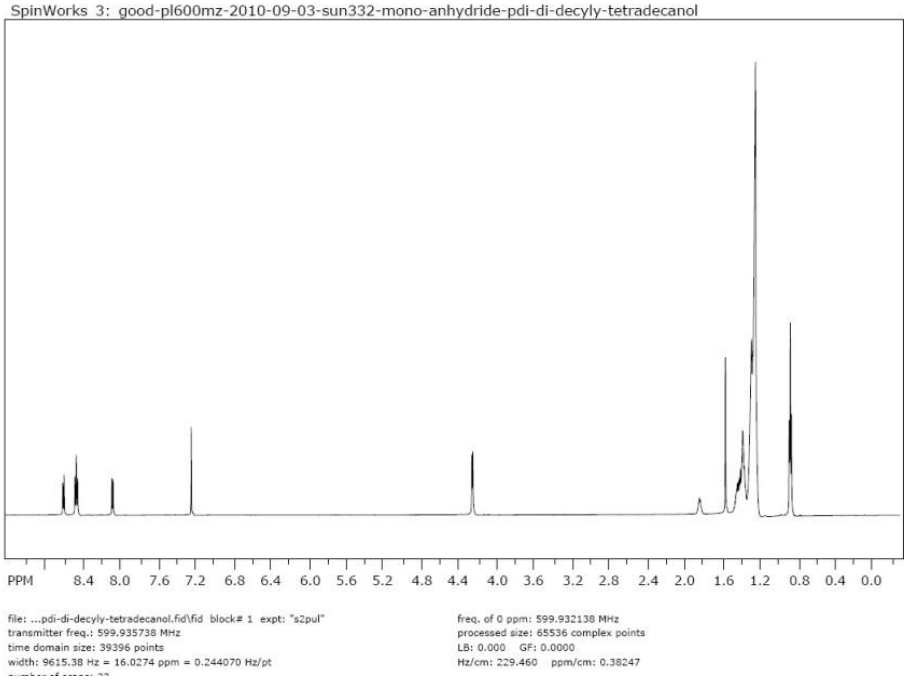

HRMS (MALDI) with benzopyrene as matrix

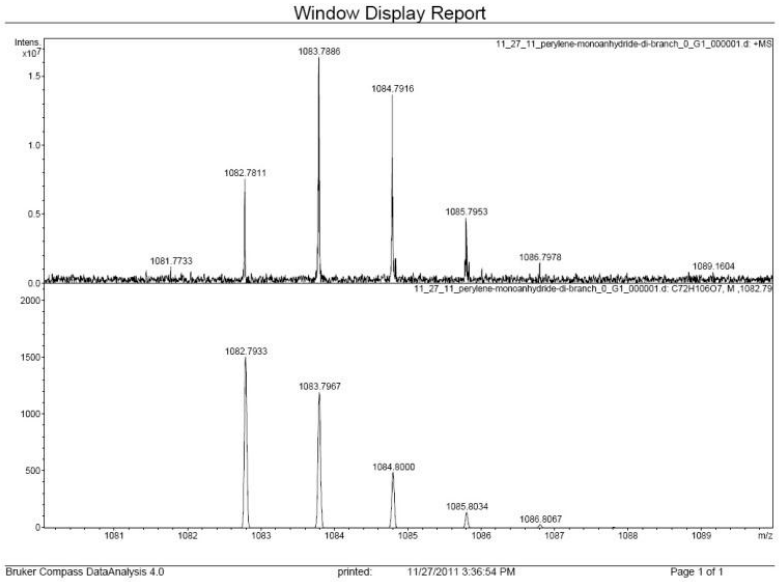

Perylene-3,4-anhydride-9-(ethyloxylcarbonyl)-10-(2-decyltetradecyloxycarbonyl) (PEA **3-19)**

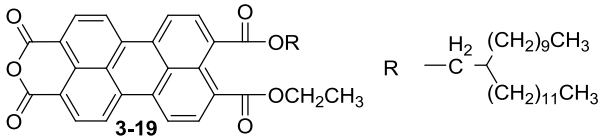

3-19

PEA **3-19** is an intermediate of reaction shown in **Scheme 3-21**. With this method, (detailed procedure was addressed in the synthesis of PEA **3-12**), PEA **3-19** was obtained with a yield of 30%.

^{1}H NMR ($CDCl_3$, 600 MHz): δ (ppm) = 8.55 (m, 2H, Ar), 8.40 (m, 4H, Ar), 8.06 (m, 2H, Ar), 4.43 (q, 2H, -OC**H$_2$**CH_3), 4.26 (d, 2H, -OC**H$_2$**CH), 1.82 (m, 1H, C**H**), 1.52 – 1.19 (m, 43H, C**H$_2$**, -OCH2**CH$_3$**), 0.85 (m, 6H, C**H$_3$**).

^{13}C NMR ($CDCl_3$, 150 MHz): δ (ppm) = 168.1 (ester **C**=O), 167.9 (ester **C**=O) 160.2 (anhydride **C**=O), 137.1 (Ar), 133.45 (Ar), 132.71 (Ar), 131.72 (Ar), 131.3 (Ar), 130.32 (Ar), 129.08 (Ar), 126.15 (Ar), 123.35 (Ar), 121.96 (Ar), 117.88 (Ar), 68.7 (O**C**H_2), 61.8 (O**C**H_2), 37.31 (**C**H), 31.93 (**C**H_2), 31.30 (**C**H_2), 29.98 (**C**H_2), 29.64 (**C**H_2), 29.62 (**C**H_2), 29.31 (**C**H_2), 26.69 (**C**H_2), 22.70 (**C**H_2), 14.13 (**C**H_3).

FT-IR (cm^{-1}): 2957 (antisymmetric CH_3), 2924 (antisymmetric CH_2), 2872 (symmetric CH_3), 2854 (symmetric CH_2), 1766 (symmetric anhydride C=O), 1729 (antisymmetric anhydride C=O), 1710 (ester C=O), 1592 (aromatic ring stretch).

HRMS (M+ 2 benzopyrene)$^-$: calcd for $C_{90}H_{86}NO_7$ 1278.6387; found 1278.6496.

^{1}H NMR of PEA **3-19**

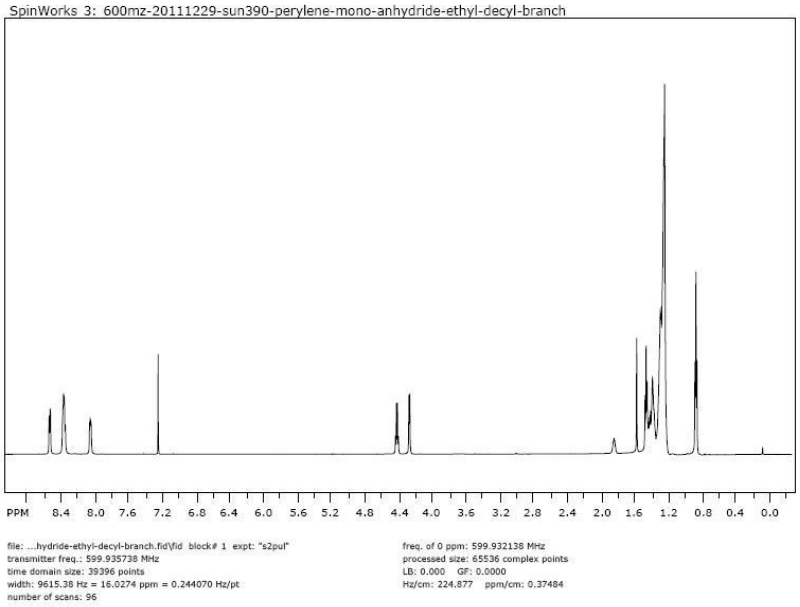

^{13}C NMR of PEA **3-19**

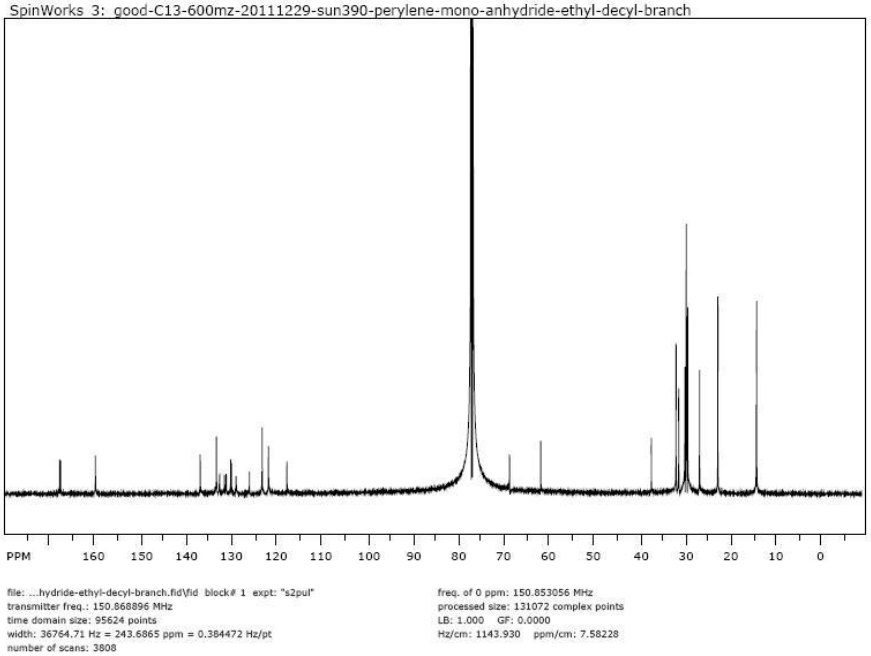

HRMS (MALDI) of PEA **3-19** with benzopyrene as matrix

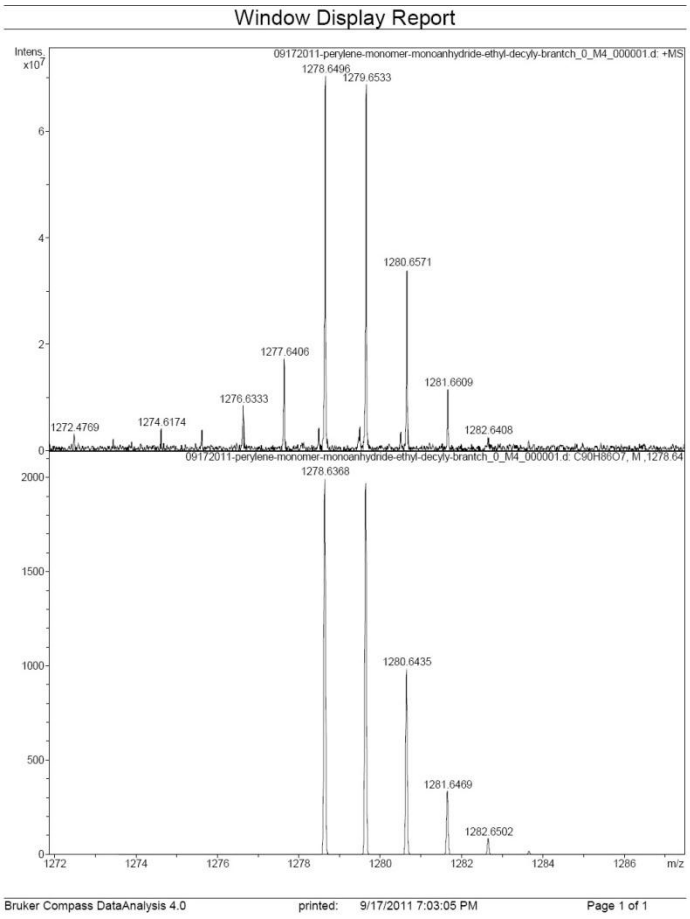

4. Design and Synthesis of Perylene Oligomers

4.1. Introduction and Design

PDI oligomers which were constructed by directly connecting PDI monomeric units with N-N bonds were shown in **Scheme 4-1**.

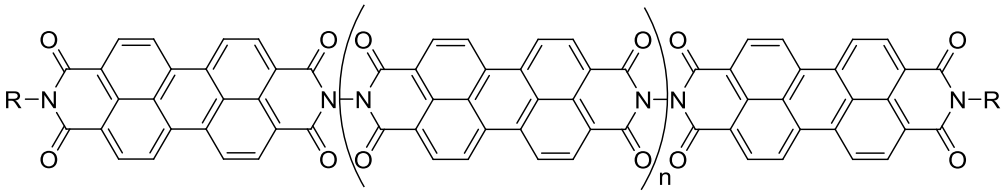

Scheme 4-1. PDI oligomer

Comparing to regular PDI derivatives, this kind of PDI oligomers have some unique properties, such as extraordinary absorbance ability and great charge transfer capability, which could have potential applications in semi-conductor fields and photovoltaic field.[1, 2]

To date, the first and only practical strategy to prepare PDI trimer was reported by Langhals and coworkers in 1998.[1] The synthesis route is shown in **Scheme 4-2**. In 2009, several PDI trimers were synthesized with the same strategy by Wasielewski's group.[2] These two articles are the only available and related literatures to date.

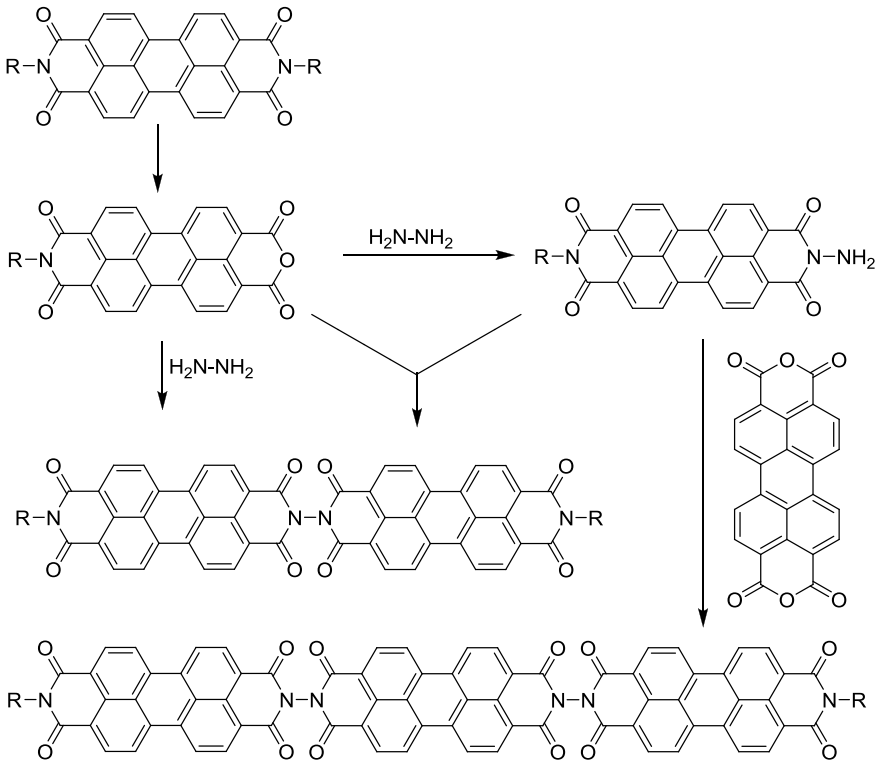

Scheme 4-2. Synthesis of PDI oligomer

There are two major issues involved in the synthesis of PDI oligomers. The first issue is the low solubility issue of PDIs, which is mainly caused by the strong **π-π** interaction between adjacent PDI molecules. This issue becomes more challenging in the synthesis of PDI oligomers, as PDI oligomers having more PDI units in one molecule.

To solve this problem, two strategies have been developed. The first strategy is to introduce bulky alky group to the bay-area of perylene core, as shown in **Scheme 1-15**.[3] This strategy was used by Wasielewski's group to prepare PDI oligomers.[2] With this strategy, the solubility of PDIs got substantial improvement. However, this improvement mainly builds on the decrease of **π-π** interaction between perylene molecules, which may lead worse performance of PDIs as charge transfer and photovoltaic materials. As our target is to obtain PDI oligomers with good solubility

and π-π interaction, this strategy can't fulfill our requirement.

The second strategy is to introduce bulky branched alky groups or swallowtails to the terminal nitrogen atoms, as shown in **Scheme 1-18**.[1] This strategy was used by Langhals' group to prepare PDI oligomers.[1] This strategy could supply the required good solubility and have less interruptions on the PDI units. It was chosen in our design for the synthesis of PDI oligomers.

Besides the solubility issue, the other issue is the preparation of key intermediate of PDI oligomers, perylene monoimide monoanhydride (PIA), which is shown in **Scheme 4-3**.

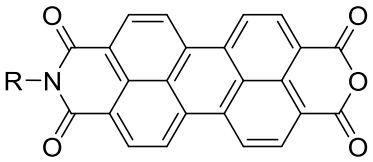

Scheme 4-3. Structure of PIA

With Langhals' strategy**,** shown in **Scheme 4-2**, saponification of PDI is the key step to prepare the PIA, which is shown in **Scheme 4-4**.

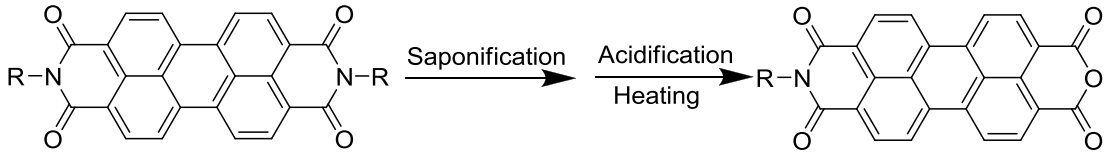

Scheme 4-4. Saponification of PDI

This strategy worked well on the synthesis of PIA. However, the saponification of PDI dimer was not successful, as shown in **Scheme 4-5**.

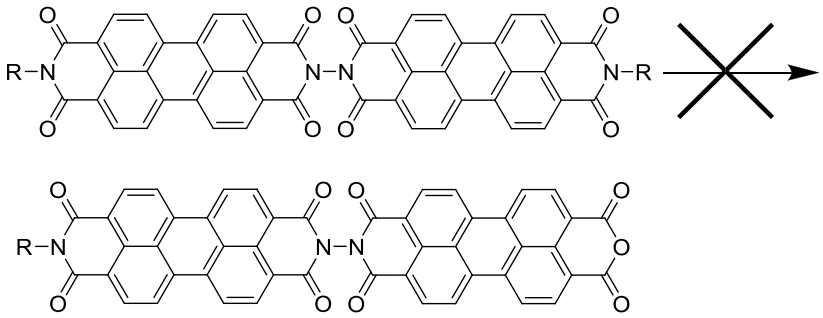

Scheme 4-5. Saponification of PDI dimer

With a thorough investigation of this reaction, we found that the reason for this failure of saponification reaction may lie in the different stabilities of internal imide bonds and terminal imide bonds, as shown in **Figure 4-1**.

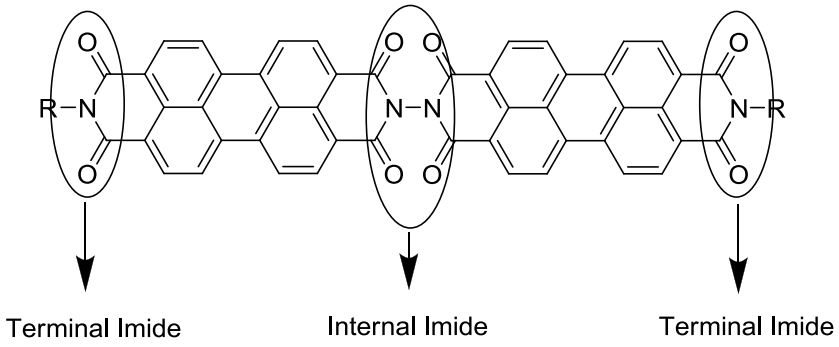

Figure 4-1. Terminal imide and internal imide of PDI dimer

In the IR spectrum of PDI dimer reported by Langhals' group, the signal peaks of terminal imide appear at 1660 cm^{-1} and 1698 cm^{-1}, which are similarly as those from terminal imide of PDI derivatives. At the same time, the signal peaks of internal imide appear at 1717 cm^{-1} and 1735 cm^{-1}, which are higher than those of imide of monomeric PDI derivatives. Generally, for carbonyl groups, higher frequency represents greater double-bond character and higher reactivity toward nucleophilic addition. Therefore, internal imides are more reactive and less stable than terminal imides.

In the saponification reaction of PDI dimer, the internal imide bonds are more

reactive toward nucleophilic attack that the terminal imide bonds. Once the internal imides are broken, the product turns out to be a monomeric PDI and a monomeric PIA instead of a PIA dimer. Due to this reason, PDI trimer is the up limit of Langhals' strategy.[1]

As PDI oligomers have potential applications in photovoltaic field, which were addressed in **Chapter 1.4.2**, efficient methods to prepare them need to be studied.

4.2. Results and Discussions

4.2.1. Preparation of PEI Dimer with *p*-Phenylenediamine

As discussed in the **Chapter 4.1**, the adjacent internal imides are less stable than terminal imides. To prevent this situation, *p*-phenylenediamine instead of hydrazine was chosen as the bridge for PEI dimer. The synthesis of PEI dimer **4-2** is shown in **Scheme 4-6**.

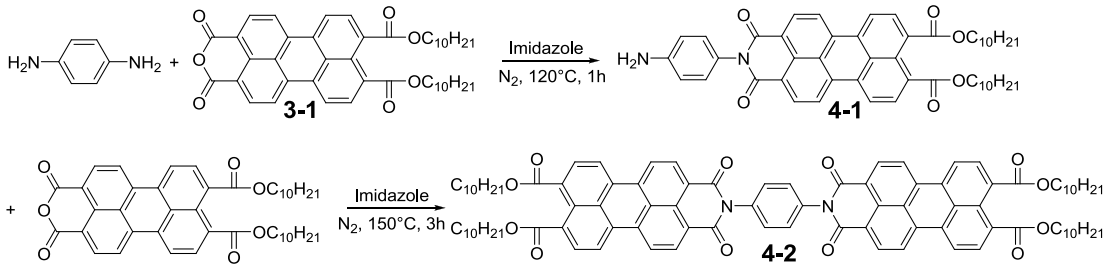

Scheme 4-6. Synthesis of PEI dimer **4-2**

The PEI **4-1** was obtained with a yield of 60%. The preparation of PEI dimer **4-2** gave a yield of 90%.

With direct condensation method, PEI dimer **4-2** could be obtained in one step reaction, which is shown in **Scheme 4-7**. The yield of this reaction turned out as 80%.

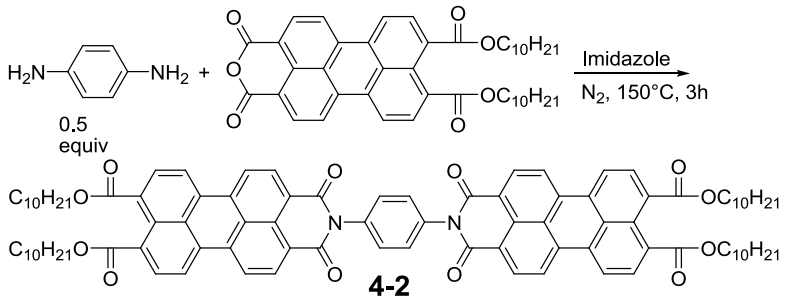

Scheme 4-7. Synthesis of PEI dimer **4-2**

The FT-IR spectrum of PEI dimer **4-2** is shown in **Figure 4-2**.

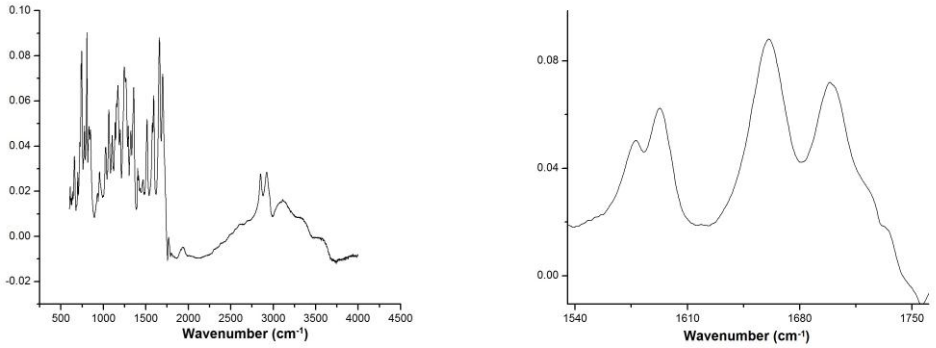

Figure 4-2. IR spectrum of PEI dimer **4-2**

In the IR spectrum, imide peaks of PEI dimer **4-2** appear at 1660 cm^{-1} and 1700 cm^{-1}. C=O of esters' peak appears at 1725 cm^{-1}. Based on our analysis in **Chapter 4-1**, C=O of esters could be less stable and more reactive than the C=O of imide bond. Therefore, a synthesis route was proposed and shown in **Scheme 4-8**.

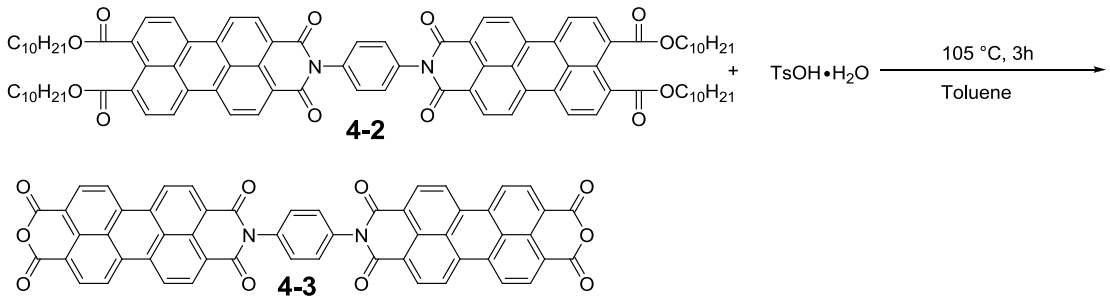

Scheme 4-8. Synthesis of PDI dimer **4-3**

PDI dimer **4-3** was obtained with a yield of 95%. It was characterized with

FT-IR. Due to the low solubility in organic solvent, the ^{1}HNMR spectrum was not obtained.

PDI dimer **4-3** could be a building block for PDI oligomers with more units. It is necessary to explore a purification method, as no available method in literatures. Based on our experience, a purification method was proposed and shown in **Figure 4-3**.

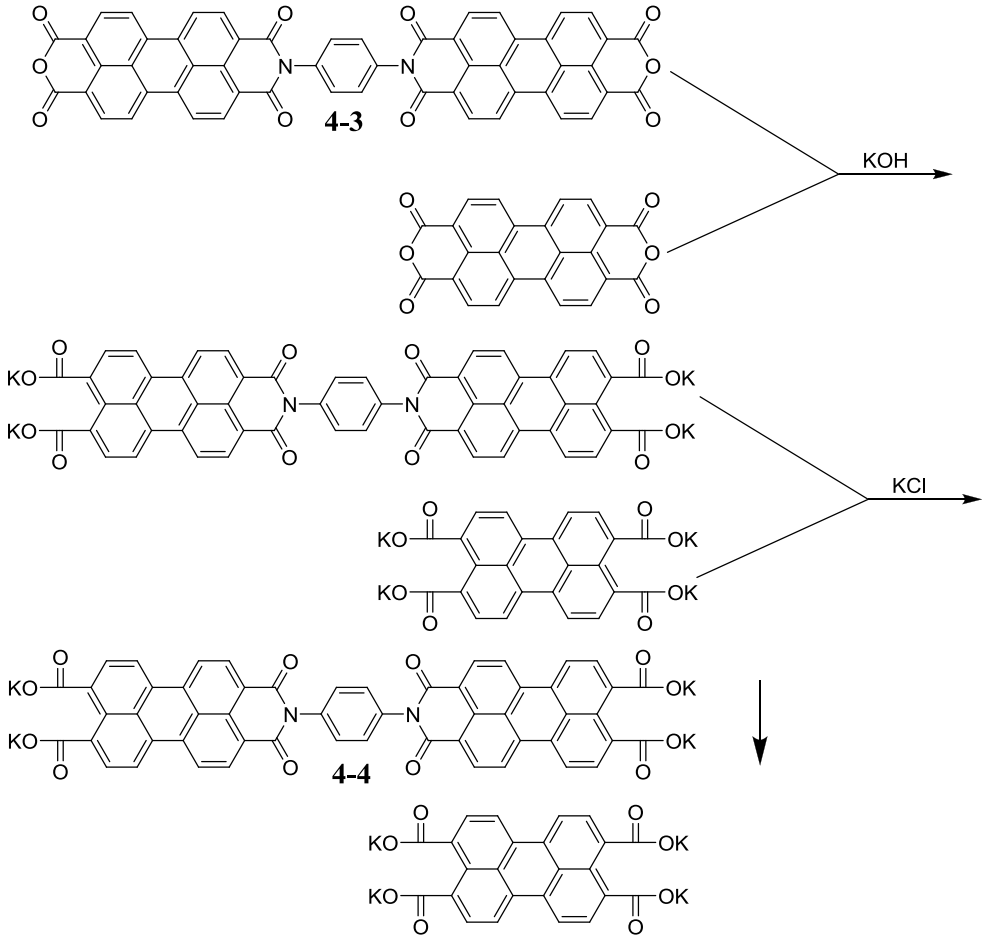

Figure 4-3. Purification of PDI dimer diananhydride **4-3**

With this method, trace amount of PDA could be removed, and high purity PDI dimer **4-3** was obtained. Starting from PDI dimer **4-3**, we could prepare PDI oligomers with 4 or more repeat PDI units.

4.2.2. Preparation of PEI Dimer with Hydrazine

PEI dimer **4-2** was obtained with our method. Through analysis the of the FT-IR spectrum of PEI dimer **4-2**, we envisioned the synthesis of PDI dimer **4-3**. The result proved the success of our design. However, PDI oligomers with direct connected PDI units are more interesting to us. The synthesis of PEI dimer **4-5** was proposed and shown in **Scheme 4-9**.

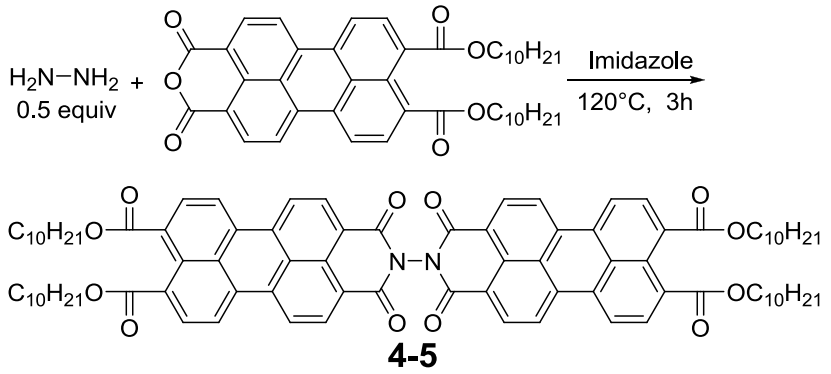

Scheme 4-9. Synthesis of PEI dimer **4-5**

Though this reaction is one step reaction, the purification process costs large amount efforts. Unlike the reaction in **Scheme 4-7**, the relative small molecule weight of hydrazine (28 g/mol), and its' volatility (b.p. 114 °C) make it difficult to keep the theoretical ratio of hydrazine and PEA. Once the theoretical ratio can't be made, the yield will be affected substantially. This reaction has been done twice, and the yield turns out ~50%.

To get better yield, another synthesis route was proposed and shown in **Scheme 4-10**. For the first step, yield turned out ~100%. Time is crucial to this reaction. The reaction need to be stopped at appropriate point under the monitoring with TLC. Shorter time will lead the reaction to low conversion. Longer than enough time,

excess hydrazine will continue react with ester groups, which could lead the reaction to a mess. For the second step, the ratio of PEA and PEI is 1.2. This arrangement could minimize the self-reacting problem of PEI and improve the yield. The yield turned out as 90%.

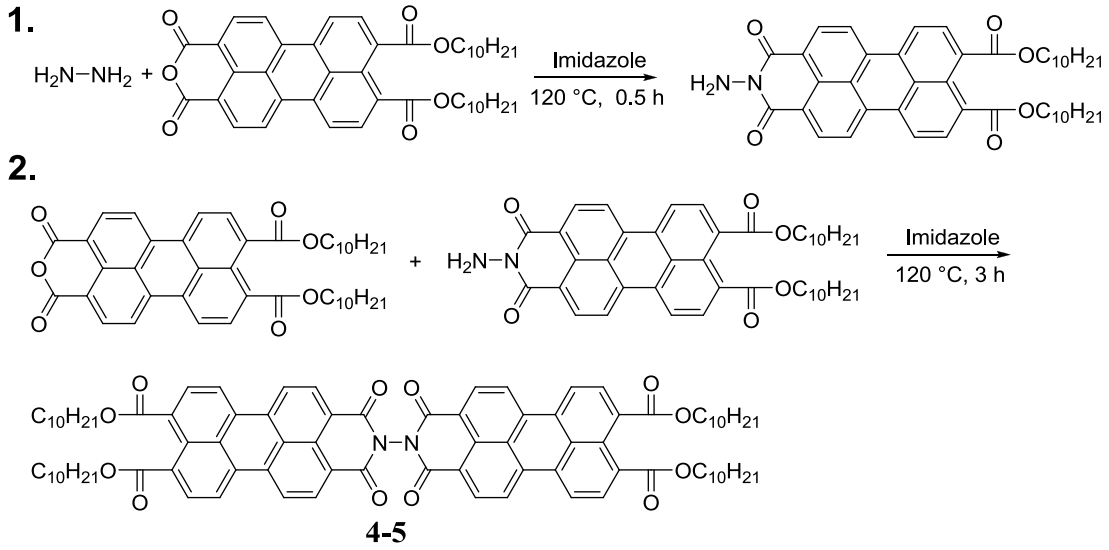

Scheme 4-10. Synthesis of PEI dimer **4-5**

4.2.3. The Synthesis of Perylene Dimer Dianhydride (PDIDMA) 4-6

The structure of PDIDMA **4-6** is shown in **Scheme 4-11**.

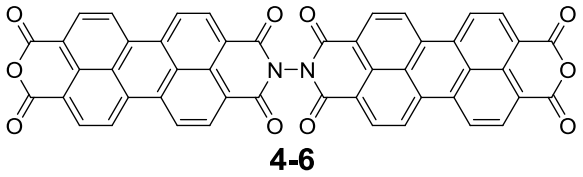

Scheme 4-11. PDIDMA **4-6**

The FT-IR spectrum of PEI dimer **4-5** was obtained and shown in **Figure 4-4**. The internal imide signal peaks appear at 1692 $cm^{-1}$and 1707 cm^{-1}, which are higher than corresponding terminal imide peaks (1665, 1690 cm^{-1}). And the esters' signal peaks are around 1725 cm^{-1}, and the signal shows like a shoulder. The C=O of ester bonds have higher frequency than those of internal imide. Therefore, the terminal

ester groups could be more reactive and less stable than internal imide groups.

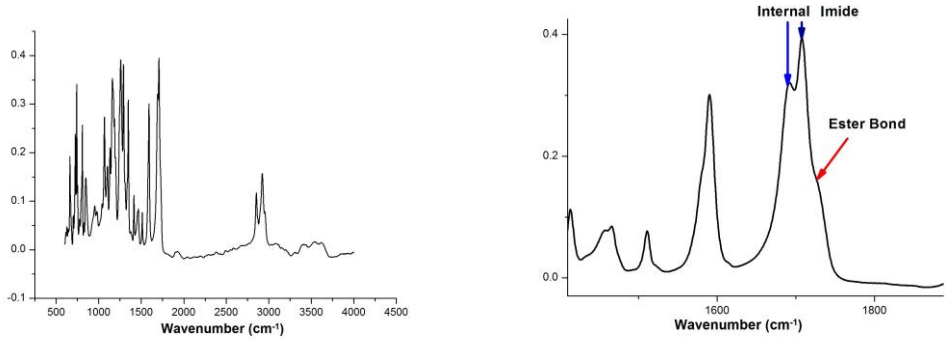

Figure 4-4. IR spectrum of PEI dimer **4-5**

Under our analysis, the synthesis route for PDIDMA **4-6** was proposed and shown in **Scheme 4-12**.

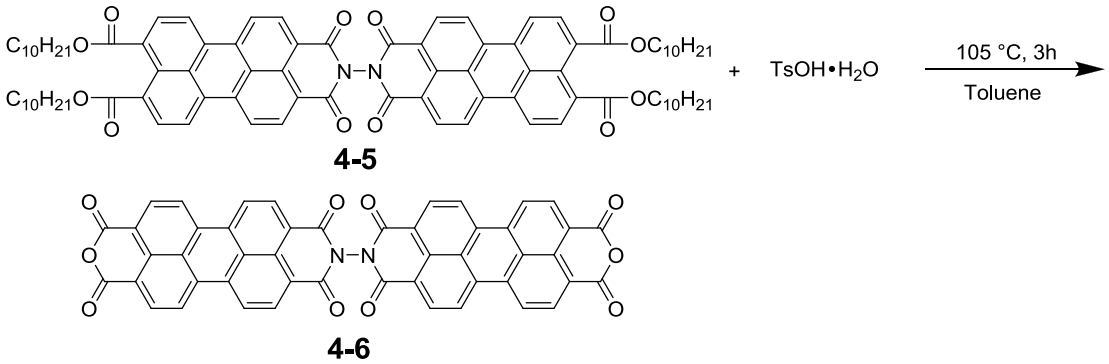

Scheme 4-12. Synthesis of PDIDMA **4-6**

This reaction is a highly efficient reaction. Within 3 hours, the conversion of reactant is near quantitative, as PEI dimer **4-5** was completely consumed. The identification of PDIDMA **4-6** is challenging due to its low solubility in normal organic solvents. To study the structure of the product of our reaction in **Scheme 4-12**, the FT-IR spectrum was obtained and shown in **Figure 4-5**.

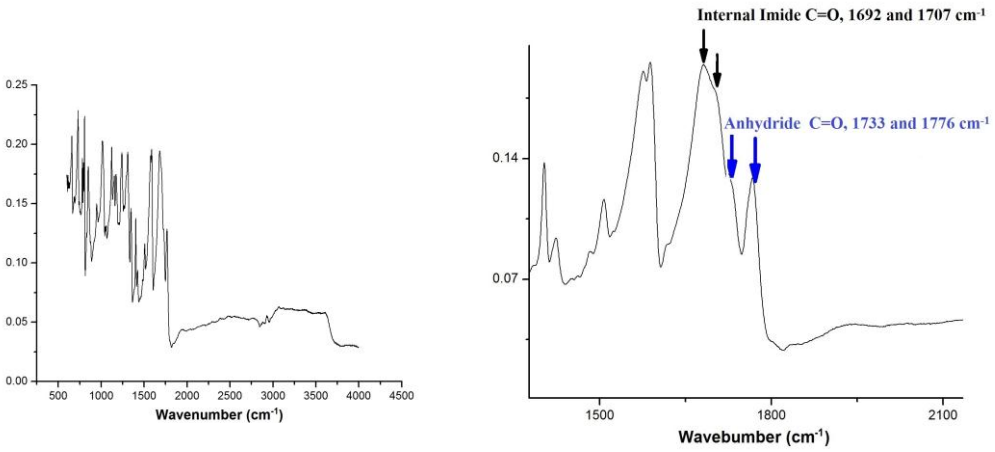

Figure 4-5. IR spectrum of PDIDMA **4-6**

In the spectrum, the terminal anhydride signal peaks were observed. And the internal imide signal peaks (1692 and 1707 cm^{-1}) also were observed.

To fully confirm the structure of PDIDMA **4-6**, one derivative of it was prepared, as shown **Scheme 4-13**.

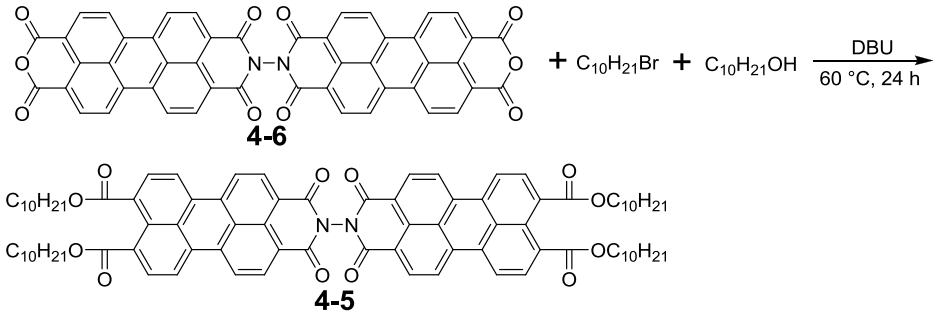

Scheme 4-13. Synthesis of PEI dimer **4-5**

With careful purification, the isolate yield of PEI dimer **4-5** was 88%.

PDIDMA **4-6** is a crucial intermediate for our design. As it has two open terminal sites, which will be useful for the growth of perylene oligomers, PDIDMA **4-6** has potential applications in the synthesis of perylene oligomers.

4.2.4. The Chemistry Involved In the Preparation of PDIDMA 4-6

The chemistry involved in the preparation of PDIDMA **4-6** is shown in **Scheme 4-14**.

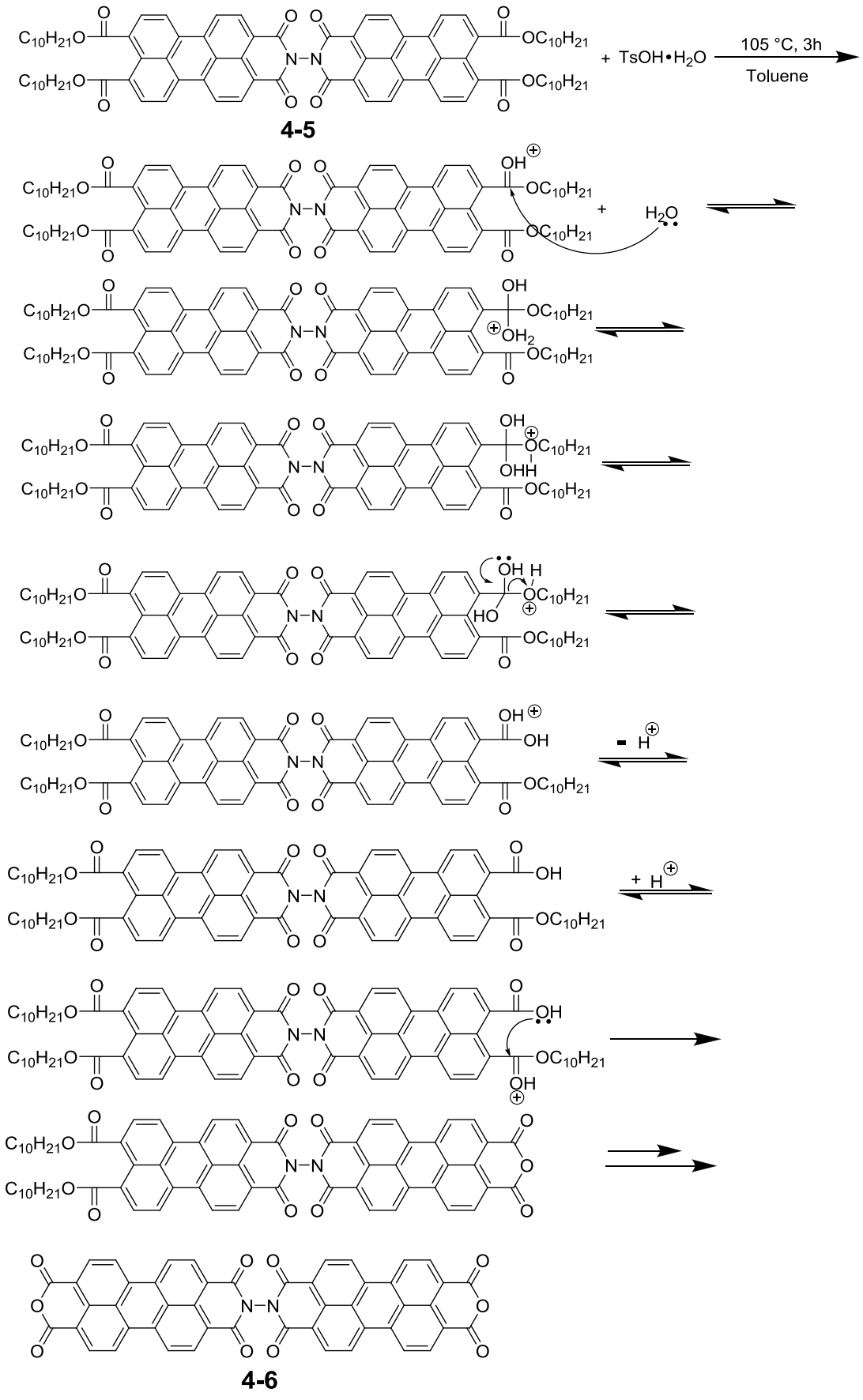

Scheme 4-14. Mechanism of cyclization of PEI dimer **4-5**

4.2.5. The Purification of PDIDMA 4-6

PDIDMA **4-6** is an important intermediate for the synthesis of PDI oligomers. It is necessary to find a method to purify this compound.

By analyzing of our planned synthesis route, we found that the most possible impurity is PDA. Removing PDA from PDIDMA **4-6** becomes the key object of our purification.

With our experience on the purification of PDI dimer **4-3**, which is shown in **Figure 4-3**, a similar procedure was proposed and shown in **Figure 4-6**.

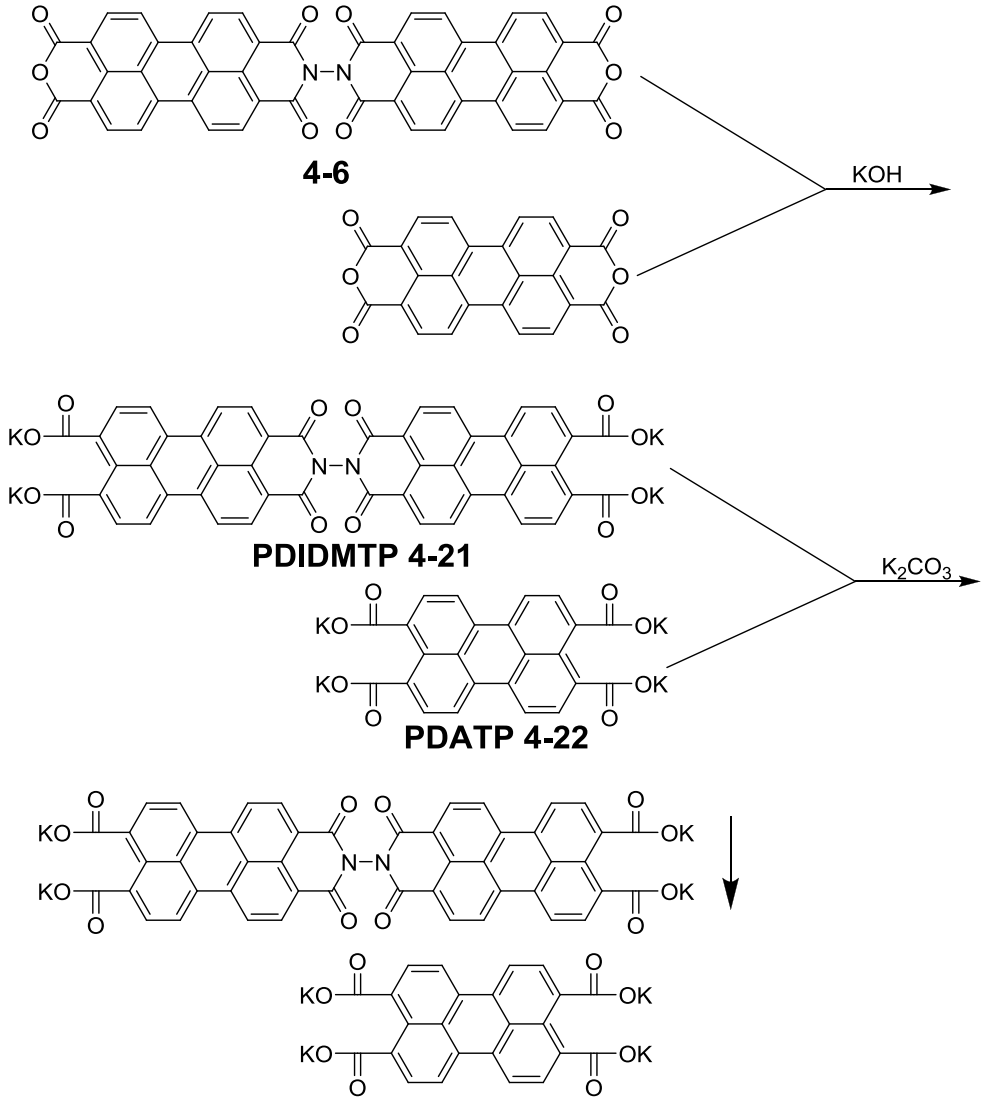

Figure 4-6. Purification of PDIDMA **4-6**

At the beginning, KCl was used to increase ion strength, as what has been done in **Figure 4-3**. However, this method was not good and convenient for the purification of PDIDMA **4-6**. There are two major problems. The first one is that PDIDMA **4-6** has difficulty to precipitate out even when the KCl solution is near saturated. The other one the slow dissolution speed of KCl in water.

To resolve these problems, a better candidate, K_2CO_3, was found. Comparing to KCl, K_2CO_3 has several advantages. Firstly, it has higher solubility, 112 g/100 ml water, comparing to KCl's 34 g/ 100 ml. Secondly, it can dissolve faster.

The excellent solubility of K_2CO_3 offers us substantial space to tune the ion strength. And we even precipitate PDA tetracaboxylate potassium salt (PDATP **4-22**), which has a solubility ~12 g/100 ml water.

To find the appropriate concentration for our purification, we did some study on ion strengths effect on the water solubility of PDIDMA **4-6** salt and PDA salt. PDIDMA **4-6** has a solubility around 0.1 g/100 ml in dilute KOH solution. And PDA has a solubility around 12 g/100 ml. K_2CO_3 is gradually added into these two solutions. Once the concentration of K_2CO_3 reaches 13.8%, given enough time (overnight), PDIDMA **4-6** tetracaboxylate potassium salt (PDIDMTP **4-21**) will all precipitate out. At the same time, PDA tetracaboxylate potassium salt (PDATP **4-22**) starts to precipitate out when the concentration of K_2CO_3 reaches 45%. If we keep K_2CO_3 concentration around 13.8%, all PDIDMTP **4-21** will precipitate out, and PDATP **4-22** will stay in the solution. After the precipitation of PDIDMTP **4-21**, separation can be done by filtration. The photo of the samples with different

concentration K_2CO_3 is shown in **Figure 4-7**.

Figure 4-7. Photo of PDIDMTP **4-21** and PDATP **4-22** solution

From left to right, **Bottle 1**, 12 g/100 ml PDA in 1.0 * 10^{-5} mol/l KOH solution; **Bottle 2**, 0.02 g/100 ml PDA in 1.0 * 10^{-5} mol/l KOH solution; **Bottle 3**, 0.02 g/100 ml PDA in 1.0 * 10^{-5} mol/l KOH solution when K_2CO_3 concentration reach 45%; **Bottle 4**, 1*10^{-3} g/100 ml PDIDMA **4-6** in 1.0 * 10^{-5} mol/l KOH solution; **Bottle 5,** 1*10^{-3} g/100 ml PDIDMA **4-6** in 1.0 * 10^{-5} mol/l KOH solution when K_2CO_3 concentration reach 13.8%.

During purification, we found that the crude PDIDMA **4-6** from reaction shown in **Scheme 4-12**, has very good quality. Only trace amount of PDA can be observed. The recycled back PDA is less than 1% of our crude product. At the same time, the PDIDMA **4-6** is more than 99% of our crude product.

With this method, relatively large amount of pure sample can be obtained at a low cost. This method may have potential application in other organic synthesis in the future.

4.2.6. The Synthesis of Perylene Dimer Tetraester with Triethylene-glycol

PDIDMA **4-6** is a very useful intermediate for preparation of other perylene derivatives. Here is an example of synthesis of perylene dimer derivatives, which is shown in **Scheme 4-15**. The isolating yield is 80%.

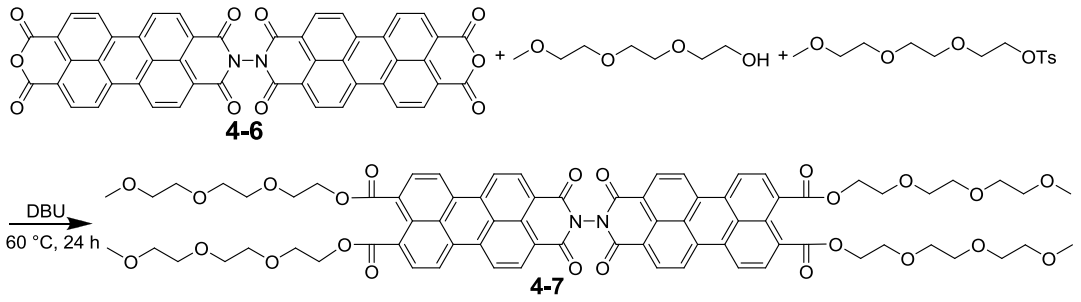

Scheme 4-15. Synthesis of PEI dimer **4-7**

Without PDIDMA **4-6**, the preparation of PEI dimer **4-7** will be more challenging. The alternate synthesis method is shown in **Scheme 4-16**, which is following the same method as in **Scheme 4-9**. However, this method is not practical due to the absence as PEA **4-8** has never been prepared.

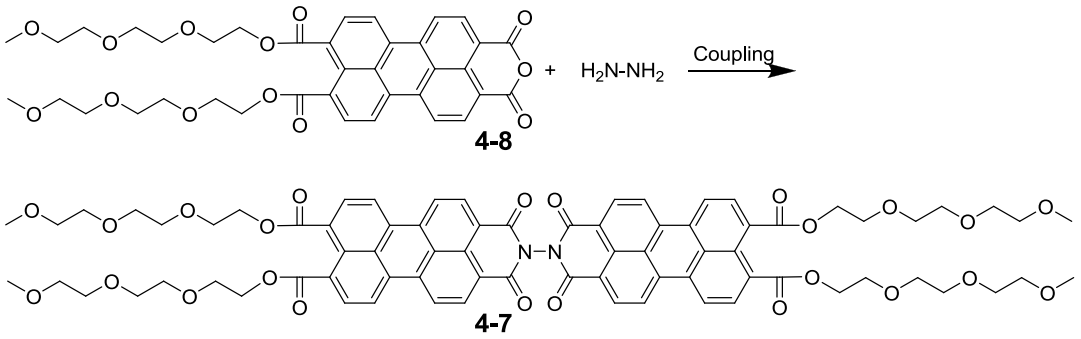

Scheme 4-16. Synthesis of PEI dimer **4-7** with coupling method

Note that PEA **4-8**, cannot be prepared by any reported method. The key issue is that ether bond is not stable in a strongly acidic environment used in our routine method (shown in **Scheme 4-12**).

4.2.7. The Synthesis of Perylene Dimer Tetraester with 2-Decyl-1-tetradecanol

The structure of PEI dimer **4-9** is shown in **Scheme 4-17**.

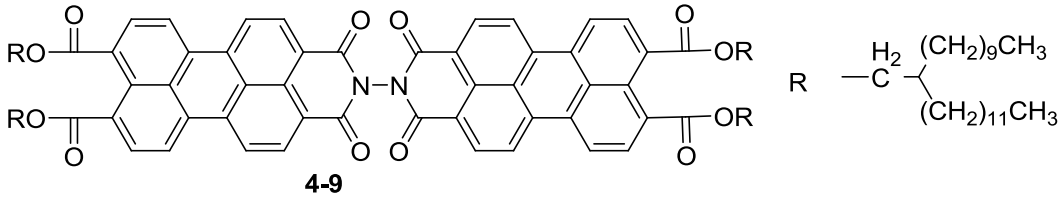

Scheme 4-17. Structure of PEI dimer **4-9**

To prepare PEI dimer **4-9**, one of the most convenient methods is shown in **Scheme 4-18**. The same strategy as in **Scheme 4-15**, is applied here. Under this condition, a small scale reaction was carried out and the yield turned out as 85%.

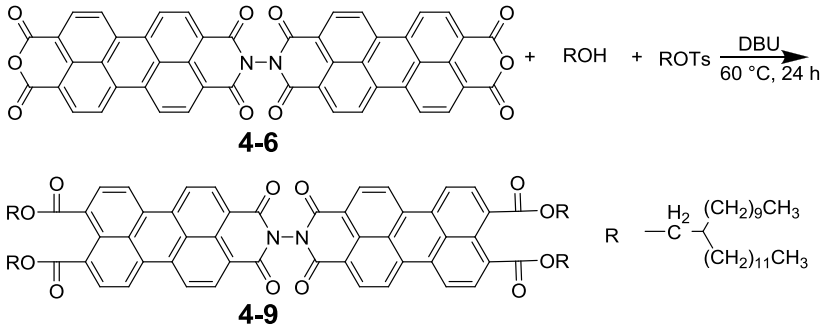

Scheme 4-18. Synthesis of PEI dimer **4-9**

However, this reaction is very sensitive to water, and it is difficult to achieve good yield in a large scale reaction. Our routine method in **Scheme 4-10** was applied on the synthesis of PEI dimer **4-9**, which is shown in **Scheme 4-19**. The yield turned out as 90%.

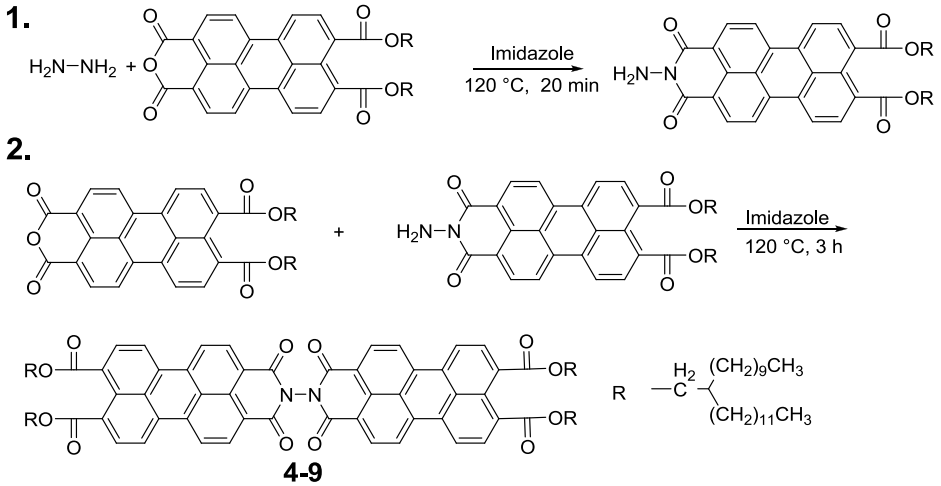

Scheme 4-19. Synthesis of PEI dimer **4-9**

4.2.8. The Synthesis of PEI Trimer

With our experience, the synthesis of PEI trimer **4-10** was proposed and shown in **Scheme 4-20**.

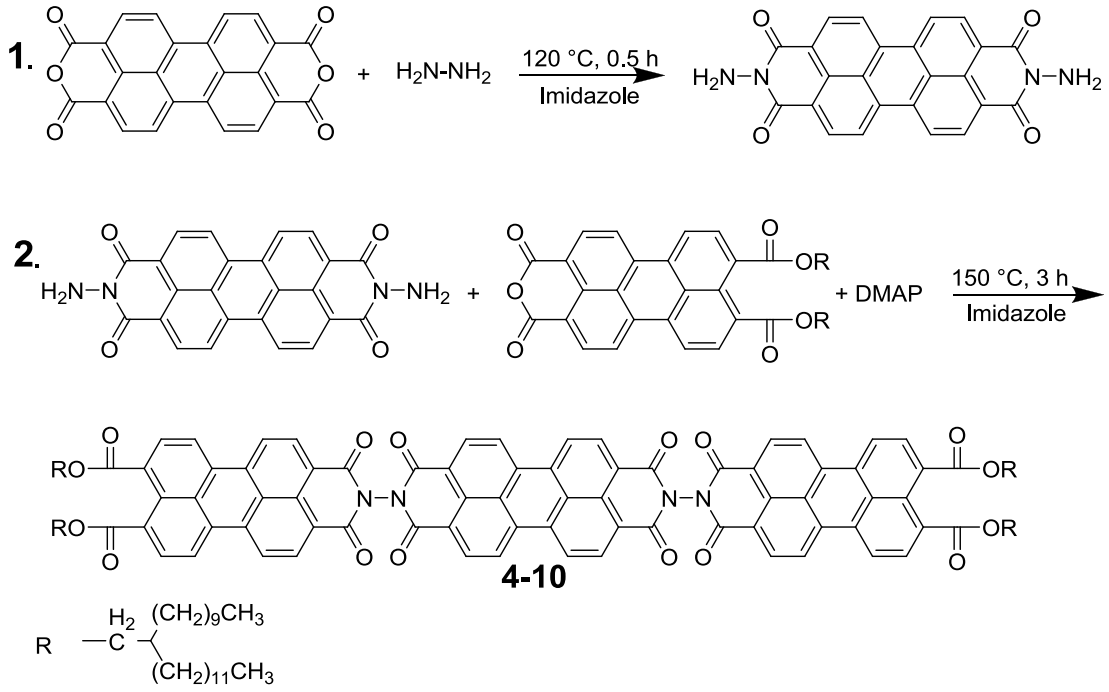

Scheme 4-20. Synthesis of PEI trimer **4-10**

In the first step, H_2N-NH_2 needs to be completely removed in the purification process. Otherwise, small amount H_2N-NH_2 could have significant effect on the yield of PEI trimer **4-10**. In the second step reaction, 2.1 equiv of PEA **3-12** is needed to suppress the side reaction between the H_2N- group and ester group.

With the strategy shown in **Scheme 4-20**, PEI trimer **4-10** was obtained with yield of 40%.

4.3. Characterization

Due to their conjugated structure, most PDIs and their derivatives have strong UV-Vis absorbance. For some PDI oligomers, the exciton effect between adjacent

PDIs is strong. The details about exciton effect were discussed in **Chapter 1.4.2**.

4.3.1. The UV-Vis Spectra of PDIDMTP 4-21 and PDATP 4-22

The structure of PDIDMTP **4-21** and PDATP **4-22** are shown in **Scheme 4-21**.

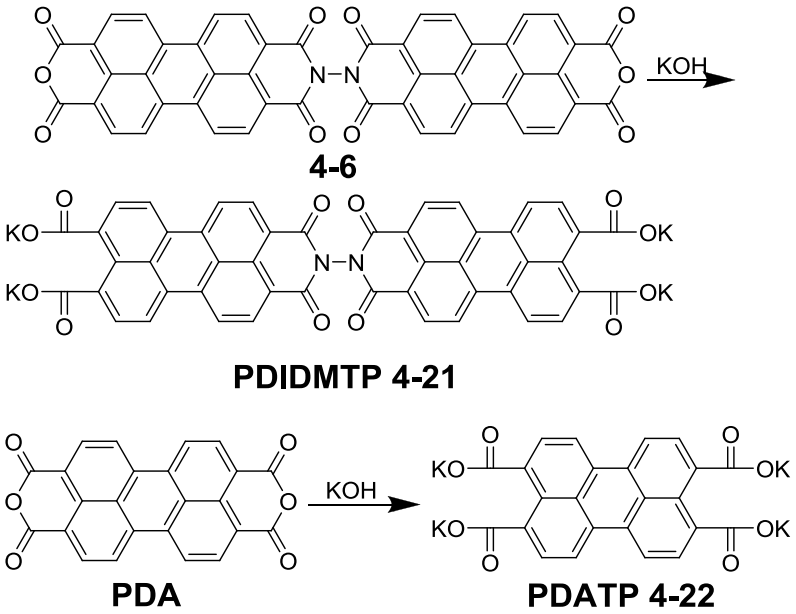

Scheme 4-21. Structure of PDIDMTP **4-21** and PDATP **4-22**

The UV-Vis spectrum of PDIDMTP **4-21** and PDATP **4-22** are shown in **Figure 4-8**.

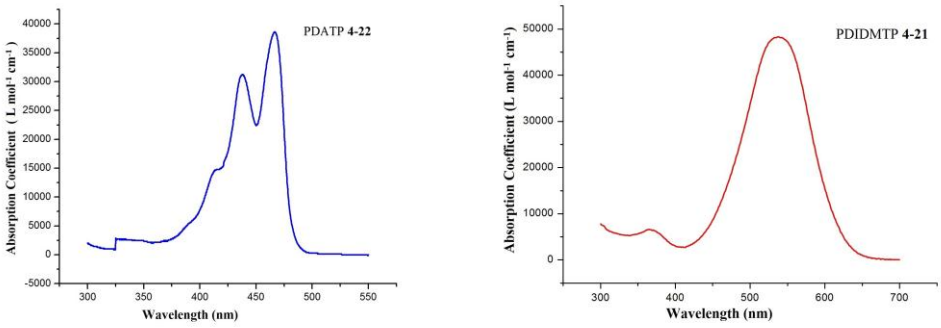

Figure 4-8. UV-Vis spectra of PDIDMTP **4-21** and PDATP **4-22**

As PDA and PDIDMA **4-6** don't dissolve in water, they were converted to the corresponding potassium salt as shown in **Scheme 4-21**. They were dissolved in

$1.0*10^{-5}$ mol/l KOH solution. For PDATP **4-22**, the absorption coefficient is 39530 L mol^{-1} cm^{-1}; λ_{max} is 466 nm. For PDIDMTP **4-21**, the absorption coefficient is 51393 L mol^{-1} cm^{-1}; λ_{max} is 543 nm.

The absorption coefficient of PDIDMTP **4-21** is less than 2 times of that of PDATP **4-22**. The reason could be the strong aggregation of PDI dimer dianhydride **4-6** salt in water, as it's the florescence quantum efficient is less than 1%. For the PDA salt, florescence quantum efficient is 100%.

To compare the absolute absorption, the integration of UV-Vis spectra of PDIDMTP **4-21** and PDATP **4-22** has been done. Integration for UV-Vis spectra of PDIDMTP **4-21** is 5949064. Integration for UV-Vis spectra of PDATP **4-22** is 2165049. The ratio turns out as 2.75. That means PDIDMTP **4-21** has much stronger ability to absorb light than PDATP **4-22**.

4.3.2. The UV-Vis Spectra of PEI Dimer 4-5

The structure of PEI and PEI Dimer **4-5** are shown in **Scheme 4-22**.

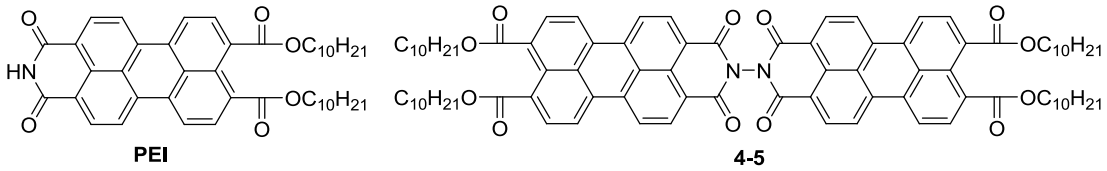

PEI 4-5

Scheme 4-22. Structure of PEI and PEI dimer

The UV-Vis spectra of PEI and PEI Dimer **4-5** are shown in **Figure 4-9**.

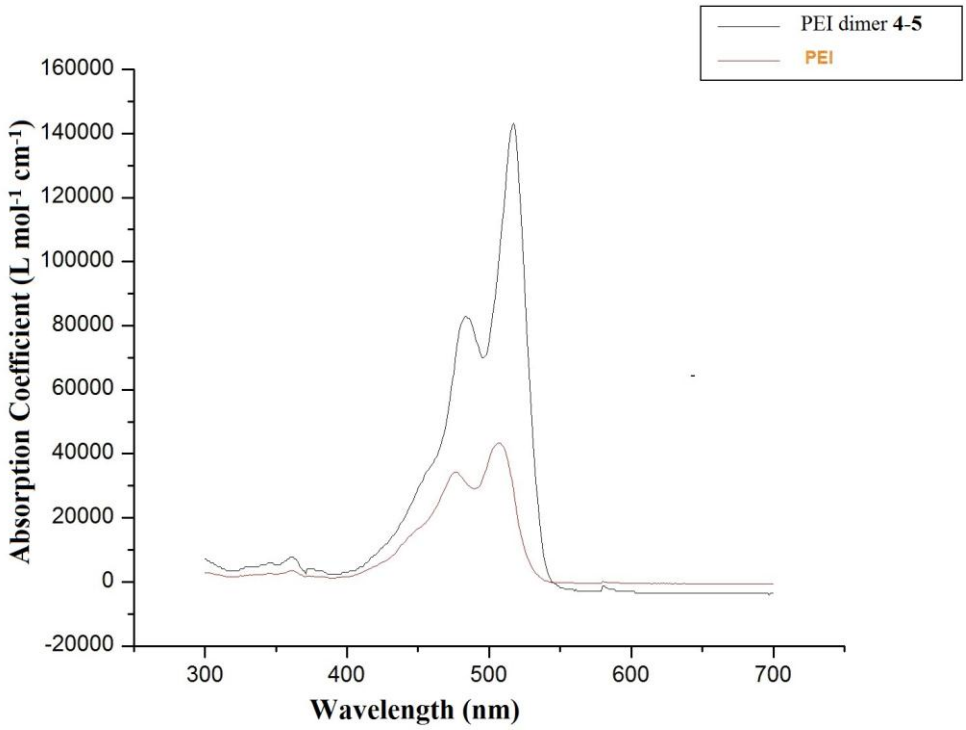

Figure 4-9. UV-Vis spectra of PEI and PEI dimer **4-5**

For PEI, the maximum absorbance peak is around 507 nm, and the coefficient is 43468 L mol^{-1} cm^{-1}. For PEI Dimer **4-5**, the maximum absorbance peak is around 507 nm, and the coefficient is 143324 L mol^{-1} cm^{-1}, which is 3.3 times of that of PEI. The substantial increase of absorbance coefficient is mainly due to the exciton effect, and the details were discussed in **Chapter 1.4.2.** This result proves that the exciton effect not only exists in ring closed system as in Langhals' report, also exists in the ring opened system.

4.3.3. The UV-Vis Spectra of PEI Dimer 4-9 and PEI Trimer 4-10

The structure of PEA **4-12**, PEI **4-20**, PEI dimer **4-9** and PEI trimer **4-10** were shown in **Scheme 4-23**.

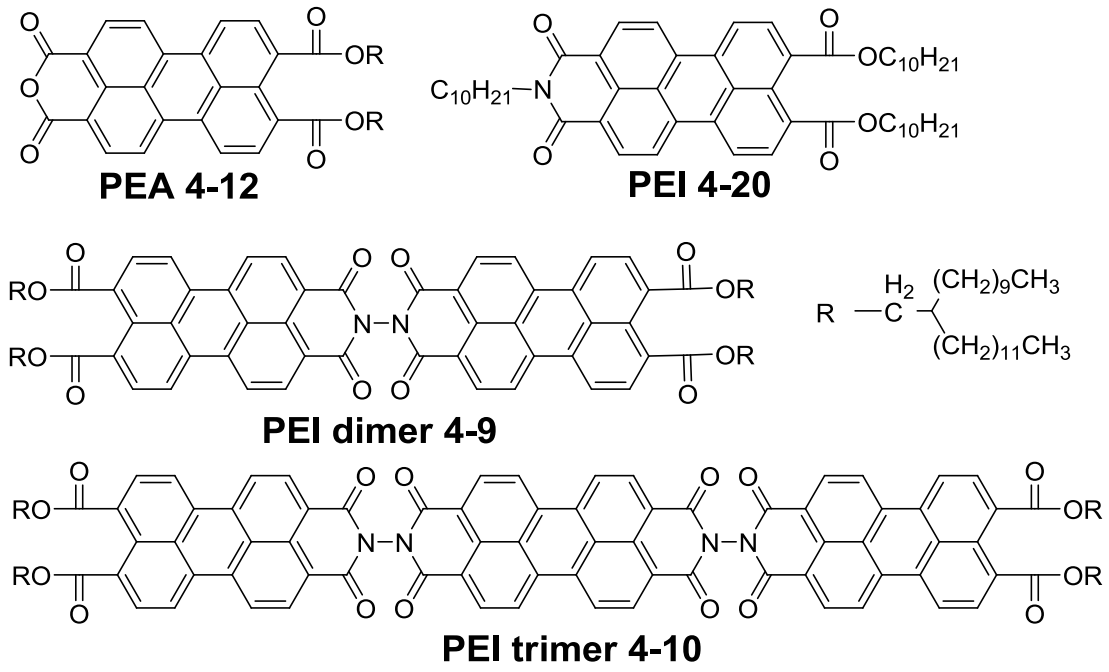

Scheme 4-23. Structure of PEI, PEA and PEI oligomers

Their UV-Vis spectra are shown in **Figure 4-10**.

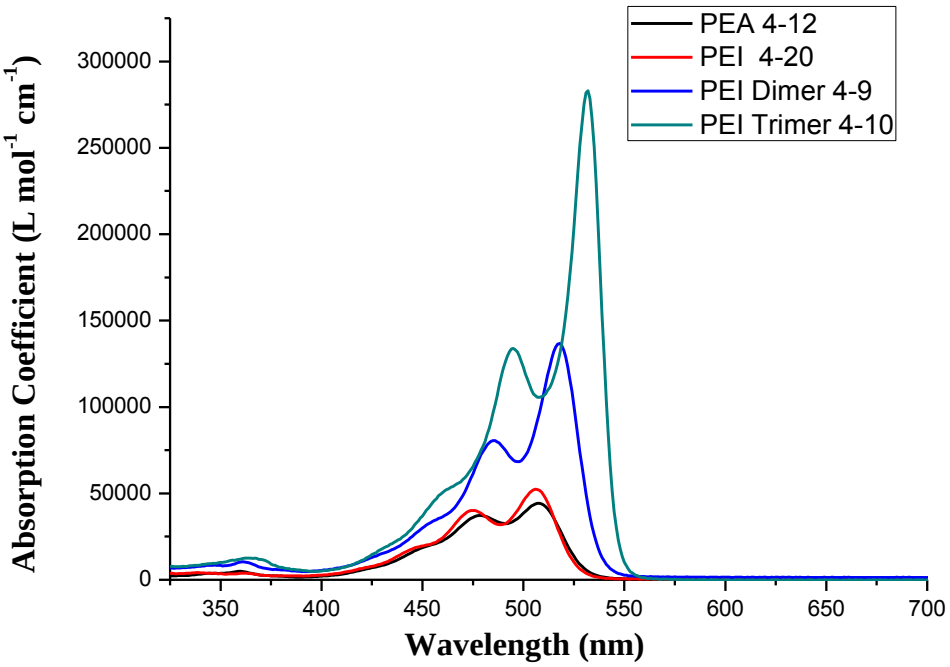

Figure 4-10. UV-Vis spectra of PEA, PEI and PEI oligomers

The λ_{max} and absorption coefficient of these compounds are shown in **Table 4-1.**

Name	**λ_{max} (nm)**	**Absorption Coefficient**
PEA 4-12	**507**	**44357**
PEI 4-20	**506**	**52166**
PEI dimer 4-9	**518**	**137458**
PEI trimer 4-10	**532**	**258542**

Table 4-1. UV-Vis spectra and absorption coefficient

From PDI monomer, to PDI dimer, then to PDI trimer, there is a significant increase of absorption coefficient. The red shift of λ_{max} also was observed. PEI trimer **4-10** is an intense colorant, which absorption coefficient is 258542 L mol^{-1} cm^{-1}. PDI tetramer and PDI oligomers with more units will have even higher absorption coefficient.

4.4. Conclusion

With the investigation of Langhals' strategy, we envisioned a method to synthesize PDIDMA **4-6**. A purification procedure for PDIDMA **4-6** also was developed. Starting from this key intermediate, several perylene oligomers were obtained. This new growing mechanism may have potential applications in the synthesis of PDI oligomers and PDI derivatives. The UV-Vis spectra of perylene oligomer were studied.

4.5. Experiments

4.5.1. Instruments and Characterizations

^{1}H and ^{13}C NMR spectra were recorded on a Varian 300 or 600 MHz NMR spectrometer with deuterated chloroform ($CDCl_3$), DMSO or THF as the solvent at room temperature. The chemical shifts were reported using TMS as the internal standard. Mass measurement was carried out in CUNY-Hunter MS center and Rutgers University at Newark. The IR spectra were acquired on a Bruker Vertex 70V FT-IR spectrometer at a resolution of 4 cm^{-1}. UV-Vis spectra were recorded on LAMBDA 650 UV-Vis Spectrophotometer.

4.5.2. Materials and Synthesis

All reagents and chemicals were purchased from Fisher scientific or VWR international and used as received. The synthesis of PEA **3-1** was addressed in **Chapter 3**. PEI **4-20** was prepared by Bin Wang, my labmate.

Synthesis of PEI 4-1

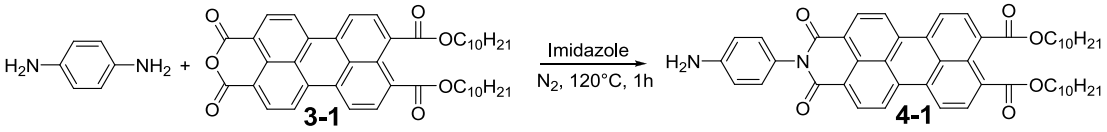

A 25 mL Schlenk flask was charged with 0.69 g (1 mmol) PEA **3-1**, 1.08 g (10 mmol) benzene-1,4-diamine and 7 g dried imidazole. The mixture was heated to 120 ℃ for 1 hour and protected with N_2. After reaction was done, the mixture was cooled to 90 ℃ and water was added into the flask to precipitate the product. Crude product was obtained with vacuum filtration and washed with water. Pure product

was obtained by column chromatography with 20/1 (v/v) $CHCl_3$/methol. Yield PEI **4-1** 0.546 g (70%) as dark red solid.

FT-IR (cm^{-1}): 2920 (antisymmetric CH_2), 2854 (symmetric CH_2), 1723 (ester C=O), 1698 (symmetric imide C=O), 1655 (antisymmetric imide C=O), 1592 (aromatic ring stretch).

Synthesis of PEI 4-2

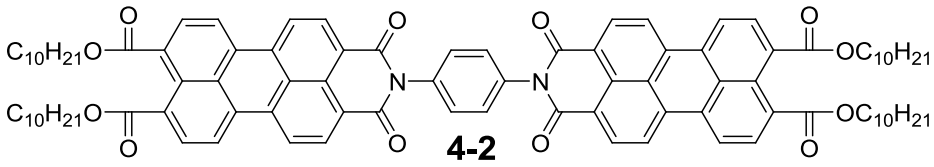

4-2

Two methods were applied in the synthesis of PEI **4-2**. The first method was shown in **Scheme 4-6**. A 25 mL Schlenk flask was charged with 0.97 g (1.40 mmol) PEA **3-1**, 0.78 g (1 mmol) PEI **4-1** and 15 g dried imidazole. The mixture was heated to 150 ℃ for 3 hour and protected with N_2. After reaction was done, the mixture was cooled to 90 ℃ and water was added into the flask to precipitate the product. Crude product was obtained with vacuum filtration and washed with water. Pure product was obtained by column chromatography with 20/1 (v/v) $CHCl_3$/acetone. Yield PDI dimer **4-2** 1.31 g (90%) as dark red solid.

The second method was shown in **Scheme 4-7**. A 10 mL Schlenk flask was charged with 0.55 g (0.8 mmol) PEA **3-1**, 0.044 g (0.4 mmol) benzene-1,4-diamine and 5 g dried imidazole. The mixture was heated to 150 ℃ for 3 hour and protected with N_2. After reaction was done, the mixture was cooled to 90 ℃ and water was added into the flask to precipitate the product. Crude product was obtained with vacuum filtration and washed with water. Pure product was obtained by column

chromatography with 20/1 (v/v) $CHCl_3$/acetone. Yield PEI dimer **4-2** 0.46 g (80%) as dark red solid.

^{1}H NMR ($CDCl_3$, 600 MHz): δ (ppm) = 8.67 (m, 4H, Ar), 8.49 (m, 8H, Ar), 8.12 (m, 4H, Ar), 7.61 (s, 4H, Ar), 4.35 (t, 8H, $CO_2C\mathbf{H_2}$), 1.86 – 1.76 (m, 8H, $CO_2CH_2C\mathbf{H_2}$), 1.50 – 1.27 (m, 56H, $CO_2CH_2CH_2(C\mathbf{H_2})_7$), 0.87 (t, J = 6.6 Hz, 12 H, $C\mathbf{H_3}$).

FT-IR (cm^{-1}): 2924 (antisymmetric CH_2), 2854 (symmetric CH_2), 1725 (ester C=O), 1701 (symmetric imide C=O), 1665 (antisymmetric imide C=O), 1591 (aromatic ring stretch).

HRMS (MALDI + H) calcd for $C_{94}H_{104}N_2O_{12}$ 1453.7662; found 1453.7533.

^{1}H NMR of PEI dimer **4-2**

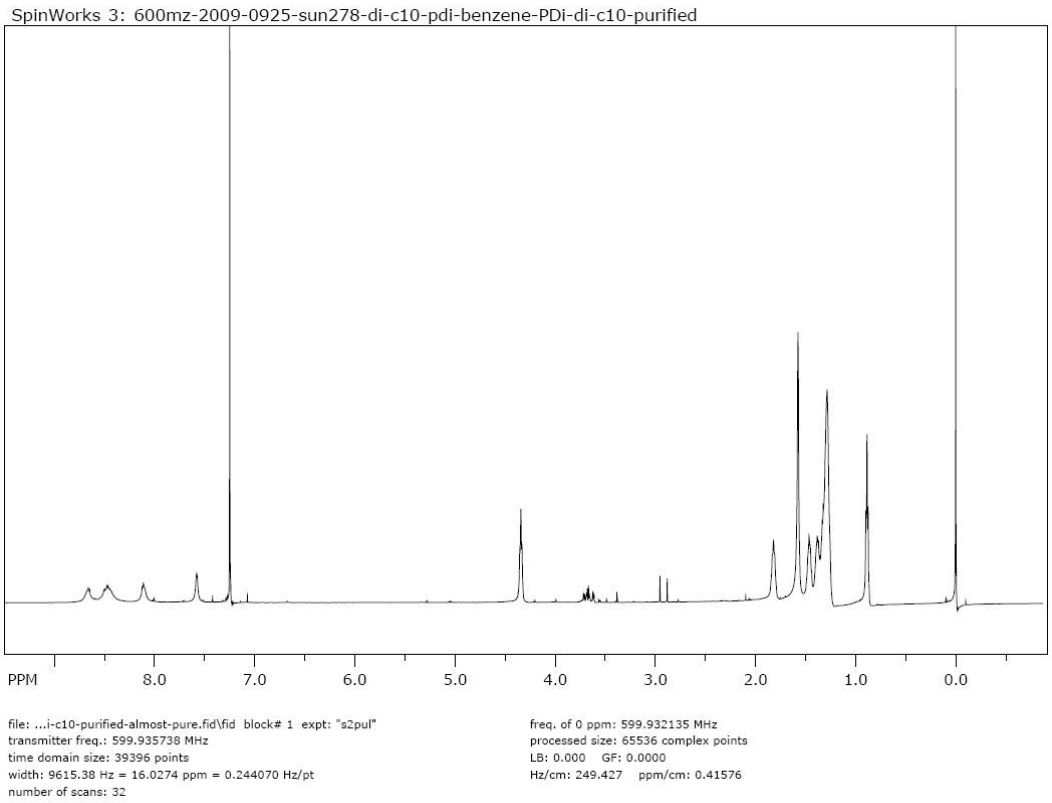

HRMS (MALDI) with benzopyrene as matrix

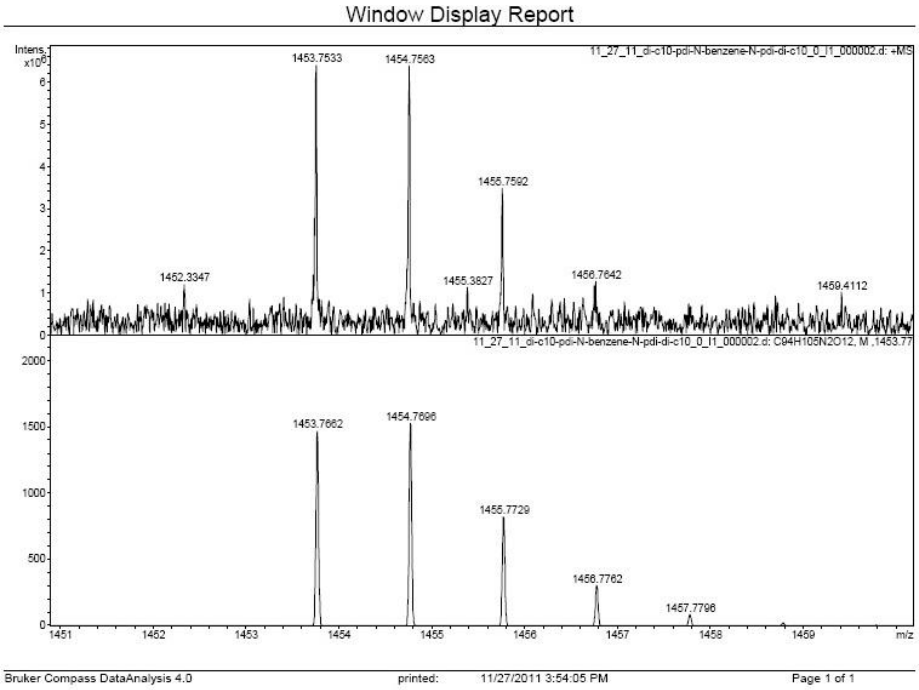

Synthesis of PDI Dimer Dianhydride 4-3

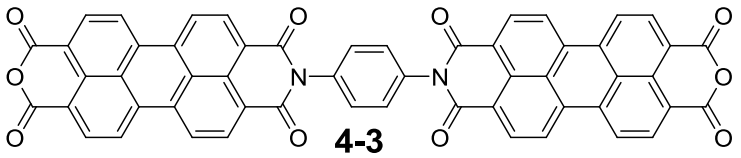

A 10 mL round-bottomed flask was charged with 0.52 g (0.36 mmol) PEI **4-2**, 10 ml toluene and 0.41 g (2.16 mmol) *p*-toluenesulfonic acid monohydrate (TsOH•H_2O). Then the mixture was heated to 105 ℃ and stirred for 3 hours. The crude product was collected by vacuum filtration and washed with water. Product was obtained by drying in vacuum at 50 ℃ overnight. Yield PDI dimer dianhydride **4-3** 0.293 g (95%) as a dark red solid.

FT-IR (cm^{-1}): 1766 (symmetric anhydride C=O), 1728 (antisymmetric anhydride C=O), 1701 (symmetric imide C=O), 1665 (antisymmetric imide C=O), 1591 (aromatic ring stretch).

Synthesis of PEI Dimer Tetraester 4-5

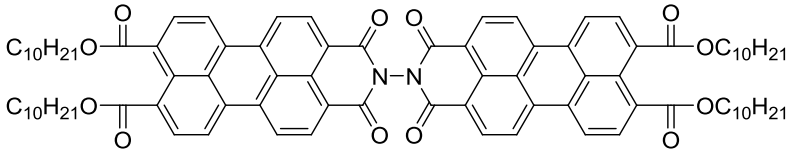

4-5

Three methods were applied in the synthesis of PEI dimer tetraester **4-5**. The first method was shown in **Scheme 4-5**. A 10 mL Schlenk flask was charged with 0.83 g (1.2 mmol) PEA **3-1**, 0.020 g (0.6 mmol) hydrazine and 5 g dried imidazole. The mixture was heated to 120 ℃ for 3 hour and protected with N_2. After reaction was done, the mixture was cooled to 90 ℃ and water was added into the flask to precipitate the product. Crude product was obtained with vacuum filtration and washed with water. Pure product was obtained by column chromatography with 20/1 (v/v) $CHCl_3$/acetone. Yield PEI dimer tetraester **4-5** 0.412 g (50%) as red solid.

The second method was shown in **Scheme 4-10**. A 10 mL Schlenk flask was charged with 0.62 g (0.9 mmol) PEA **3-1**, 0.38 g (13.5 mmol) hydrazine and 5 g dried imidazole. The mixture was heated to 120 ℃ for 0.5 hour and protected with N_2. After reaction was done, the mixture was cooled to 90 ℃ and water was added into the flask to precipitate the product. Crude product was obtained with vacuum filtration and washed with dilute HCl. The intermediate PEI was dried in vacuum at 50 ℃ overnight. Yield PEI 0.601 g (95%) as red solid.

In the second step, 0.601 g (0.86 mmol) PEI, 0.712 g (1.03 mmol) PEA **3-1** and 15 g dried imidazole were added into a 25 ml Schlenk flask. The mixture was heated to 120 ℃ for 3 hour and protected with N_2. After reaction was done, the mixture was cooled to 90 ℃ and water was added into the flask to precipitate the

product. Crude product was obtained with vacuum filtration and washed with water. Pure product was obtained by column chromatography with 20/1 (v/v) $CHCl_3$/acetone. Yield PEI dimer tetraester **4-5** 1.06 g (90%) as red solid.

The third method was shown in **Scheme 4-13**. 50 mg (0.064 mmol) PDIDMA **4-6**, 38 mg (0.25 mmol) DBU, and 202 mg (1.28 mmol) 1-Decanol were added into a 10 ml round-bottomed bottle. The bottle was sealed and heat to 60 ℃ for 3 hours. Then 424 mg (1.92 mmol)1-decylbromide was added into bottle. Subsequently, the mixture was stirred and heated at 60 ℃ over night. Then the mixture was added into 50 ml methanol. Crude product was obtained by vacuum filtration and washed with methanol. Pure product was obtained by column chromatography with 20/1 (v/v) $CHCl_3$/acetone. Yield PEI dimer tetraester **4-5** 77 mg (88%) as red solid.

^{1}H NMR ($CDCl_3$, 600 MHz): δ (ppm) = 8.52 (m, 4H, Ar), 8.17 (m, 8H, Ar), 7.99 (m, 4H, Ar), 4.35 (t, 8H, $CO_2C\mathbf{H_2}$), 1.86 – 1.76 (m, 8H, $CO_2CH_2C\mathbf{H_2}$), 1.50 – 1.27 (m, 56H, $CO_2CH_2CH_2(C\mathbf{H_2})_7$), 0.87 (t, J = 6.6 Hz, 12 H, $C\mathbf{H_3}$).

FT-IR (cm^{-1}): 2957 (antisymmetric CH_3), 2924 (antisymmetric CH_2), 2870 (symmetric CH_3), 2854 (symmetric CH_2), 1720 (ester C=O), 1701 (symmetric imide C=O), 1689 (antisymmetric imide C=O), 1591 (aromatic ring stretch).

HRMS (MALDI + H) calcd for $C_{88}H_{100}N_2O_{12}$ 1377.7349; found 1377.7476.

UV-Vis (in $CHCl_3$): 479, 508 nm (λ_{max}).

^{1}H NMR spectrum of PEI dimer tetraester **4-5**

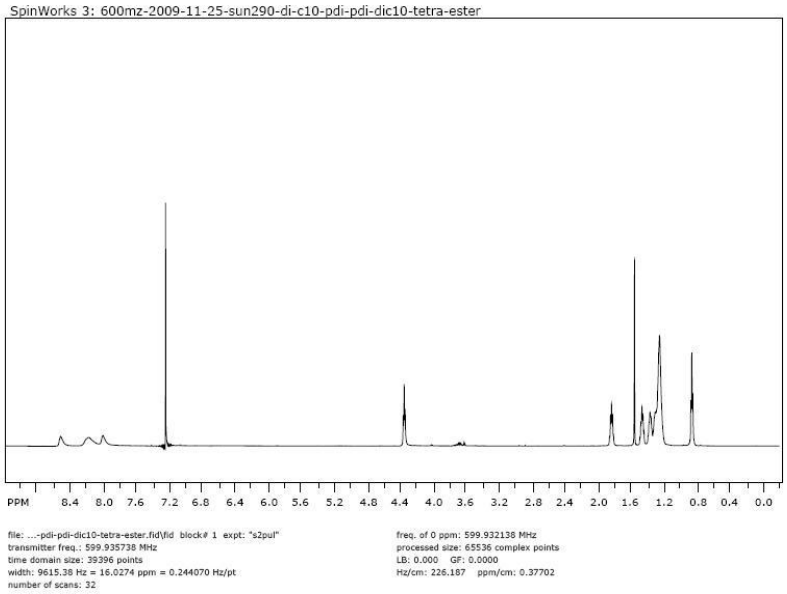

HRMS (MALDI +) of PEI dimer tetraester **4-5**

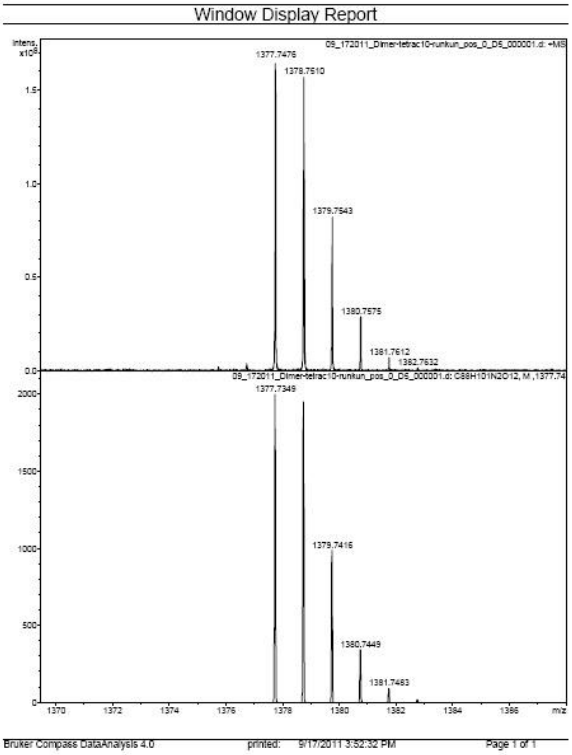

Synthesis of PDI Dimer Tetraester 4-7

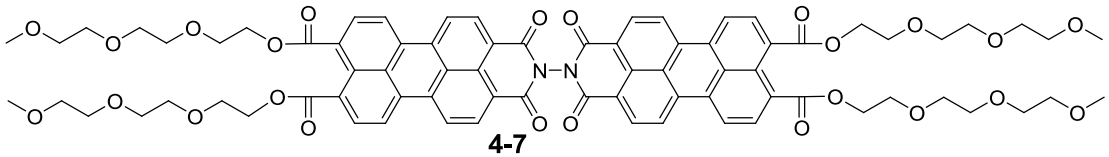

4-7

As shown in **Scheme 4-15**, 60 mg (0.077 mmol) PDIDMA **4-6**, 47 mg (0.31 mmol) DBU, and 262 mg (1.6 mmol) triethylene glycol monomethyl ether were added into a 10 ml round-bottomed bottle. The bottle was sealed and heat to 60 ℃ for 3 hours. Then 636 mg (1.6 mmol) triethylene glycol monomethyl tosylate was added into bottle. Subsequently, the mixture was stirred and heated at 60 ℃ for 24 hours. Then the mixture was added into 50 ml methanol. Crude product was obtained by vacuum filtration and washed with methanol. Pure product was obtained by column chromatography with 40/1 (v/v) $CHCl_3$/acetone. Yield PEI dimer tetraester **4-7** 85 mg (80%) as dark red solid.

^{1}H NMR ($CDCl_3$, 600 MHz): δ (ppm) = 8.53 (m, 4H, Ar), 8.17 (m, 8H, Ar), 8.04 (m, 4H, Ar), 4.53 (t, 8H, $CO_2C\mathbf{H_2}$), 3.90 (t, 8H, $CO_2CH_2C\mathbf{H_2}O$), 3.70 (t, 8H, $CO_2CH_2CH_2OC\mathbf{H_2}$), 3.65 (t, 8H, $CO_2CH_2CH_2OCH_2C\mathbf{H_2}$), 3.60 (t, 8H, $CO_2CH_2CH_2OCH_2CH_2OC\mathbf{H_2}$), 3.60 (t, 8H, $CO_2CH_2CH_2OCH_2CH_2OCH_2C\mathbf{H_2}$), 3.32 (s, 12H, $OC\mathbf{H}_3$)

^{13}C NMR ($CDCl_3$, 75 MHz): δ (ppm) = 168.06 (ester **C**=O), 160.40 (imide **C**=O), 135.90 (Ar), 132.30 (Ar), 131.52 (Ar), 130.63 (Ar), 129.38 (Ar), 128.81 (Ar), 128.58 (Ar), 123.09 (Ar), 121.92 (Ar), 121.78 (Ar), 121.32 (Ar), 71.87 ($CO_2\mathbf{C}H_2CH_2$), 70.67 ($CO_2CH_2\mathbf{C}H_2$), 68.91 ($O\mathbf{C}H_2\mathbf{C}H_2$), 64.67 ($O\mathbf{C}H_2\mathbf{C}H_2$), 59.01 ($O\mathbf{C}H_3$)

FT-IR (cm^{-1}): 1723 (ester C=O), 1701 (symmetric imide C=O), 1689 (antisymmetric imide C=O), 1591 (aromatic ring stretch).

HRMS (MALDI+252) of PEI dimer tetraester **4-7** with benzopyrene calcd for $C_{76}H_{76}N_2O_{24}$1400. 48; found 1652.5965.

^{1}H NMR spectrum of PEI dimer tetraester **4-7**

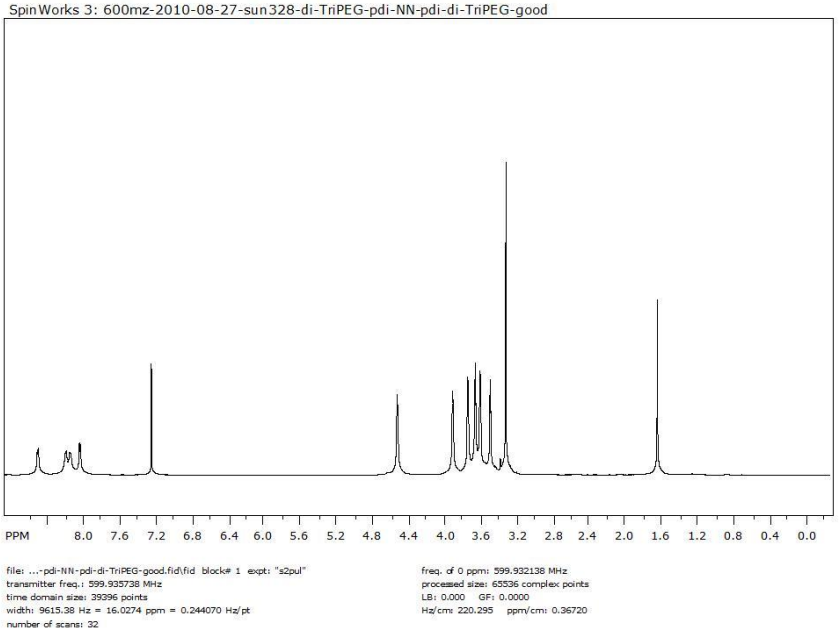

HRMS (MALDI +252) of PEI dimer tetraester **4-7** with benzopyrene as matrix

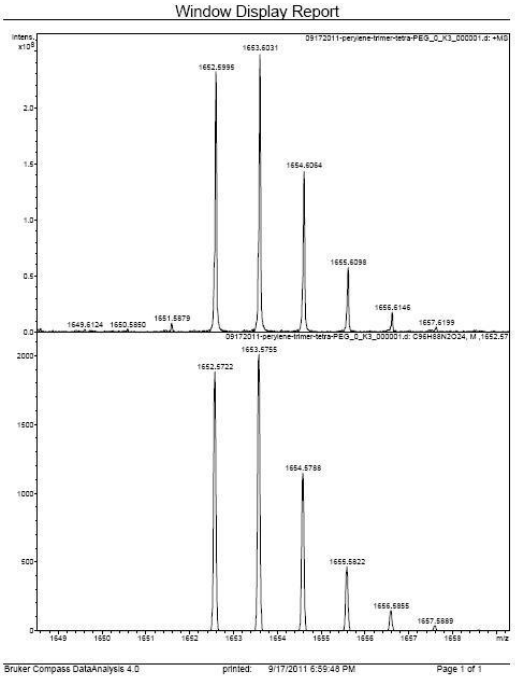

Synthesis of PDI Dimer Tetraester 4-9

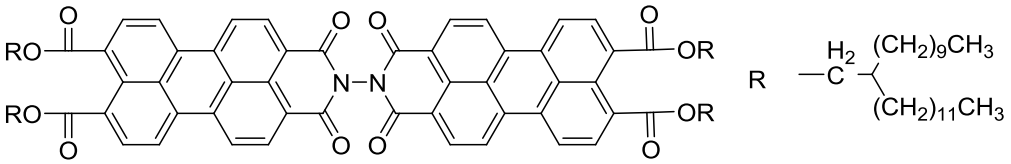

4-9

Two methods were applied to the synthesis of PEI dimer tetraester **4-9**. The first was shown in **Scheme 4-18**. A 10 ml round-bottomed bottle was charged with 50 mg (0.064 mmol) PDIDMA **4-6**, 30 mg (0.20 mmol) DBU and 158 mg (0.448 mmol) 2-decyltetradecan-1-ol. The bottle was sealed and heat to 60 ℃ for 3 hours. Then 228 mg (0.448 mmol) 2-decyl-1-tetradecyl-1-tosylate was added into the bottle. Subsequently, the mixture was stirred and heated at 60 ℃ for 24 hours. Then the mixture was added into 50 ml methanol. Crude product was obtained by vacuum filtration and washed with methanol. Pure product was obtained by column chromatography with 20/1 (v/v) $CHCl_3$/acetone. Yield PEI dimer tetraester **4-9** 117 mg (85%) as dark red solid.

The second method was shown in **Scheme 4-19**. A 10 ml Schlenk flask was charged with 30 mg (0.028 mmol) PEA **3-12**, 25 mg (0.023 mmol) PEI, 1.5 mg (0.01 mmol) DMAP, and 2g dried imidazole. The mixture was heated to 120 ℃ for 3 hour and protected with N_2. After reaction was done, the mixture was cooled to 90 ℃ and water was added into the flask to precipitate the product. Crude product was obtained with vacuum filtration and washed with water. Pure product was obtained by column chromatography with 20/1 (v/v) $CHCl_3$/acetone. Yield PEI dimer tetraester **4-9** 45 mg (90%) as dark red solid.

^{1}H NMR ($CDCl_3$, 600 MHz): δ (ppm) = 8.53 (d, J= 8.4 Hz, 4H, Ar), 8.36 (m, 8H, Ar), 8.08 (d, J= 7.8, 4H, Ar), 4.28 (d, J= 6.0 Hz, 8H, $CO_2C\mathbf{H_2}$), 1.86 – 1.76 (m, 4H, $CO_2CH_2C\mathbf{H}$), 1.50 – 1.27 (m, 160H, $C\mathbf{H}_2$), 0.87 (m, 24 H, $C\mathbf{H_3}$).

^{13}C NMR ($CDCl_3$, 150 MHz): δ (ppm) = 168.30 (ester C=O), 160.65 (imide C=O), 136.40 (Ar), 132.46 (Ar), 131.62 (Ar), 130.15 (Ar), 129.73 (Ar), 129.14 (Ar), 128.96 (Ar), 126.17 (Ar), 123.16 (Ar), 121.78 (Ar), 121.45 (Ar), 68.57 ($CO_2\mathbf{C}H_2CH_2$), 37. 41 ($CO_2CH_2\mathbf{C}H$), 31.93 ($\mathbf{C}H_2$), 31.31 ($\mathbf{C}H_2$), 30.05 ($\mathbf{C}H_2$), 29.37 ($\mathbf{C}H_2$), 26.75 ($\mathbf{C}H_2$), 22.768 ($\mathbf{C}H_2$), 14.10 ($\mathbf{C}H_3$)

FT-IR (cm^{-1}): 2954 (antisymmetric CH_3), 2924 (antisymmetric CH_2), 2870 (symmetric CH_3), 2854 (symmetric CH_2), 1725 (ester C=O), 1708 (symmetric imide C=O), 1690 (antisymmetric imide C=O), 1591 (aromatic ring stretch).

HRMS (MALDI +252) of PEI dimer tetraester **4-9** with benzopyrene as matrix: calcd for $C_{144}H_{212}N_2O_{12}$ 2163. 23; found 2415.6700.

UV-Vis (in $CHCl_3$): 485 nm, absorption coefficient 80828 L mol^{-1} cm^{-1}; 518 nm (λ_{max}), absorption coefficient 137453 L mol^{-1} cm^{-1}.

^{1}H NMR of PEI dimer tetraester **4-9**

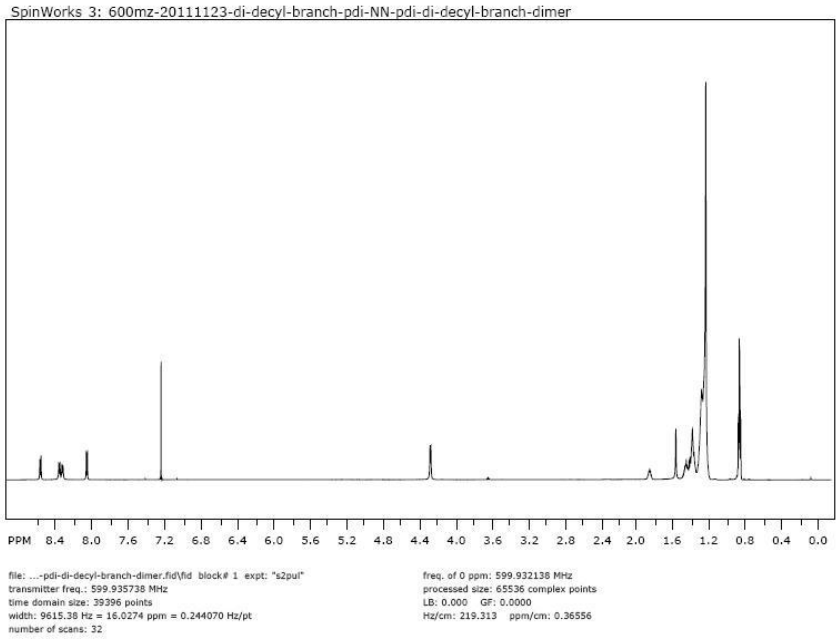

^{13}C NMR of PEI dimer tetraester **4-9**

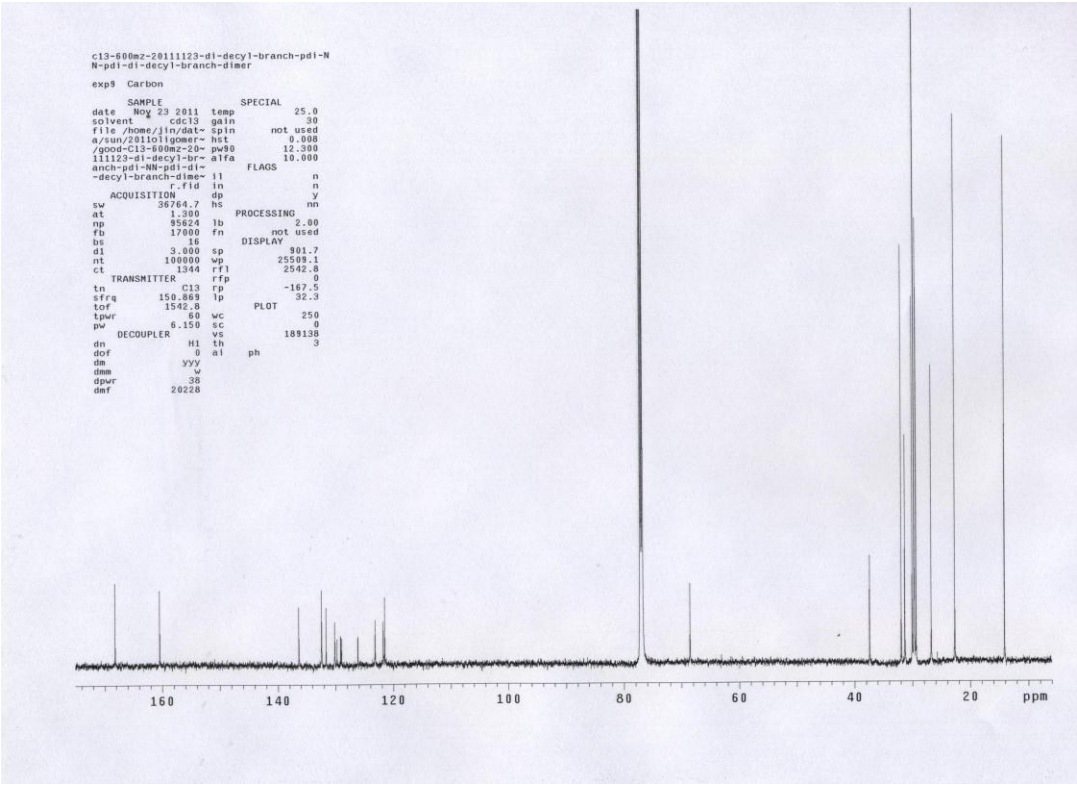

HRMS (MALDI +252) of PEI dimer tetraester **4-9** with benzopyrene

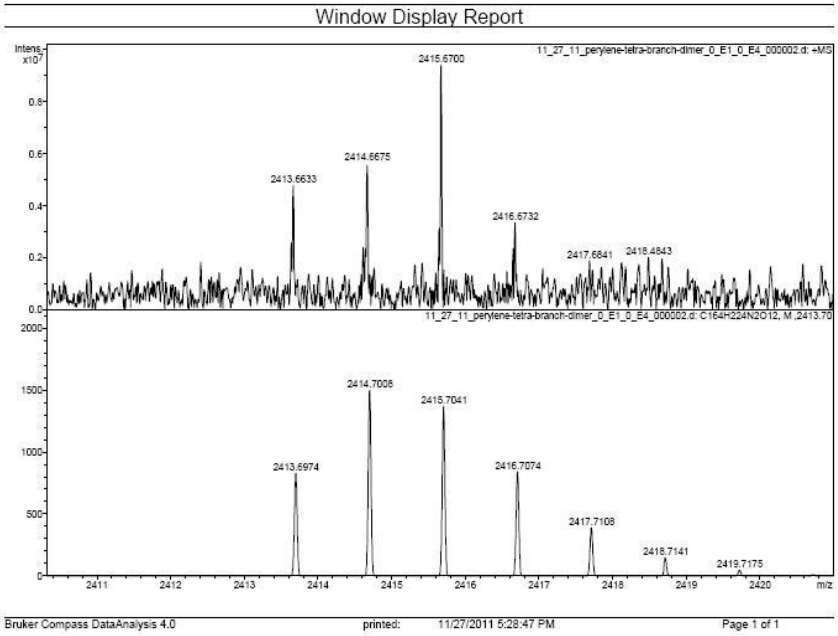

Synthesis of PEI Trimer Tetraester 4-10

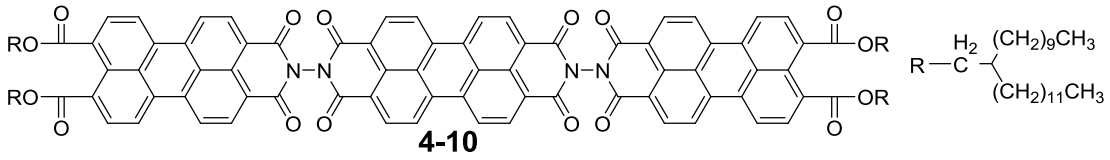

4-10

As shown in **Scheme 4-20**, PEI trimer tetraester **4-10** was synthesized with two step reaction.

Firstly, a 25 mL Schlenk flask was charged with 0.782 g (2 mmol) PDA, 1.0 g (20 mmol) H_2N-NH_2.H_2O and 8g dried imidazole. The mixture was heated to 120 ℃ for 1 hour and protected with N_2. After reaction was done, the mixture was cooled to 90 ℃ and water was added into the flask to precipitate the product. Crude product was obtained with vacuum filtration and washed with dilute HCl. Produt was dried in vacuum oven at 50 ℃ over night. Yield PDI 0.83 g (99%) as dark red solid.

Secondly, a 10 ml Schlenk flask was charged with 10 mg (0.024 mmol) PDI, 54

mg (0.0498 mmol) PEA **3-12**, 5 mg (0.04 mmol) DMAP and 1 g imidazol. The mixture was heated to 150 ℃ for 3 hour and protected with N_2. After reaction was done, the mixture was cooled to 90 ℃ and water was added into the flask to precipitate the product. Crude product was obtained with vacuum filtration and washed with water. After dried in vacuum oven overnight, the crude product was purified by column chromatography with 40/1 (v/v) $CHCl_3$/acetone. Yield ^{1}H NMR of PEI trimer tetraester **4-10** 25 mg (40%) as dark red solid.

^{1}H NMR ($CDCl_3$, 600 MHz): δ (ppm) = 8.75-8.05 (m, 24H, Ar), 4.28 (d, J= 6.0 Hz, 8H, $CO_2C\mathbf{H_2}$), 1.86 – 1.76 (m, 4H, $CO_2CH_2C\mathbf{H}$), 1.50 – 1.27 (m, 160H, $C\mathbf{H}_2$), 0.87 (m, 24 H, $C\mathbf{H_3}$).

^{13}C NMR ($CDCl_3$, 150 MHz): δ (ppm) = 168.16 (ester **C**=O), 160.28 (imide **C**=O), 136.40 (Ar), 131.03 (Ar), 128.96 (Ar), 122.94 (Ar), 121.07 (Ar), 68.59 ($CO_2\mathbf{C}H_2CH_2$), 37. 69 ($CO_2CH_2\mathbf{C}H$), 31.93 ($\mathbf{C}H_2$), 31.29 ($\mathbf{C}H_2$), 30.12 ($\mathbf{C}H_2$), 29.70 ($\mathbf{C}H_2$), 29.40 ($\mathbf{C}H_2$), 26.78 ($\mathbf{C}H_2$), 22.65 ($\mathbf{C}H_2$) 14.10 ($\mathbf{C}H_3$)

FT-IR (cm^{-1}): 2958 (antisymmetric CH_3), 2920 (antisymmetric CH_2), 2870 (symmetric CH_3), 2851 (symmetric CH_2), 1725 (ester C=O), 1708 (symmetric imide C=O), 1692 (antisymmetric imide C=O), 1591 (aromatic ring stretch).

UV-Vis (in $CHCl_3$): 497 nm, absorption coefficient 118442 L mol^{-1} cm^{-1}; 532 nm (λ_{max}), absorption coefficient 258543 L mol^{-1} cm^{-1}.

^{1}H NMR of PEI trimer tetraester **4-10**

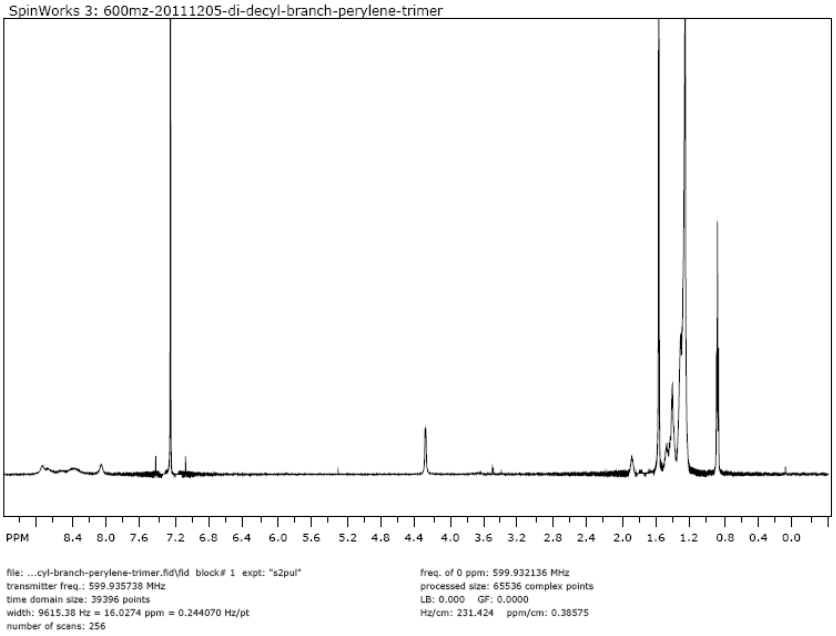

UV-Vis (in $CHCl_3$) spectrum of PEI trimer tetra ester **4-10**

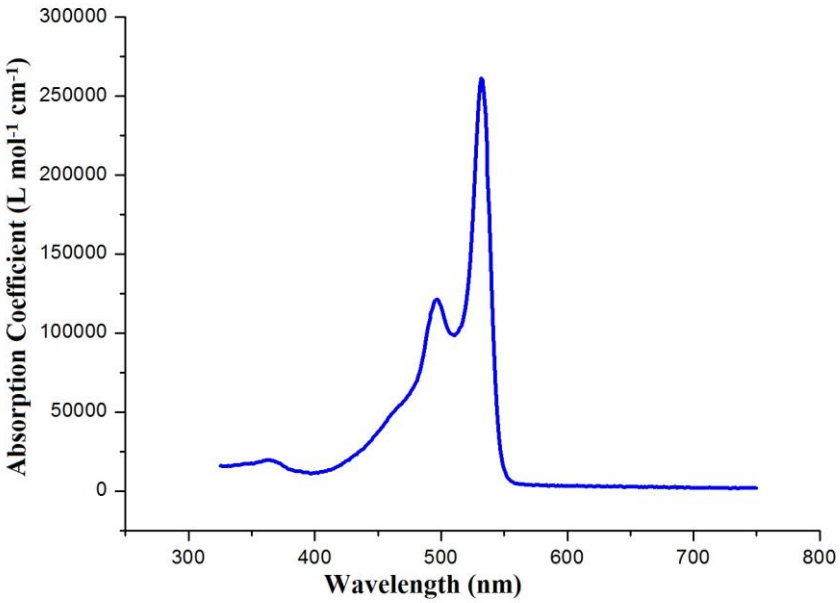

BIBLIOGRAPHY

Chapter 1

1. D. M. Donaldson, J. M. Robertson, J. G. White, *Proc. R. Soc. Lond. A.* **1953**, *220*, 311.

2. S. R. Forrest, Y. Zhang, *Phys. Rev. B.* **1994**, *49*, 11297.

3. S. R. Forrest, M. L. Kaplan, P. H. Schmidt, in: R. A. Huggins (Ed.), *Ann. Rev. Mater. Sci., Annual Reviews.* Vol. 17, PaloAlto, CA, **1987**.

4. I. Chizhov, A. Kahn, G. Scoles, *Journal of Crystal Growth.* **2000**, *208*, 449.

5. S. R. Forrest, M. L. Kaplan, P. H. Schmidt, T. Venkatesan, A. J. Lovinger, *J. Appl. Phys. Lett.* **1982**, *41*, 708.

6. A. J. Lovinger, S. R. Forrest, M. L. Kaplan, P. H. Schmidt, T. Venkatesan, *J. Appl. Phys.* **1984**, *55*, 476.

7. S. R. Forrest, M. L. Kaplan, P. H. Schmidt, *J. Appl. Phys.* **1984**, *55*, 1492.

8. S. R. Forrest, M. L. Kaplan, P. H. Schmidt, W. L. Feldmann, E. Yanowski, *Appl. Phys. Lett.* **1982**, *41*, 90.

9. J. Danziger, J-P. Dodelet, P. Lee, K. W. Nebesny, N. R. Armstrong, *Chem. Mater.* **1991**, *3*, 821.

10. U. Zimmermann, G. Schnitzler, N. Karl, E. Umbach, *Thin.Solid.Films.* **1989**, *175*, 85.

11. S. R. Forrest, M. L. Kaplan, P. H. Schmidt, *J. Appl. Phys.* **1984**, *56*, 543.

12. R. B. Taylor, Z. Shen, S. R. Forrest, *Top Mtg on Organic Thi Film for Photonics Applications Tech Dig.* **1995**, p 38.

13. K. Tanigaki, S. Kuroshima, T. Ebbesen, T. Ichihashi, *Mol. Cryst. Liq. Cryst. Sci. Technol. Nonlinear Optics.* **1992**, *B2*, 179.

14. C. Seidel, C. Awater, X. D. Liu, R. Ellerbrake, H. Fuchs, *Surf. Sci.* **1997**, *371*, 123.

15. M. Mobus, N. Karl, T. Kobayashi, *J. Cryst. Growth.* **1992**, *116*, 495.

16. F. Würthner, *Chem. Comm.* **2004**, *14*, 1564.

17. F. J. M. Hoeben, P. Jonkheijm, E. W. Meijer, A. P. H. J. Schenning, *Chem. Rev.* **2005**, *105*, 1491.

18. R. F. Kelley, W. S. Shin, B. Rybtchinski, L. E. Sinks, M. R. Wasielewski, *J. Am. Chem. Soc*. **2007**, *129*, 3173.

19. S. Yagai, Y. Monma, N. Kawauchi, T. Karatsu, A. Kitamura, *Org. Lett.* **2007**, *9*, 1137.

20. H. Langhals, W. Jona, *Angew. Chem., Int. Ed*. **1998**, *37*, 952.

21. M. Kardos, *Chem. Ber*. **1913**, *46*, 2608.

22. C. Liebermann, M. Kardos, *Chem. Ber.* **1914**, *47*, 1203.

23. C. Liebermann, M. Zsuffa, *Chem. Ber.* **1911**, *44*, 202.

24. W. Herbst, K. Hunger, *Industrial Organic Pigments: Production,Properties, Applications*, 2nd edn., WILEY-VCH, Weinheim, **1997**.

25. G. Geissler, H. Remy (Hoechst AG), *Ger. Pat. Appl.* DE 1130099, **1959** (*Chem. Abstr.*, **1962**, ***57***, P11346f).

26. C. W. Struijk, A. B. Sieval, J. E. J. Dakhorst, M. V. Dijk, P. Kimkes, R. B. M. Koehorst, H. Donker, T. J. Schaafsma, S. J. Picken, *J. Am. Chem. Soc.* **2000**, *122*, 11057.

27. Z. An, J. Yu, S. C. Jones, S. Barlow, S. Yoo, B. Domercq, P. Prins, L. D. A. Siebbeles, *Adv. Mater*. **2005**, *17*, 2580.

28. V. Dehm, Z. J. Chen, U. Baumeister, P. Prins, L. D. A. Siebbeles, F. Würthner, *Org. Lett.* **2007**, *9*, 1085.

30. L. Schmidt-Mende, A. Fechtenkötter, K. Müllen, E. Moons, R. H. Friend, J. D. MacKenzie, *Science*. **2001**, *293*, 1119.

31. A. Yakimov, S. R. Forrest, *Appl. Phys. Lett.* **2002**, *80*, 1667.

32. H. Langhals, R. Ismael, O, Yürük, *Tetrahedron.* **2000**, *56*, 5435.

33. H. Langhals, J. Karolin, L. B. A. Johansson, *J. Chem. Soc.Faraday. Trans*. **1998,**

94, 2919.
34. A. Rademacher, S. Markle, H. Langhals, *Chem. Ber*. **1982**, *115*, 2927.

35. F. Würthner, *Chem. Comm.* **2004**, *14*, 1564.

36. F. J. M. Hoeben, P. Jonkheijm, E. W. Meijer, A. P. H. J. Schenning, *Chem. Rev.* **2005**,*105*, 1491.

37. R. F. Kelley, W. S. Shin, B. Rybtchinski, L. E. Sinks, M. R. Wasielewski, *J. Am. Chem. Soc.* **2007**, *129*, 3173.

38. S. Yagai, Y. Monma, N. Kawauchi, T. Karatsu, A. Kitamura, *Org. Lett*. **2007**, *9*, 1137.

39. X. Q. Li, V. Stepanenko, Z. J. Chen, P. Prins, L. D. A. Siebbeles, F. Würthner, *Chem. Comm.* **2006**, 3871.

40. Y. J. Xu, S. Leng, C. M. Xue, R.K. Sun, J. Pan, J. Ford, S.Jin, *Angew. Chem. Int. Ed.* **2007**, *46*, 3896.

41. R. K. Sun, C. M. Xue, M. Owak, R. M. Peetz, S. Jin, *Tetrahedron. Lett.* **2007**, *48*, 6696.

42. H. Langhals, H. Jaschke, U. Ring, P. Unold, *Angew. Chem. Int. Ed.* **1999**, *38*, 201.

43. T. Weil, U. M. Wiesler, A. Herrmann, R. Bauer, J. Hofkens, F. C. De. Schryver, K. Müllen, *J. Am. Chem. Soc.* **2001**, *123*, 8101.

44. T.Weil, E. Reuther, K. Müllen, *Angew. Chem., Int. Ed.* **2002**, *41*, 1900.

45. R. Gronheid, J. Hofkens, F. Köhn, T. Weil, E. Reuther, K. Müllen, F. C. De Schryver, *J. Am. Chem. Soc.* **2002**, *124*, 2418.

46. G. De. Belder, G. Schweitzer, S. Jordens, M. Lor, S. Mitra, J. Hofkens, S. De . Feyter, M. Van. Der. Auweraer, A. Herrmann, T. Weil, K. Müllen, F. C. De. Schryver, *Chem. Phys. Chem.* **2001**, *1*, 49.

47. H. R. Schweizer. 'Kunstliche organische Farbstoffe und ihre Zwischenprodukte' 1st ed., Springer-Verlag, Berlin, **1964**.

48. E. Spietschka, M. Urban (Hoechst AG), *Ger. Pat. Appl.*, DE 3208192, **1982** (*Chem. Abstr*. **1983**, *99*, 214170y)

49. I. Lukac and H. langhals, *Chem. Ber.* **1983**, *116*, 3524.

50. A. Rademacher, S. Markle, H. Langhals, *Chem. Ber.* **1982,** *115*, 2927.

51. H. Langhals, *Chem. Ber.* **1985**, *118*, 4641.

52. H. Langhals (Hoechst AG), *Ger. Pat. Appl.*, DE 3703513, **1987** (*Chem. Abstr.* **1988**, *109*, P2123760w)

53. D. Volker, Z. J. Chen, D. A. Laurens, F. Würthner, *Org. Lett.* **200**7, *9*, 1085.

54. H. Langhals, *Heterocycles*. **1995,** *40*, 477.

55. M. Kardos, *D. R. P.* 276956. *Friedlanders. Fortschr. Teerfarbenfabr.*, **1917**, *12*, 493.

56. Kalle & Co, *D. R. P.* 386057. *Friedlanders. Fortschr. Teerfarbenfabr.*, **1926**, *14*, 484.

57. G. N. Vorozhtsov, V. A. Ryabinin, V. F. Starichenko, S. M. Shein, *Zh. Org. Khim.* **1982,** *18*, 1024.

58. V. A. Ryabinin, V. F. Starichenko, G. N. Vorozhtsov, S. M. Shein, *Zh. Org. Khim.* **1979**, *15*, 1566.

59. Y. nagao, YTanabe, T. Misono, *Nippon. Kagaku. Kaishi.* **1979,** 528.

60. Y. Nagao and T. Misono, *Bull. Chem. Soc. Jpm.* **1981**, *54*, 1269.

61. H. Troster, *Dyes Pigm*. **1983**, *4*, 171.

62. H. Kaiser, J. Lindner, H. langhals, *Chem. Ber.* **1991**,*124*,529.

63. G. Seybold, G. Wagenblast, *Dyes Pigm.* **1989**, ***11***, 303–317; G. Seybold, A. Stange (BASF AG), *Ger. Pat.*, DE 35 45 004, **1987** (*Chem. Abstr.* **1988**, *108*, 77134c).

64. A. Stange, G. Wagenblast, G. Seybold, *BMFT-Bericht T 86–216*, Fachinformationszentrum Karlsruhe, Germany, **1986**.

65. A. Böhm, H. Arms, G. Henning, P. Blaschka, (BASF AG), *Ger. Pat. Appl.*, DE 19547209 A1, **1997** (*Chem. Abstr.* **1997**, *127*, 96569g).

66. A. Böhm, H. Arms, G. Henning and P. Blaschka (BASF AG), *Ger. Pat. Appl.*, DE 19547210 A1, **1997** (*Chem. Abstr.* **1997**, ***127***, 96570a).

67. M. J. Ahrens, M. J. Fuller, M. R. Wasielewski, *Chem. Mater.* **2003**, *15*,

2684–2686.

68. Y. Zhao, M. R. Wasielewski, *Tetrahedron. Lett.* **1999**, *40*, 7047.

69. A. S. Lukas, Y. Zhao, S. E. Miller and M. R. Wasielewski, *J. Phys. Chem. B*. **2002**, *106*, 1299.

70. B. A. Jones, M. J. Ahrens, M-H. Yoon, A. Facchetti, T. J. Marks, M. R. Wasielewski, *Angew. Chem. Int. Ed.* **2004**, *43*, 6363.

71. F. Würthner, *Chem. Commun.* **2004**, 1564.

72. M. Sadrai, G. R. Bird, *Opt. Commun.* **1984**, *51***,** 62.

73. H. Langhals, S. Demmig, H. Huher, *Spectrochim. Acra.* **1988**, *44A***,** 1189.

74. Xerox Corp., ***JP*** 03024059 A2 (Fehr. 1, 1991) ***(****Chem. Abstr.* **1991**, *115*, 123841a).

75. H. Langhals, *Chem. Phys. Lett.* **1988**, *150*, 321.

76. H. Langhals, S. Demmig, ***D.O.S.*** 4007618.0 (March 10, 1990) ***(****Chem. Abstr.* **1992**, *116*,117172n).

77. Y. Yang, S. Yang, Z. Wang, *Hmue. Shiji***, 1984**, *6*, 167 ***(****Chem. Abstr.* **1984**, *101*, 221163m).

78. H. Langhals, S. Demmig, T. Potrawa, *J. Prakt. Chem.* **1991**, *333*,733.

79. H. Langhals, J. Karolin, L. B.-A. Johansson, *J. Chem. Soc. Faraday. Trans.* **1998**, *94*, 2919.

80. F. Würthner, C. Thalacker, S. Diele, C. Tschierske, *Chem. Eur. J.* **2001**, *7*, 2245.

81. M. G. Dirk, P. N. Jhb, K-D. Asmuslb, *J. Phys. Chem.* **1994,** *98***,** 4617.

82. M. J. Ahrens, M. J. Fuller, M. R. Wasielewski, *Chem. Mater.* **2003**, *15*, 2684.

83. J. A. Letizia, A. Facchetti, C. L. Stern, M. A. Ratner, T. A. Marks, *J. Am. Chem. Soc.* **2005**, *127*, 13476.

84. S. Tatemichi, M. Ichikawa, T. Koyama, Y. Taniguchi, *Appl. Phys. Lett.* **2006**, *89*, 112108.

85. A. J. Brooks, A. Facchetti, M. R. Wasielewski, T. J. Marks, *J. Am. Chem. Soc.* **2007**, 129, 15259.

86. K. Petritsch, R. H. Friend, A. Lux, G. Rozenberg, S. C. Moratti, A. B. Holmes, *Synthetic. Metals.* **1998**, *102*, 1776.

87. C. W. Tang, *Appl. Phys. Lett.* **1986**, *48*, 183.

88. L. Schmidt-Mende, A. Fechtenkotter, K. Müllen, E. Moons, R. H. Friend, J. D. MacKenzie1, *Science*. **2001**, *293*, 1119.

89. T. Habheider, S. A. Benning, M. W. Lauhof, H.-S. Kitzerow, Mol., *Cryst. Liq. Cryst.* **2004**, *413*, 461.

90. F. Graser, E. Hädicke, *Liebigs Ann. Chem.* **1980**, 1994.

91. F.Graser, E. Hädicke, *Liebigs Ann. Chem.* **1984**, 483.

92. W. Herbst, K. Hunger, *Industrial Organic Pigments: Production, Properties, Applications*, 2nd edn., WILEY-VCH, Weinheim, **1997**.

93. S. Ghosh, X-Q. Li, V. Stepanenko, F. Würthner, *Chem. Eur. J.* **2008**, *14*, 11343.

94. F. Würthner, C. Thalacker, S. Diele, C. Tschierske, *Chem. Eur. J.* **2001**, ***7***, 2245.

95. R. A. Cormier, B. A. Gregg, *J. Phys. Chem. B.* **1997**, *101*,11 004; R. A. Cormier, B. A. Gregg, *Chem. Mater.* **1998**, *10*, 1309.

96. C. Thalacker, F. Würthner, *Adv. Funct. Mater.* **2002**, *12*, 209.

97. R. Dobrawa, D. G. Kurth, F. Würthner, *Polymer Preprints*, **2004**, *45*(1), 378–379; R. Dobrawa, F. Würthner, *Chem. Commun.* **2002**, 1878.

98. H. Langhals and W. Jona, *Angew. Chem. Int. Ed.* **1998**, *37*, 952.

99. T. M. Wilson, M. J. Tauber, M. R. Wasielewski, *J. Am. Chem. Soc.* **2009**, *131*, 8952.

100. W. Kuhn, *Trans. Faraday. Soc.* **1930**, *26*, 293.

Chapter 2

1. H. Langhals, *Heterocycles.* **1995**, *40*, 477.

2. H. Langhals, W. Jona, F. Einsiedl, S.Wohnlich, *Adv. Mater.* ***1998***, *10*, 1022.

3. R. Samudrala, X. Zhang, R. M. Wadkins, D. L. Mattern, *Bioorg. Med. Chem.* **2007**, *15*, 1861.

4. H. Langhals, R. Ismael, O. Yuruk, *Tetrahedron.* **2000**, *56*, 5435.

5. H. Langhals; J. Karolin, L. B. A. Johansson, *J. Chem. Soc. Faraday. Trans.* **1998**, *94*, 2919.

6. A. Rademacher, S, Markle, H. Langhals, *Chem. Ber.* **1982**, *115*, 2927.

7. C. W. Struijk, A. B. Sieval, J. E. J. Dakhorst, M. V. Dijk, P. Kimkes, R. B. M. Koehorst, H. Donker, T. J. Schaafsma, S. J. Picken, *J. Am. Chem. Soc.* **2000**, *122*, 11057.

8. Z. An, J. Yu, S. C. Jones, S. Barlow, S. Yoo, B. Domercq, P. Prins, L. D. A. Siebbeles, *Adv. Mater.* **2005**, *17*, 2580.

9. V. Dehm, Z. J. Chen, U. Baumeister, P. Prins, L. D. A. Siebbeles, F. Würthner, *Org. Lett.* **2007**, *9*, 1085.

10. F. Würthner, *Chem. Comm.* **2004**, *14*, 1564.

11. F. J. M. Hoeben, P. Jonkheijm, E. W. Meijer, A. P. H. J. Schenning, *Chem. Rev.* **2005**, *105*, 1491.

12. R. F. Kelley, W. S. Shin, B. Rybtchinski, L. E. Sinks, M. R. Wasielewski, *J. Am. Chem. Soc.* **2007**, *129*, 3173.

13. Y. nagao, Y. Tanabe, T. Misono, *Nippon. Kagaku. Kaishi.* **1979,** 528.

14. H. Troster, *Dyes. Pigm*. **1983**, *4*, 171.

15. H. Kaiser, J. Lindner, H. Langhals, *Chem. Ber.* **1991**, *124*, 529.

16. R. Gomez, J. L. Segura, N.Martin, *Org. Lett.* **2005**, *7*, 717.

17. S. Fukuzumi, K. Ohkubo, J. Ortiz, A. M. Gutierrez, F. Fernandez-Lazaro, A. Sastre-Santos, *Chem. Commun.* ***2005***, *30*, 3814.

18. L. D. Wescott, D. L. Mattern, *J. Org. Chem.* **2003**, *68*, 10058.

19. G. J. Mohr, U. E. Spichiger, W. Jona, H. Langhals, *Anal. Chem.* **2000**, *72*, 1084.

20 L. Zang, R. Liu, M. W. Holman, K. T. Nguyen, D. M. Adams, *J. Am. Chem. Soc.* **2002**, *124*, 10640.

21. N. Soh, T. Ariyoshi, T. Fukaminato, K. Nakano, M. Irie, T. B. Imato, *Med. Chem. Lett.* **2006**, *16*, 2943.

22. E. E, Neuteboom, E. H. A. Beckers, S. C. J. Meskers, E. W. Meijer, R. A. Janssen, *J. Org. Biomol. Chem.* **2003**, *1*, 198.

23. A. M. Ramos, S. C. J. Meskers, E. H. A. Beckers, R. B. Prince, L. Brunsveld, R. A. Janssen, *J. Am. Chem. Soc.* **2004**, *126*, 9630.

24. H. Langhals, W. Jona, *Angew. Chem. Int. Ed.* **1998**, *37*, 952.

25. H. Langhals, O. Krotz, *Angew. Chem. Int. Ed.* **2006**, *45*, 4444.

26. M. J. Tauber, R. F. Kelley, J. M. Giaimo, B. Rybtchinski, M. R. Wasielewski, *J. Am. Chem. Soc.* **2006**, *128*, 1782.

27. P. Yan, A. Chowdhury, M. W. Holman, D. M. Adams, *J. Phys. Chem. B*, **2005**, *109*, 724.

28. E. E. Neuteboom, P. A. Hal, R. A. Janssen, *J. Chem. Eur.* **2004**, *10*, 3907.

29. D. Medvedeva, A. Bobrovsky, N. Boiko, V. Shibaev, V. Shirinyan, M. Krayushkin, *Macromol. Chem. Phys.* **2006**, *207*, 770.

30. S. M. Lindner, M. Thelakkat, *Macromolecules.* **2004**, *37*, 8832.

31. Y. J. Xu, S. Leng, C. M. Xue, R.K. Sun, J. Pan, J. Ford, S. Jin, *Angew. Chem. Int. Ed.* **2007**, *46*, 3896.

32. R. K. Sun, C. M. Xue, M. Owak, R. M. Peetz, S. Jin, *Tetrahedron. Lett.* **2007**, *48*, 6696.

Chapter 3

1. Y. Nagao, T. Misono, *Bull. Chem. Soc. Jpm.* **1981**, *54*, 1269.

2. H. Troster, *Dyes. Pigm*. **1983**, *4*, 171.

3. H. Kaiser, J. Lindner, H. langhals, *Chem. Ber.* **1991**,*124*, 529.

4. R. K. Sun, C. M. Xue, M. Owak, R. M. Peetz, S. Jin, *Tetrahedron. Lett.* **2007**, *48*, 6696.

5. S. Benning, H. S. Kitzerow, H. Bock, M. F. Achard, *Liq. Cryst.* **2000,** *27*, 901.

6. M. J. Yang, S. L. Lu, Y. J. Li, *Mater. Sci. Lett.* **2003**, *22*, 813.

7. T. Sheider, S. A. Benning, M. W. Lauhof, H. S. Kitzerow, H. Bock, M. D. Watson, K. Müllen, *Mol. Cryst. Liq. Cryst.* **2004**, *413*, 2597.

8. C. Xue, R. Sun, R. Annab, D. Abadi, T*etrahedron. Lett.* **2009**, *50*, 853.

9. H. Langhals, W. Jona, *Angew. Chem. Int. Ed.* **1998**, *37*, 952.

10. H. Troster, *Dyes. Pigm*. **1983**, *4*, 171.

11. C. F. H. Allen, J. W. Gates, *Organic. Synthesis*. **1945**, *25*, 9.

12. O. Ryu, K. B. Sharpless, *Organic. Synthesis.* **1996**, *73*, 1.

13. Y. J. Xu, S. Leng, C. M. Xue, R. K. Sun, J. Pan, J. Ford, S.Jin, *Angew. Chem. Int. Ed.* **2007**, *46*, 3896.

14. G. D. Beal, *Organic. Synthesis*. **1926**, *6*, 379.

15. H. R. Snyder, L. A. Brooks, S. H. Shapiro, *Organic. Synthesis*. **1931**, *11*, 42.

16. H. Langhals, *Helvetica. Chimica. Acta.* **2005**, *88*, 1309.

17. H. Tamiaki, T. Obata, Y. Azefu, K. Toma, *Bull. Chem. Soc. Jpn.* **2001**, *74*, 733.

Chapter 4

1. H. Langhals, W. Jona, *Angew. Chem. Int. Ed.* **1998**, *37*, 952.

2. T. M. Wilson, M. J. Tauber, M. R. Wasielewski, *J. Am. Chem. Soc.* **2009**, *131*, 8952.

3. G. Seybold, G. Wagenblast, *Dyes. Pigm.* 1989, **11**, 303–317.

4. H. Langhals, S. Demmig, T. Potrawa, *J. Prakt. Chem.* **1991,** *333*, 733.

5. C. M. Xue, R. K. Sun, S. Jin, *Tetrahedron. Lett.* **2009**, *50*, 853.